5-2015

CONTROL OF RADIATION EXPOSURE TO PAEDIATRIC PATIENTS AT CONVENTIONAL RADIOLOGY AND CARDIAC CENTERS AT DUBAI HOSPITAL

Najlaa Khalfan Saeed Almazrouei

United Arab Emirates University

College of Science

Department of Physics

CONTROL OF RADIATION EXPOSURE TO PAEDIATRIC PATIENTS AT CONVENTIONAL RADIOLOGY AND CARDIAC CENTERS AT DUBAI HOSPITAL

Najlaa Khalfan Saeed Almazrouei

This thesis is submitted in partial fulfilment of the requirements for the degree of Master of Science in Physics

Under the Supervision of Dr. Adel Hashish

May 2015

Declaration of Original Work

I, Najlaa Khalfan Saeed Almazrouei, the undersigned, a graduate student at the United Arab Emirates University (UAEU), and the author of this thesis entitled "*Control of radiation exposure to paediatric patients at conventional radiology and cardiac centers at Dubai Hospital*", hereby, solemnly declare that this thesis is an original research work that has been done and prepared by me under the supervision of Dr. Adel Hashish, in the College of Science at UAEU. This work has not been previously formed as the basis for the award of any academic degree, diploma or a similar title at this or any other university. The materials borrowed from other sources and included in my thesis have been properly cited and acknowledged.

Student's Signature_____ Date _____

Advisory Committee

1) Advisor: Dr. Adel Hassan Hashish
   Title: Associate Professor
   Department of Physics
   College of Science, UAEU

2) Member: Dr. Jamila Salem Alsuwaidi
   Title: Consultant - Radiation in Medicine Developments
   Department of Medical Education
   Dubai Health Authority, UAE

Approval of the Master Thesis

This Master Thesis is approved by the following Examining Committee Members:

1) Advisor (Committee Chair): Dr. Adel Hassan Hashish
   Title: Associate Professor
   Department of Physics
   College of Science, UAEU

   Signature _____ Date _____

2) Member: Dr. Jamila Salem Alsuwaidi
   Title: Consultant - Radiation in Medicine Developments
   Department of Medical Education
   Dubai Health Authority, UAE

   Signature _____ Date _____

3) Member: Dr. Bashar Issa
   Title: Professor
   Department of Physics
   College of Science, UAEU

   Signature _____ Date _____

4) External Examiner: Dr. Renato Padovani
   Title: Professor
   International Centre for Theoretical Physics (ICTP), Consultant
   Trieste, ITALY

   Signature _____ Date _____

This Master Thesis is accepted by:

Dean of the College of Science: Professor Frederick Chi-Ching Leung

Signature _____ Date _____

Dean of the College of the Graduate Studies: Professor Nagi T. Wakim

Signature _____ Date _____

Copy ____ of ____

Abstract

In view of increasing the number of x-ray examinations over the years, paediatric radiation safety is considered as one of the critical subjects in the modern medical imaging. Paediatric patients are at higher risk from ionizing radiation than adults if they receive same amount of dose. This project was conducted to evaluate paediatric patient radiation dose levels in digital radiology (both fixed and mobile x-ray units) and interventional cardiology at Dubai Hospital. The results of this study are expected to contribute in establishing local and national diagnostic reference levels in United Arab Emirates (UAE).

A combination of phantom studies and patient data collection were utilized in this paediatric dosimetry project. The patient data collection was obtained through both manual contributions from radiographers and data obtained from Digital Imaging and Communications in Medicine (DICOM) header. The first method was performed using Polymethyl methacrylate phantom with different thicknesses to represent different age groups of paediatrics; whereas the second method was without phantom where the exposure factors extracted from DICOM header. Then, effective dose was estimated using Monte Carlo dose calculation software.

The primary measured and estimated radiation dose quantity was the incident air kerma. The entrance surface air kerma was calculated from the incident air kerma and then executed with the application of appropriate backscatter factors. For the fixed x-ray machine, the radiation dose levels were lower than the recommended values and other published data while for the mobile x-ray the findings were comparable and slightly higher than other surveyors. In interventional cardiology, the radiation dose values were higher compared to other values shown in previous researches. The variation in entrance skin air kerma values between the published data and the findings in this study are related to the use of different equipment, exposure parameters and it is significantly related to the professional awareness towards ionizing radiation hazards. Evidently, the values of effective doses showed that the radiation risk is higher with small ages.

In UAE, this study is considered as one of the first structured studies performed on paediatric dosimetry. Further researches are needed to include image

quality assessment to stress on obtaining optimum image quality with lower radiation dose.

Keywords: Ionizing radiation, patient dosimetry, paediatric radiation safety, radiation protection, diagnostic radiology, x-ray, effective dose, DRLs

Title and Abstract in Arabic

مراقبة التعرض الإشعاعي للأطفال في الأشعه الإعتياديه و مركز القلب في مستشفى دبي

الملخص

أدت تكنولوجيا التصوير الطبي الحديثه الي زيادة فحوصات الأشعة السينية للمرضى الأطفال على مر السنين. السلامة الإشعاعيه لطب الأطفال تعتبرإحدى الموضوعات الهامة في التصوير الطبي. إن الإشعاعات المؤينة تشكل خطر أكبرعلى الأطفال منها على البالغين إذا تعرضوا لنفس القدر من الجرعة الإشعاعيه. فالهدف من هذه الأطروحه هو تقييم الجرعات الإشعاعية للمرضى الأطفال في الأشعة الرقميه (أجهزة الأشعة السينية الثابتة والمتحرك)، وجهازأمراض القلب التداخلي في مستشفى دبي. ومن المتوقع أن نتائج هذه الدراسة ستساهم في إرساء مستويات مرجعية للفحوصات الإشعاعيه التشخيصية للأطفال على المستوى المحلي والوطني في دولة الإمارات العربية المتحدة.

لقد تم اجراء مجموعه من الدراسات التجريبيه المحاكيه (phantom studies) بالإضافه الى جمع بيانات المرضى بشكل يدوي بمساعدة فني الأشعة وتجميع البيانات من خلال قاعدة بيانات المرضى الإلكترونيه لتقدير قياس جرعات المريض الإشعاعية، حيث أن الكميه الأساسيه التى يتم قياسها وتقديرها تدعى (Incident Air Kerma). تم استخدام طريقتان لعملية القياس و التقدير، الأولى طريقة المحاكاة (Phantom) بسماكات مختلفة لتمثيل الفئات العمرية للأطفال. والطريقه الثانيه من دون استخدام أداة المحاكاة حيث ان عوامل التعرض الإشعاعيه للتصوير الطبي تم استخراجها من قاعدة بيانات المرضى الإلكترونيه. بعد ذلك تم حساب الجرعه الإشعاعيه على مستوى سطح جسم المريض والتي يطلق عليها (Entrance Surface Air Kerma) من خلال استخدام عامل التشتت الإرتدادي للاشعه و الجرعه الإشعاعيه المقاسه. وتم تقديرقيمة الجرعه المؤثره (effective dose) باستخدام برنامج مونت كارلو.

نتائج هذه الدراسه أظهرت أن مستوى الجرعة الإشعاعية في أجهزة الأشعه السينيه الثابته كانت أقل من القيم الموصى بها وكذلك أقل من نتائج الدراسات الأخرى المنشورة في حين أجهزة الأشعة السينية المتحركه أظهرت نتائج مقاربه وأعلى قليلا من الدراسات الأخرى. فيما يخص جهاز أمراض القلب التداخلي كانت النتائج أعلى من الدراسات الأخرى. هنالك كثير من العوامل التي تؤدي الى إختلاف النتائج بين الباحثين في مستويات الجرعات الإشعاعيه للمرضى من فئة الأطفال منها على سبيل المثال : نوعية الأجهزة، عوامل التعرض الإشعاعيه في التصوير الطبي و مستوى الوعي بمخاطر الأشعه المؤينه بين المهنيين. وفي هذه الدراسه، بينت قيم الجرعات المؤثره مدى خطر الإشعاع على الأطفال الأقل عمرا.

تعتبر هذه من أوائل الدراسات المنظمة على مستوى الدوله أجريت على قياس الجرعات الإشعاعيه للأطفال و هناك حاجة إلى المزيد من الدراسات لتشمل تقييم جودة التصوير الإشعاعي للحصول على صور إشعاعيه مثلى مع جرعات إشعاع أقل.

Acknowledgements

First, I am especially grateful to my academic advisor Dr. Adel Hashish; Associated Professor in the Department of Physics/ UAEU, for his support, advice, mentor and encouragement along the hard process of the preparation of this thesis.

Greatly and foremost I would like to express my sincere gratitude to my supervisor Dr. Jamila Salim Alsuwaidi; Consultant Medical Physicist/ Dubai Health Authority (DHA), for her continuous support, patience, motivation and enthusiasm. Her guidance helped me in all the time of research and writing of this thesis.

I would like to express my gratitude to Dubai Hospital (DH) administration and to my colleagues at medical physics section for their patience and support during my MSc. study. Moreover, I highly thank the staff at Radiology department and cardiac center at DH for their cooperation and support during the practical part of my thesis. Thanks to DHA higher authorities and the DHA Ethics Committee for there continues support through this project. I appreciate the support from my colleagues at the Military and Alain Hospitals for providing me with the tools for my project. Furthermore, I would like to thank Philips Company for purchasing PCXMC 2.0 software to carry out part of this project. I extend my appreciation to all members of the Physics Department at UAEU. Especially Prof. Maamar Benkraouda the head of the Physics Department and Prof. Mofreh Zaghloul the coordinator of physics MSc. program. I would like to thank the thesis committee members; Dr. Bashar Issa (internal examiner) and Dr. Renato Padovani (External Examiner) for dedicating their time and effort towards this project.

I owe my dearest thanks to the most precious people in my life, my parents, brothers, sisters and AlMazrouei family for their support and encouragement.

Dedication

To UAE and my beloved family

Table of Contents

List of Tables

List of Figures

List of Abbreviations/ Nomenclatures/Symbols

The following notation is used throughout the text; other terms appear less frequently. Symbols used in all equations are defined where they occur.

KERMA	Kinetic Energy Released per Unit Mass
ESD	Entrance Surface Dose
ESAK	Entrance Surface Air Kerma
IAK	Incident Air Kerma
KAP	Kerma Area Product
P_{AK}	Kerma Area Product
K_i	Incident Air Kerma
K_e	Entrance Surface Air Kerma
DRL	Diagnostic Reference Level
HVL	Half Value Layer
mAs	X-ray tube current multiplied by the time
kVp	X-ray tube potential
TLD	Thermo luminescence Dosimeter
B	Back scatter factor
ICRP	International Committee on Radiological Protection
IAEA	International Atomic Energy Agency
UNSCEAR	United Nations Scientific Committee on the Effects of Atomic Radiation
WHO	World Health Organization
BSS	Basics Safety Standards
NRPB	National Radiological Protection Board

IC	Interventional Cardiology
E	Effective dose
DICOM	Digital Imaging and Communications in Medicine
PMMA	Polymethyl methacrylate
Cath lab	Catheterization Laboratory
d_{FTD}	Tube focus to table distance
d_{FSD}	Tube focus to skin distance
d_m	Distance between the dosimeter reference point and table top

Glossary of Terms

The following glossaries of terms were taken from IAEA TRS.457 [14] and ICRP 121 [1].

Automatic Exposure Control (AEC)	A mode of operation of an X ray machine by which the tube loading is automatically controlled and terminated when a preset radiation exposure to the imaging receptor is reached. The tube potential may or may not be automatically controlled.
Backscatter factor (B)	The ratio of the entrance surface air kerma to the incident air kerma.
Calibration	A set of operations that establish the relationship between values of quantities indicated by the instrument under reference conditions and the corresponding values realized by standards.
Calibration Coefficient	For a detector assembly with an associated measuring assembly, the coefficient that converts the indication, corrected to stated reference conditions, to the conventional true value of the dosimetric quantity at the reference point of the detector.
Calibration of a diagnostic dosimeter	The comparison of the indication of the instrument under test with the conventional true value of the air kerma or air kerma rate with the objective of determining the calibration coefficient.
Entrance surface air kerma	The air kerma at a point in a plane corresponding to the entrance surface of a specified object, e.g. a patient's breast or a standard phantom. The radiation incident on the object and the backscattered radiation are included
Exposure parameters	The settings of x ray tube voltage (kV), tube current (mA) and exposure time (s)
Heel effect	The non-uniform distribution of air kerma rate and of the beam hardness in an x- ray beam in planes perpendicular to the beam axis and in the direction cathode to anode
Incident air kerma	The air kerma at a point in a plane corresponding to the entrance surface of a specified object, e.g. a patient's breast or a standard phantom. Only the radiation incident on the object and not the backscattered radiation is included
kerma area	Product of the area of a cross-section of a radiation beam and the average value of a kerma related quantity over that cross-section.

product	This quantity is available clinically either by direct measurement with a KAP meter or by calculator and display on a KAP indicator.
Patient dose (exposure)	A generic term used for a variety of quantities applied to a patient or group of patients. The quantities are related and include absorbed dose, incident air kerma, entrance surface air kerma, etc.
Phantom	An object used to absorb and/or scatter radiation equivalent to that of a patient and hence to aid estimation of radiation doses and test imaging systems without actually exposing a patient. It may be an anthropomorphic or a physical test object.
Reference Person	An idealized person for whom the organ or tissue equivalent doses are calculated by averaging the corresponding doses of the Reference Male and Reference Female. The equivalent doses of the Reference Person are used for the calculation of the effective dose by multiplying these doses by the corresponding tissue weighting factors
Reference phantom	Voxel phantoms for the human body (male and female voxel phantoms based on medical imaging data) with the anatomical and physiological characteristics defined in the report of the ICRP Task Group on Reference Man (Publication 89, ICRP 2002).
Semiconductor detector	A device that uses a semiconductor to detect and measure the number of charge carriers set free in the detector by ionizing radiation.
X- ray tube	Vacuum tube designed to produce X rays by bombardment of the anode with a beam of electrons accelerated through a potential difference.

Chapter 1: Introduction

1.1 Patient Safety in Diagnostic Radiology

Diagnostic radiology is considered as one of the most valuable inventions as well as a key area for future innovations and improvement. It encompasses different advanced imaging modalities and methods from conventional x-rays into fluoroscopically and fluorography guided procedures, which are used to image different parts of the patient's body for the diagnosis and treatment of many kinds of diseases. Usually, in addition to initial scans doctors are frequently in need of more scans to monitor the progress of a disease already being diagnosed or treated. Hence, digital radiology has an important role in the improvement of public health in all patients through all age ranges. Despite the fact that digital radiology dose clearly have many advantages, it is important to highlight its ionizing radiation which may cause harm to the human biological tissues [1].

In the United Nations Scientific Committee on the Effects of Atomic Radiation (UNSCEAR) 2008 Report, it has been stated that the medical exposure represents the second largest source of ionizing radiation exposure to human globally and it contributes over 95% of the man-made radiation exposure [2]. In the period between 1997 and 2007 covered by the UNSCEAR 2008 survey, it was found that the number of the imaging studies per year was approximately 3.6 billion; this includes diagnostic imaging and also dental examinations.

The exposure to ionizing radiation in childhood should be highly monitored as this group has a higher readiness to develop cancer than adults when receiving the same dose [1]. Therefore, special attention for paediatric patients of different age

groups has been given by various international organizations such as the World Health Organization (WHO), UNSCEAR, the International Committee of Radiological Protection (ICRP) and the International Atomic Energy Agency (IAEA). These international organizations have recommended the implementation of a set of best practice procedures which are documented in the Basics Safety Standards (BSS) guidelines. These guidelines focus on radiology practices to ensure the establishment of radiation safety, quality assurance and quality control programs to protect patients, staff and the general public from unnecessary radiation exposures [2, 4, 5].

All diagnostic exposures to ionizing radiation shall follow the main radiation protection principles of justification and optimization, particularly in paediatric care. This exposure increases by two to three times the risk of cancer induction compared to the adult [1]. Therefore, radiation safety for paediatric is extremely important where the longer life expectancy in children allows more time for any harmful effects of radiation to arise. For instance the ICRP also provides guiding principles of radiological protection for referring clinicians and clinical staff performing diagnostic imaging and interventional procedures specifically focuses on paediatric patients [1].

In a recent IAEA publication, it has been stated that there is relatively little quantitative literature and practical guidelines on the protection of paediatric patients from radiation during diagnostic procedures, which makes it difficult to justify whether the international radiation safety requirements are implemented as recommended by the BSS [4]. Furthermore, survey reports recently conducted by IAEA recognize the lack of information on image quality and patients doses in most

Asian countries. As a consequence, a number of IAEA Technical Cooperation (TC) projects were initiated. The purpose of these TCs was to assess the status of imaging technology, practice in conventional radiography, mammography, computed tomography (CT) and interventional procedures, and to implement optimization actions in the developing world's [3].

In general, a key area of medical concerns is to limit the levels of radiation exposures when handling paediatric patients. However, any doses must be sufficient for a diagnosis to be performed according to a principle of "as low as reasonably achievable" (ALARA). Indeed many studies had been performed to define the optimal paediatric radiation doses [6, 7, 8, 9, 10]. A study conducted in the UK, based on epidemiological and data collection surveys found that there is a need for nationwide surveys to estimate fetal and childhood radiation doses from common diagnostic procedures [6]. Though radiation doses from conventional radiology might be low, paediatric patients often receive repeated examinations over time to evaluate their clinical conditions, which could result in relatively high cumulative radiation doses that increase the risk of developing cancer in their future life as late radiation biological effects [11].

The prolonged x-ray procedures such as the x-ray guided cardiac catheterizations perform to examine paediatric patient with heart defects induce high level of radiation doses. Therefore, it is very important to justify and optimize the procedures and keep the radiation dose level as low as possible [12].

It is clear from the literature reviewed by the researcher that the goal of radiation protection is important and in short it is to minimize the probability of

radiation biological effects stochastic risks and to prevent the occurrence of deterministic effects [15]. These potential radiation risks to humans are widely discussed among medical communities, in the media and even by politicians [16]. Hence, the international organizations and associations concerning with radiation protection state that the data related to the radiation risk caused to the patient should be available, and special attention should be paid to paediatric imaging [13, 17]. It is widely argued that medical practitioners must better understand the risk and science behind diagnostic radiology in order to be able to apply medical diagnostic and interventional radiation carefully by weighing the benefits with the risks prior to each patient request [17]. Furthermore, it is asserted that the standard dose quantities registered by all x-ray examinations should work towards provide sufficient data to estimate the radiation risk. The patient dosimetry in terms of measurements, recording, monitoring and auditing are important part of any quality assurance program when an x-ray machine is installed or used in any human medical context [13, 14, 15].

1.2 Paediatric Dosimetry

The dosimetry for paediatric patients undergoing diagnostic radiology requires special considerations. This is because the organs and tissues are closer together in small children and, hence, are harder to exclude from the primary beam and to protect from scatter radiation [4, 18]. Furthermore, most of the paediatric radiological examinations are performed in a mixed environment with adult radiology; as a consequence of this, a special care be given when dealing with paediatric in radiological examination. In 2007, the IAEA published a code of practice, Dosimetry in Diagnostic Radiology (TRS 457), recommends procedures for

dosimetric measurement and calibration for standardized implementation [14]. In a subsequence document, IAEA specifically focus on the dosimetry of the paediatric diagnostic radiology [18]. The document highlights the complex nature of paediatric and recommends this area to be studied as an independent field; reasons for this include:

a) They have longer life expectancy which allows more time for any harmful effects of radiation to arise.
b) Higher radiosensitivity than adults which vary with gender and age.
c) The data collection and analysis are complex process due to wide variety in the paediatric population size even within the same age group.

The document points out that paediatric examination should differ from adult examinations in a number of ways such as different radiological equipment, different technique factor and beam quality. Moreover, the type of diagnostic examination performed and the skills of the staff who carry out this examination should be observed carefully. It recommends that there is a need for a specialized phantoms and radiation measurements equipment such as more sensitive air kerma area product (KAP) meters [18].

Quantification of radiation exposures for the paediatric patients in the diagnostic radiology reflects one of the main goals to optimize the patient's protection. Also, it may expect to reduce the stochastic effects without compromising the quality of the diagnostic image [14, 18].

1.3 Biological Effect of Ionizing Radiation

The human body is composed of about 80 % water which is an important element of radiation effects. The remaining molecular composition of the body is about 15% proteins, 2 % lipids (fats), 1% carbohydrates, and about 1% nucleic acids. These molecules are organized primarily within the living cells of the body, of which there are many types including epithelial (skin) cells, osteocytes (bone cells), nerve cells, and blood cells [25].

Radiation interactions that produce biological changes are classified as either direct or indirect which is defined in Figure (1). The change takes place by direct action if a biological macromolecule such as DNA, RNA, or protein becomes ionized or excited by an ionizing particle or photon passing through or near them [26].

Indirect effects are the result of radiation interactions within the medium which create reactive chemical compound that in turn interact with the target molecule. Because the majority of living systems is composed of water, the vast majority of radiation-induced damage from medical irradiation is mediated through indirect action on water molecules. The absorption of radiation by a water molecule results in an ion pair (H_2O^+ & H_2O^-). The H_2O^+ ion is produced by the ionization of H_2O, whereas the H_2O^- ion is produced via capture of a free electron by a water molecule as shown below (Eq.1 and Eq.2). These ions are very unstable; each detaches to form another ion and a free radical, which is symbolized by a dot on the right-hand side of the chemical symbol [26]:

$$\mathbf{H_2O^+ \rightarrow H^+ + OH^{\cdot}} \qquad (1)$$

$$\mathbf{H_2O^-} \rightarrow \mathbf{H^{\cdot}} + \mathbf{OH^-} \qquad (2)$$

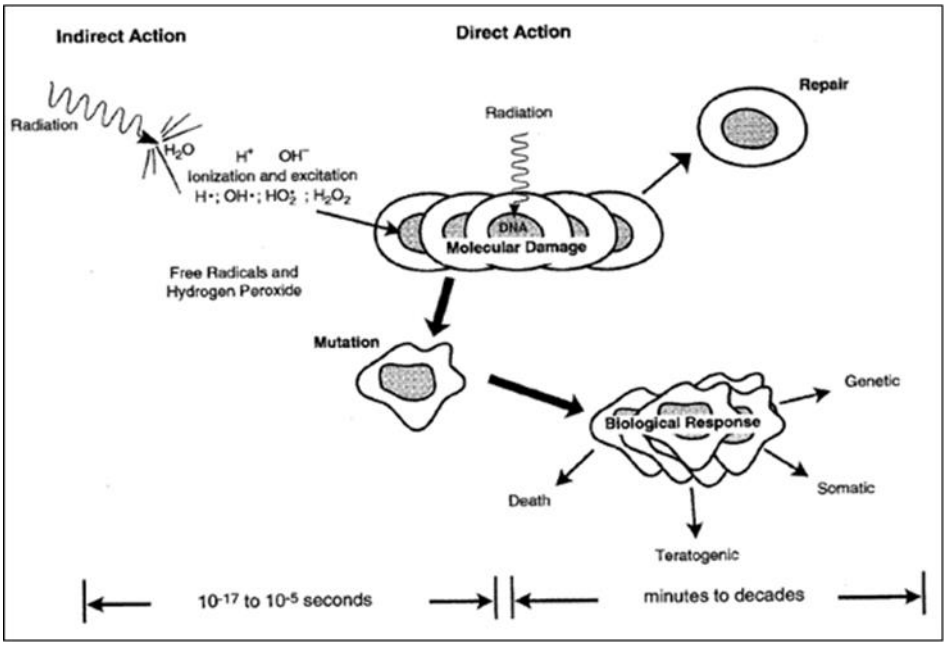

Figure 1: Physical and Biological response to ionizing radiation [26]

Free radicals may inactivate cellular mechanisms directly or via damage to genetic material, specifically DNA and RNA, when they are the primary cause of biological damage from low linear energy transfer (LET) radiation [26]. Most of the time damage to the DNA caused by radiation is repaired by specialized molecular mechanisms or the cell dies, but sometimes the affected cell may survive with a mutation in its genetic code. This mutated cell could possibly cause unregulated cell division, which could lead to a cancerous tumor. In case of the living cells irradiated with high amount of radiation doses, the damage to these cells will be high. When a sufficient number of cells are killed, tissue reactions such as erythema (reddening of the skin), epilation (hair loss), cataracts and infertility may occur [26, 27].

Organs and tissues are distributed differently and are more susceptible to radiation during childhood. Propagation of cellular and subcellular levels during growth periods is likely to be associated with increased susceptibility. Because of

longer life expectancy for children the possibility for tumor to develop is manifest while they are alive. On the other hand, adult patients may have died from other causes before the manifestation of induced cancers [4].

The biological effects of radiation can be grouped into two types: stochastic effects (cancer and heritable effects) and deterministic effects (tissue reactions) [1].

1.3.1 Stochastic: this term is defined as an affect that increases in probability in proportion to dose, while their severity is independent of dose level [25]. Stochastic effects do not require a threshold dose to occur even at very low dose levels. There is always a chance that the radiation dose received might cause the disease or effect. It is the primarily concern in a diagnostic radiology department. They are generally associated with low level radiation and usually follow a linear, non-threshold response curve [25].

Most late effects are stochastic in nature which takes many months or years to become revealed. These include congenital (birth) defects, life-span shortening, cataracts and various cancers [25].

1.3.2 Deterministic also called non-stochastic effects are those which increase in severity with increasing dose above a certain threshold level. The severity of the disease or effect is a function of an increasing number of cells which have been damaged [25]. Deterministic effects occur only as a consequence of large doses of radiation, such of that might be received in a radiation therapy department. Moreover, radiation levels from extended C-Arm fluoroscopy procedures or extended angiographic fluoroscopy can be high enough to cause deterministic effects [25].

Deterministic are early effect which are revealed within a short period of time (hours, days, few weeks or months) after radiation exposure. Most early effects are somatic (affecting the organism itself but not its offspring), and deterministic. They tend to follow a nonlinear, threshold response curve. Examples of deterministic effects include most early effects of radiation such as decreased blood cell counts, erythema, epilation, fibrosis, atrophy or sterility [25]. The following Figure (2) is an example of a deterministic effect (skin injury from interventional cardiac procedure) and the overall dose-time relationships for several tissue reactions are shown graphically in Figure (3) [28].

Figure 2 : Deterministic effect at 18–21 months after procedure [28]

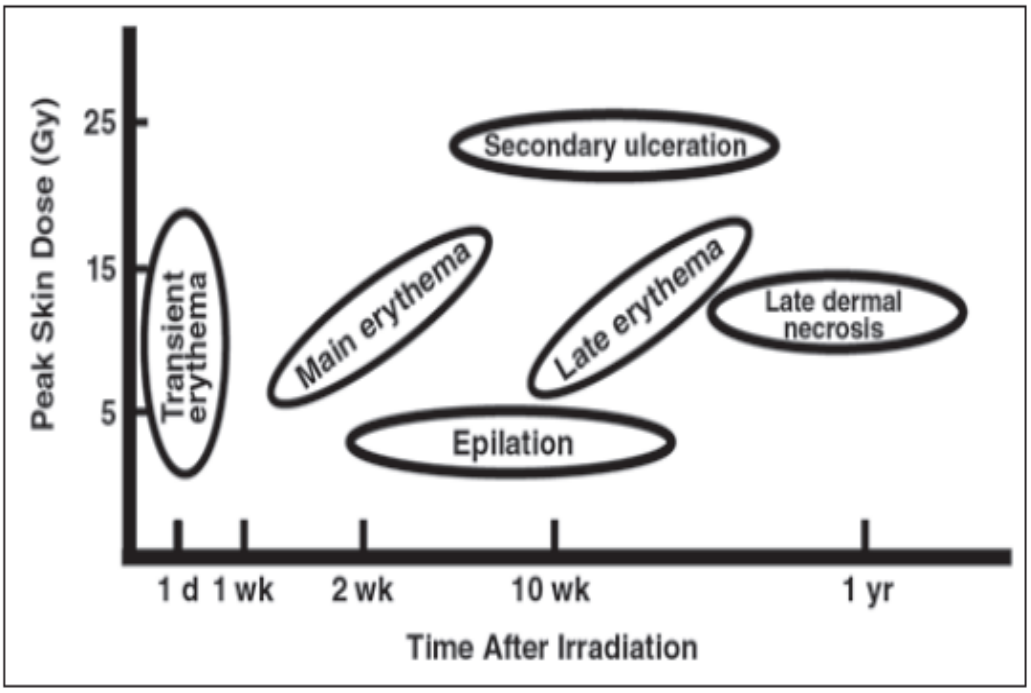

Figure 3: Tissue skin reaction as a function of dose and time in the fluoroscopy guided procedure [28]

1.4 Basic Concepts of Radiation Protection (Quantities and Units)

1.4.1 Average absorbed dose in organs

Several quantities are used to quantify the magnitude of the exposure to the patient in diagnostic radiology such as entrance surface dose (ESD), entrance surface air kerma (ESAK) and kerma area product (KAP) [17]. The averaged absorbed dose is the energy deposited in the organ divided by the mass of that organ. It represents the basic physical quantity that can be correlated with the stochastic or the deterministic effects [1].

The SI unit for absorbed dose is joule per kilogram (J/kg) and its commonly known as the Gray (Gy). The average absorbed dose is given by the following equation (Eq.3):

$$\mathbf{D_T} = \frac{\varepsilon_T}{m_T} \qquad (3)$$

Where ε_T is the energy imparted to the organ or tissue over the mass m_T of that organ or tissue [4].

1.4.2 Equivalent dose

The equivalent dose H_T to an organ or tissue T is used to describe the effects of different radiation types in causing stochastic effects [4]. It is recommended by the ICRP for risk–benefit assessment as shown below (Eq.4). It is equal to the product of a radiation weighting factor w_R for the type of radiation R as show in Table 1 and the organ dose D_T:

$$\mathbf{H_T} = \mathbf{w_R}\, \mathbf{D_T} \qquad (4)$$

The SI unit of the dose equivalent is the Sievert (Sv).

Table 1: Radiation weighting factor for different radiation type [15]

Radiation Type	**Radiation weighting factor (w_R)**
B, γ and X-rays	1
Electrons and muons	1
Protons and charged pions	2
Alpha particles, fission fragments, heavy ions	20

1.4.3 Effective dose

Effective dose (E) was first introduced by the ICRP in Publication 60 [19] and revised in the ICRP 113 [35]. It is defined as the sum of over all of the body

organs and tissues, which are the product of the equivalent dose H_T of organ or tissue and the tissue weighting factor w_T for that organ or tissue [18]:

$$\mathbf{E} = \sum \mathbf{w_T}\, \mathbf{H_T} \qquad (5)$$

This quantity measures the combined detriment from stochastic effects for all organs and tissues on the basis of mean doses to a reference person. Also, it is used for the comparison of the risk related dose burdens from different types of diagnostic procedure, or in inter-comparison of procedures performed in different hospitals or countries [18]. The tissue weighting factors w_T are shown in Table 2 taking into account variations in radiation sensitivity between organs.

Table 2: Tissue weighting factors [18]

Tissue or organ	**Tissue weight factor w_T**	$\sum w_T$
Bone marrow, colon, lung, stomach, breast, remainder tissues	0.12	0.72
Gonads	0.08	0.08
Urinary bladder, esophagus, liver, thyroid	0.04	0.16
Bone surface, brain, salivary glands, skin	0.01	0.04

The SI unit for effective dose is similar to the equivalent dose Sievert (Sv). To avoid misinterpretation of the dose value, the dose quantity (i.e. equivalent dose or effective dose) should always be clearly stated [18].

In paediatric imaging, it should be recognized that the relative tissue weighting for organs may not be appropriate for paediatric patients as it is shown below (Figure (4)). The organ and tissue radiosensitivity depend on the age and gender; however, the effective dose does not accurately reflect that. Instead, the

equivalent dose does not depend on the tissue weighting factors and, thus, it is more dosimetric than effective dose [18].

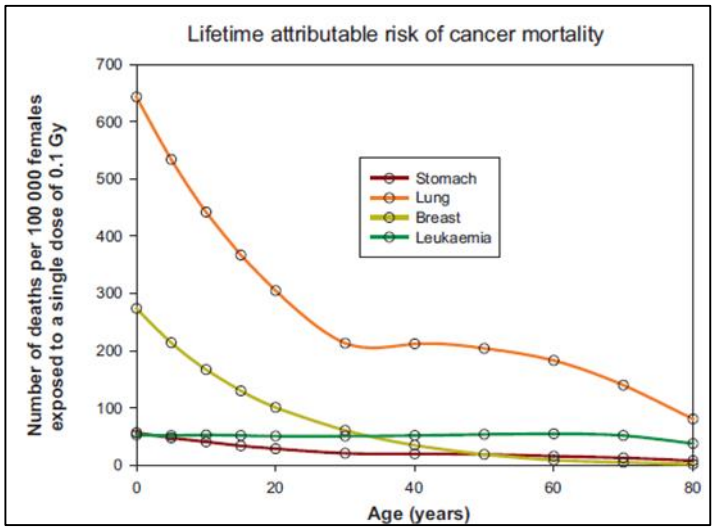

Figure 4: Lifetime attributable risk of cancer mortality in females for irradiation of single selected organs [18]

1.4.4 Risk assessment

The assessment of the risk associated with stochastic health effects of x- ray procedures can be performed to assess the mean organ doses and applying an appropriate risk coefficients. Mean organ doses can be assessed using Monte Carlo simulations [21]. Monte Carlo software program (PCXMC 2.0) is an easy method for calculating patient organ doses and effective doses in medical x-ray examinations. It was developed by the Finnish Nuclear and Safety Authority (Stuk, Helsinki, Finland). The effective radiation dose was calculated based on the current tissue weighing factors of the ICRP publication 103 and old tissue weighting factor of the ICRP publication 60 [22].

The Monte Carlo calculation of photon transport is based on stochastic mathematical simulation of interactions between photons and matter. Photons are

emitted (in a fictitious mathematical sense) from an isotropic point source into the solid angle specified by the focal distance and the x-ray field dimensions. It is followed by random interactions with the phantom according to the probability distributions of the physical processes that may undergo, such as the photo-electric absorption, coherent (Rayleigh) scattering or incoherent (Compton) scattering. At each interaction point the energy deposition to the organ at that position is calculated and stored for dose calculation and the maximum photon energy used is up to 150 keV [24].

A large number of independent random photon histories are generated and estimated the mean values of the energy depositions in the various organs of the phantom used for calculating the dose in these organs [23].

In PCXMC simulation anatomical data based on the mathematical hermaphrodite phantom models of Cristy and Eckerman (1987) was used to describe patients of six different age groups: newborn (0), 1, 5, 10, 15-year-old and adult patients [23], as shown in Figure 5.

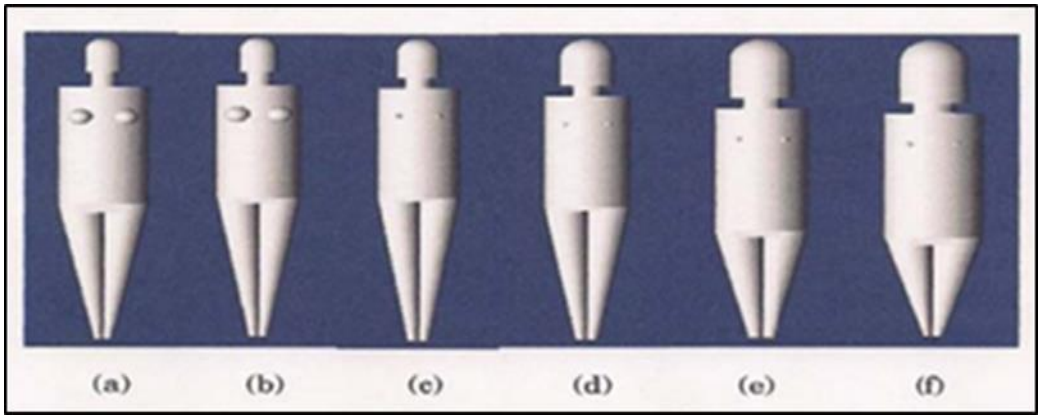

Figure 5: (a) adult phantom,(b) 15-year old phantom, (c) 10-year old phantom, (d) 5-year old phantom,(e) 1-year old phantom & (f) new born phantom [23].

The PCXMC 2.0 software calculation depends on the amount of radiation to be as an input [23]:

1- Entrance exposure free in air without backscatter with unit of (milliRontegen**)** mR.
2- Air-kerma-area product with unit of ($mGy.cm^2$) or Dose-area product ($R \cdot cm^2$).
3- If the previous information is not available, the program is able to estimate the incident air kerma from x-ray tube current-time product (mAs) and other parameters such as the x-ray tube voltage (kVp), the total filtration in the radiation beam and the distance from the x-ray tube focal spot to the patient's skin (FSD).

Due to the fact that the mathematical phantoms refer to a reference man/baby, these assessments cannot be applied to a specific patient.

1.5 Radiological Protection in Paediatric Diagnostic Imaging

The general radiological protection principle has been recommended by the ICRP 103 to be use in any ionizing examination [1]. The responsibility to monitor the basis of radiation protection in paediatric radiology is usually extended from the level of hospital administration to the operational level [18]. The pillars of patient radiation protection in diagnostic radiology are explained below.

1.5.1 Justification of diagnostic radiology procedures

The ICRP states that the principle of justifying any decision that alters the radiation exposure situation should be more beneficial and less harmful [4]. Justification is considered one of the most critical steps in medical radiation protection as stated by the European Society of Radiology (ESR) [16]. Many

researchers show the deficit in knowledge about diagnostic imaging risks among medical professionals, both referring doctors and radiological staff. Hence, the biological impact of the examination must be clear for the referring clinicians and radiologist, whereas the justification implies that the necessary results cannot be achieved with other methods that would pose a lower risk for the patient [1, 16]. Moreover, it is very important that the radiological examination is indicated for paediatric patients where the examination request shall include the clinical information and signed by the referring clinician before the examination performed. Justification includes three main levels [30].

a) General justification of the practice by weighing the diagnostic or therapeutic benefit against the radiation risk taking into account the availability of alternative modality that does not involve ionizing radiation.
b) Generic justification of clinical procedure done by the health authority in cooperation with appropriate professional bodies should be updated frequently bearing in mind the advances in knowledge and technological developments.
c) Individual justification for patients carried out through consultation between the radiologist and the referral paediatricians. The patient's request shall be appropriate wherein it should include the history of the patient's clinical situation, previous radiological procedure, the urgencies for this radiological procedure and the characteristic of radiological exposure.

The implementation of the justification principle is mainly achieved through the Referral Guideline for each patient in the diagnostic radiology.

1.5.2 Optimization of radiological protection

Once examinations are justified, they are required to be optimized (performed at a lower dose while maintaining efficiency and accuracy) [4]. The basic aim of the optimization is adhering to principle of (as low as reasonably achievable) ALARA for each radiological procedure [1, 16]. Optimization of patient's examinations includes three main aspects [1]. First, the radiological equipment should work properly, delivering the appropriate exposures and compliant with established standards of installation and performance during the installation time and after the routine use.

Second, the adequate selection of technical imaging parameters to optimize the radiation exposure level according to the size of the child should be considered carefully. Third, implementation of diagnostic reference levels (DRLs) to ensure patient safety.

1.5.2.1 Diagnostic reference levels (DRL)

The guidance level for radiological imaging has been recommended by international organizations and ICRP as a mean of patient dose reduction and tool of optimization. A DRL value is advisable for investigation if the dose value exceeds the regulatory value but it is not a dose limit for patient undergoing medical exposure. The concept of DRL is applied to dose quantity (e.g. incident air kerma, entrance surface air kerma and kerma area product, etc.) [1,4]. The upper DRL is taken as the high level of radiation dose for the patient (third quartile value of dose distribution obtained in the survey) and ICRP does not specify the quantity. Yet it

should meet the needs of respective area of the local bodies where it is considered as a national task [1].

There are many studies worldwide on this subject for paediatric patients in different diagnostic medical procedures [6, 7, 8, 9, 10, 11, 17]. This thesis contributes to setting out and establishing the DRL for paediatric patients who undergo diagnostic procedures in conventional radiology and IC, in Dubai hospital (member of Dubai Health Authority-DHA). DRLs value can be expected to change over time due to both technological advances and increased optimization [18].

A new approach for optimization procedures, which is similar to DRLs concept, is introduced at the beginning of 2015. It states that the hospital should adapt acceptable quality dose (AQD) for their own needs. The AQD is based primarily on the image quality and secondary on the radiation dose governing all age groups. The DRL is known as a good tool in previous years but it does not reflect the optimum performance [31].

1.5.2.2 Patient dosimetry through Digital Imaging and Communications in Medicine (DICOM) structures

X-ray equipment can provide the parameters which are related to patient doses displayed on the equipment console and also stored in Digital Imaging and Communications in Medicine (DICOM) structures [18]. As an example for these parameters in modern digital x-ray machines, the air kerma area product, $P_{KA,}$ is recorded within the DICOM header which can be used to estimate the entrance surface air kerma, K_e [18]. Hence, the dosimetric data could be used for dose audit purposes but it has to be kept in mind that there are differences between the manufactures of the x-ray systems regarding the dosimetric information in the

DICOM header. Additionally, the units of some dosimetric quantities vary between different x-ray manufactures. Therefore, the calibration factor for these quantities should be verified by local medical physicists before starting the patient dose audit where the auditing considers one of the patient optimization tools [1, 29].

1.6 Purpose and Structure of the Thesis

Our region is developed fast in radiation medical imaging and there is a lack of complete information on paediatric dosimetry that has been reported and stated worldwide in general and in particular in the UAE. This project will contribute in highlighting radiology radiation doses levels for the paediatric patients group in Dubai Health Authority (DHA) - Dubai Hospital, and will help to set up local DRLs. Moreover, it will fulfil the radiation safety requirements set by the Federal Authority for Nuclear Regulations (FANR) in UAE.

In Dubai hospital, the radiological procedures of paediatric patient are performed in a mixed environment with the adult's patients. This project aims at evaluating the radiation safety practices, the radiation exposure level for this group of patients and to estimate the radiation risk associated with the different diagnostic procedures. Moreover, endorse the paediatric DRLs, and to provide new data on patient doses for optimization purposes in diagnostic radiology. The diagnostic modalities which were evaluated in this thesis includes: conventional radiology (fixed x-ray unit and the mobile x-ray unit which dedicated to the premature and newborn patients in the neonatal intensive care unit (NICU)) and the interventional cardiology (IC) the catheterization laboratory (Cath lab). The thesis provides information on the paediatric examination protocols, ESD or ESAK and KAP for

different paediatric age groups. The paediatric patients were classified according to the age: newborn (0-1m), > 1m-1y, >1y-5y, >5y-10y and >10y-15y.

This thesis falls into six chapters:

1. The introductory chapter concerns with the patient safety in diagnostic radiology and the paediatric dosimetry reflecting the literature surveys as well as pointing out the international organizations finding in this field.
2. Chapter two includes the literature review, focusing on the findings of the other researchers in the paediatric radiation levels in conventional radiology, NICU and IC.
3. Chapter three demonstrates the implementation of the IAEA TRS 457 and IAEA safety series No.24 in measuring the paediatric radiation dose.
4. Chapter four illustrates the results of this study compared to the finding of other researches.
5. Chapter five contains the discussion on the results.
6. Then, the thesis ends up with a conclusion highlighting the summary of overall results.

Chapter 2: Literature Review

There is growing concerns about the paediatric radiation exposure levels in diagnostic radiology. Moreover, medical imaging developments have an impact on increasing the radiation exposure levels to the paediatric patients because of the wide spread and easy use of radiology digital systems. Radiation has been long known for it is harmfulness to the human. The risk of diagnostic radiology can be either stochastic or deterministic depends upon the radiation dose to individual organs or tissues [3,16]. As a consequence, international organizations such as ICRP have managed to introduce recommendations and advices as a framework for radiation protection to reduce this concern [15, 33, 34, 35].

In order to apply these recommendations, it is essential to understand the factors that affect the radiation exposure to be able to evaluate the paediatric doses in different diagnostic radiology modalities. Patient dose has often been described by the ESD or ESAK where it is measured in the center of the x-ray beam. ESD/ESAK is measured directly using Thermo luminescence Dosimeter (TLD) placed on the skin of the patient where the backscatter radiation is already included during the measurements or indirectly from the measurements of KAP which is fitted in the x-ray tube. It is important to remember that the KAP measurement represents the total energy incident on the patient (accumulated air kerma) and the planes of measurement do not include a significant contribution from backscattered radiation from the patient or phantom; the backscatter factor should be used to calculate the ESD [44]. Moreover, the ESD can be calculated from the x-ray tube output and the

exposure parameter where the IAK will be measured first using ionization or solid state detectors then it will be multiplied by an appropriate backscatter factor.

The diagnostic modalities included in this thesis were: Digital fixed x-ray machine, digital mobile x-ray machine for general radiology imaging and fluoroscopy machine equipped with flat panel detector for the interventional procedures. This chapter illustrates other countries experience on evaluating the radiation dose to the paediatric patient in the diagnostic radiology and their recommendations.

2.1 Paediatric Radiation Dose in General Radiography

Several surveys on radiation doses to paediatric patients have been conducted in UK under the umbrella of National Radiological Protection Board (NRPB)*. They started with adult dose in 1985 then within a five-year span they reviewed the national patient dose data and analyzed the information collected. Each study was focusing on different type of radiological examination. Survey was carried out from 1996-2000 and published in 2002. While the other surveys were carried out from 2001-2006 published in 2007 including the paediatric groups [36,37]. These surveys include the radiation dose for three common radiographic and fluoroscopic procedures for five age groups: newborn, 1, 5, 10 and 15 years. It is found that the radiation doses received by paediatric patient increases with increasing age [38]. The initial data of previous surveys was not harmonized, as consequent, Smans K. et al., (2008) [41] conducts other surveys requesting both data and information on the

* The Health Protection Agency Act 2004 repealed the Radiological Protection Act. On 1 April 2005, NRPB became the Radiation Protection Division of the Health Protection Agency (HPA).

applied dose measurement methodology and protocols, 13 countries responded to this survey. The dose data includes the measurements for both the ESD and KAP for three examinations (chest, abdomen and pelvis) for the following age groups: <1 y, 1–2 y, 2–3 y, 3–8 y, 8–12 y and >12 y. This survey shows that there was a clear need for standardization if data from several centers are to be combined in a single DRL. Future studies should include evaluation of image quality beside the dose measurements and data collection would be straightforward and systematic through DICOM headers for digital images.

A study was performed by Emmanuel N. et al., (2007) [39], using 289 TLDs to evaluate the ESD and the effective dose (E) for the common radiological examination at two dedicated paediatric hospital in Greece. The examination were: chest AP/PA*, skull AP/LAT**, pelvis AP/LAT, lumber spin AP/LAT and full spin AP/LAT. Their ESD results were higher than DRLs proposed by the NRPB-R318 and European Commission (EC). The main reason responsible for the high ESD observed in certain cases were: the use of low tube potentials, the absence of additional filtration for chest radiography, the routine use of the grid and the worst among all is the use of fluoroscopy for positioning. They found that a lot of work has to be done in order to achieve optimization of the radiological techniques in close cooperation of medical physicists with both radiologists and radiographer.

Other study was performed on Sudan by Suliman et al., (2008) [40] to determine the radiation doses to 459 patients from common paediatric x-ray examinations in three hospitals in Khartoum state. ESD was determined from exposure settings using DosCal

* PA= Posterior anterior projection, AP= Anterior posterior projection

** LAT = Lateral projection

software for chest, skull, abdomen and pelvis. DosCal software developed by the radiological protection center of Saint George' Hospital, London. The x-ray tube outputs, in mGy (mA s)$^{-1}$ were measured using Unfors Xi dosimeter and the other parameter such as the patient demographic information and exposure parameters were entered to the software to calculate the ESD. Their study showed that there is a statistically significant correlation between patient dose and size and there is no significant difference in correlation when patient size is expressed in age or weight. Also, the ESD for the newborns and 1y old patients were higher than the other published results due to the use of x-ray generator (single phase) in one of the hospitals, filtration and the use of grid with younger children.

In order to establish an initial national DRL for paediatric dose in Sudan (Khartoum state), a survey on 2013 were conducted by Suliman et al., [7] in seven hospitals to evaluate the radiation dose delivered to patients in chest x-ray examinations in general radiology. Data were collected using specially prepared forms. The radiographers were requested to collect the information on the actual exposure parameter used for children of different age group: 0, 1, 5, 10 and 15 y. The patient doses were measured in terms of the ESAK using the Unfors Xi dose-rate meter. The results shows that the values of the ESAK measured are close to the UK reference doses and doses reported in similar studies for children aged, 5 y, while for children aged 10-15 were higher. This is due to use of 3-phase 12-pulse generator and high tube output compared to the remaining units. They recommended that frequent dose measurements are important for the optimization of x-ray examination for paediatric patient.

L.A. Ribeiro et al., (2008) [42] carried out a survey on paediatric dose in radiological examinations in paediatric hospital of the city of Sao Paulo, Brazil, using the TLD attached to the skin of the children to measure the ESD. Moreover, a phantom was used to represent the younger children to obtain the ESD because of used of small tube potential and the TLD will not read small doses and it can make an artifact on the image. The results showed that the majority of paediatric patients are below 4 years, and that about 80% of the examinations correspond to chest projections. Four kinds of paediatric examinations were investigated: three conventional examinations (chest, skull and abdomen) and a fluoroscopic procedure (barium swallow). The results presented in this survey showed that it is necessary to investigate the technical parameters to perform the radiographs, to introduce practices to control paediatric patient's doses and to improve the staff skills in performing paediatric examinations wherein the technical parameters showed wide variation in kVp and mAs chosen, giving rise to large dose intervals.

In order to establish national DRL in Austria, Billinger et al., (2010) [10], conducted a survey between September 2006 and September 2007 to determine radiation doses to paediatrics in x-ray examinations including: chest, skull AP/PA/LAT and abdomen. Among 91 hospitals, 14 hospitals were participated in this survey. The paediatric were classified into: newborns, 1, 5, 10 and 15 year olds. DRL was taken as third quartile values in term of IAK, ESAK and KAP were presented. The Data collection includes the patient demographic information, exposure factors and KAP reading if available. The IAK values were calculated from reported data using tube output measurements performed for all x-ray units. According to this study calculating IAK from the exposure factor is replacing the use

of TLDs in diagnostic radiology. The ESAK and KAP results of this study were compare to European, British and German reference values. The Austrian DRLs was provided in term of IAK and KAP values.

In Ireland, K. Matthews et al., (2013) [43], conducted a nationwide survey including 18 hospitals to investigated the common paediatric radiography examinations and the possible approach for improvement. The radiological examinations studied were chest, mobile chest, pelvis, skull, abdomen, lumbar spine and full supine. Forms were distributed among the hospital radiographic rooms including the following information: referral information, technique factors and dose data (KAP) reading, along with patient demographics such as weight and age. This approach was followed in order to evaluate the justification practice, radiation dose level, DRLs and if there is any possibility for optimization improvement. They found that their DAP reading is comparable with other published data and the justification was followed for the paediatric patient but always there is a room for more optimization. Furthermore, they were highlighting the fundamental role of the radiographer in ensuring that the principle of optimization is achieved where most of the optimization factor is under the radiographer control.

2.2 Neonatal Radiation Dose in the Intensive Care Unit

A study was performed by Brindhaban and Al-Khalifah (2004) [45], to determine the ESD and effective dose (E) to premature infants at three neonatal intensive care units in Kuwait. Three x-ray examinations were involving the abdominal, chest and skull x- rays using a simple water phantom equivalent to a premature infant and ionization chamber, exposed under the clinical condition. Computer program Child Dose was used to calculate the E. This program uses

NRPB-R279 and NRPB-SR279 data files for calculation. Among the three NIC units there were a variation on ESD values and E-values; this was direct to the variation of the quality in the half value layer (HVL) for each x-ray beam. Their study results were comparable with other studies that perform same method in using the ionization chamber or TLD. They recommended increasing the filtration and tube voltage for more dose reduction. The use of computed radiography (CR) machines instead of screen film was recommended to be investigated for the neonates.

A survey carried out by Donadieu et al., (2006) [49], on the number of examinations performed on prematurely born children in a large French hospital. The doses received by the infants, the ESD and E were calculated by the PCXMC software program. The Cumulative effective dose (CED) was calculated by taking into account the number and types of examinations performed during the NICU stay. The median number of radiographs per patient was 10.6 (range: 0 – 95) and the median CED equivalent was 138 µSv (range: 0 – 1450 µSv). Factors that influenced the CED were: age, weight, intensity of medical management and its monitoring and clinical condition of the patient. The more sick the patient, the more radiographer examinations he/she will undergo.

Şorop and Dãdulescu (2009) [11], describes the distribution, frequency of radiological examinations and estimate the ESD using the technical parameter for chest and combined chest abdomen radiological examinations for the newborn babies within an intensive care unit (ICU). The issue is not the ESD for one single exposure, but the repeated examinations during the child's hospitalization period, leading to cumulative doses and it is likely that many others may be added during childhood. The average values of ESD were higher than the other reference levels; this is due to

use of screen film technology and the type of the x-ray generator. The medical staff awareness on the means and methods of patient's protection, levels of irradiation child may be exposed, and the risks may occur by repeating such exposures are highly recommended. Working protocols should be developed at the hospital level to improve the optimization.

A survey was conducted by Frayre et al., (2012) [46], General Hospital of Mexico City to evaluate the level of radiation exposure received by neonate in NICU from chest x-rays. The quantum noise level is also taken in account to not affect the diagnostic image quality. TLDs were used to measure the ESD and placed in position that not affecting the radiographic image. CR digital radiography was used for chest examination and the study involved 208 chest x-rays of 12 neonates admitted and treated in NICU. ESD values for chest x-rays are higher than the DRL of 50 mGy proposed by the NRPB. Then, optimum ESD was estimated for additional 20 chest x-rays by increasing kVp and reducing mAs until quantum noise affects image quality and the results was below the NRPB value. They found that chest x-rays in neonates are safe when used with care, but it is necessary that radiologists, paediatricians and x-ray technologists to be trained in radiation protection in patients and biological effects of x-rays to minimize the radiation risks.

In Belgium, Jeremie Dabin et al., (2013) [47], conducted a nation survey including seventeen NICU to investigate the radiation exposure of premature newborns. Two examinations were evaluated, chest and combined chest-abdomen. The ESAK were calculated form the tube output measurements and exposure parameter while KAP were available on machine console for recording. The organ doses were calculated with PCXMC. They found that their ESAK results were less

than NRPB and EC values. Their ESAK DRL is also comparable to NRPB reference doses and lower than EC values. The lower dose was for the chest examination but they highlighted the cumulative dose received could be high and should be considered by the medical practitioners. The wide variation in radiographer doses attributed to the different technical settings used among the radiographer in hospitals. Hence, the practice should be harmonized and the principle of DRL should be applied to achieve the optimization.

Alzimami et al., (2014) [48], conducted a survey for 135 neonates to evaluate the patient ESD, organ dose and effective dose for neonates in the special care baby unit (SCBU) up to 28 days after birth in Kingdom of Saudi Arabia (KSA) at Omduran Maternity hospital. ESDs were calculated from patient exposure parameters and tube output measurement using DosCal software. The tube output measured by using Unfors Xi dosimeter, E was calculated using software from the NRPB. The radiation dose in this study was higher compared to other studies. This can be attributed to the machine filtration and exposure factors where a wide variation occur due to patient weight, tube voltage and tube current time product. They found also that mathematical equations provide accurate results of ESD which can be used in the absence of other passive or active dosimeters.

2.3 Paediatric Radiation Dose in the Interventional Cardiology

A study was carried in the largest Cardiac Centre in Greece by Tsapaki et al., (2008) [50], in the period from January to March, to investigate paediatric doses in coronary angiography (CA) and percutaneous transluminal coronary angioplasty (PTCA). The clinical and technical data were collected for 40 patients including patient weight, height, age, fluoroscopy time (FT), total number of images (N) and

KAP. The x-ray machine with which the paediatric IC procedures were performed was a Philips Integris Allura 9. The investigation of age distribution revealed that 25% were, <1 y old (Group 1), 37.5% were 1–10 y old (Group 2) and the remaining 37.5% were > 10 y (Group 3). The results showed that CA and PTCA were performed in all age groups had no linear relationship between KAP and the main clinical and technical parameters that would give straight forward conclusions. This could be partially attributed to the small sample of patients and to the numerous other factors that affect the dose such as complexity of clinical case, orientation of C-arm, zoom factor, copper filtration for dose reduction and the experience of operator. Moreover they observe that as age increased, cine dose percentage decreased, whereas total radiation dose increased. Median paediatric FT and N recorded reached or even exceeded adult DRL and should be optimized. Hence, the main conclusion is that the paediatric DRL should be set.

Another survey conducted by Dragusin et al., (2008) [51], for 273 paediatric catheterizations to investigate the radiation doses delivered by flat detector fluoroscopy in Belgium. They aim to investigate the radiation exposure parameters: KAP for fluoroscopy and cine - angiography, FT, number of cine-angiographic images, calculation of E using the PCXMC software and to establish DRL. Patients divided into six age groups: A(0 –30d), B(>1– 12m), C(>1– 3y), D (>3–5y), E(>5 –10y) and F(>10–15y). The x-ray machine with which the paediatric IC procedures were performed was biplane Siemens Artis dBC system. The 75^{th} percentile of the FT for diagnostic procedures are 18 min for neonates, 11 min for Group B, 14 min for C and D, 10.5 min for E and 16.5 min for F. For therapeutic procedure FT was longer than in diagnostic procedures where the FT was found not statistically different in

relation to the various age groups. Therapeutic procedures have higher KAP values (because of longer FT and more cine-angiographic images). For therapeutic interventions, the 75th percentile of KAP values were 6.5, 9.2, 12.5, 22.2, 27 and 74.4 Gy cm^2 (group A-E). The E is higher in therapeutic than those for diagnostic procedures in all age groups. Moreover, it has been observed that the E decrease with increasing the age in diagnostic procedure for all groups and in therapeutic procedure only for the groups from A to C. This step considered as a first step in the optimization process to make full use of the dose reduction potential of flat-panel systems.

In a hospital in Sweden, Karambatsakidou et al., (2009) [53], carried out a survey to establish conversion factors (CF_S) for E in paediatric IC, and to evaluate the impact of radiation geometry and age on these factors. The x-ray machine used was biplane Philips Integris H 5000C. This study included 249 paediatric patient performed on the same x-ray equipment during a 6-year period. The patients were divided into five age groups (neonate (0), 1 y, 5 y, 10 y and 15 y) and the entrance radiation field size used was varies with age. Clinical data and examination reports containing information on cine and fluoroscopy data acquisitions were retrieved for all patients. Two methods were used to calculate the effective dose, one using data published from other researchers and the second by using the PCXMC software. There is a clear trend for increases in total KAP with increasing age where the KAP values include fluoroscopy and cine from both the frontal and lateral planes. The results of CF_s were almost same using both methods A and B, as evaluated for a subset of 52 patients and it was slightly dependence on the geometry. Moreover, it is

found that the effective dose in paediatric IC is of much greater concern than the skin dose and their results were in range of 0.2 to77.2 mSv.

McFadden et al., (2013) [52] said in his survey that there is a lack of information worldwide on radiation exposure in paediatric IC. Currently in UK, at present, there is an established national DRL for adult IC procedures but little data is available for paediatric. IC is considered the highest ionizing radiation contributors to medical exposure especially among children, which invites another study to determine the radiation dose levels in paediatric IC to establish local diagnostic reference levels (LDRL). The records of 354 paediatric patients were examined including the kerma Area Product meter along with examination details. Procedures were categorized as either diagnostic or therapeutic. Paediatric patient were divided into five age groups: newborn <1 year, 1 <5 years, 5 <10 years, 10 <15 years and ≥ 15 years. LDRLs were calculated from the mean KAP readings. The mean patient age was 2.6 years and weight was 14.9 kg. LDRL for the five age groupings were calculated as 190, 421, 582, 1289 and 1776 cGycm2, respectively. This LDRL has been proposed for paediatric IC and can be used as a standard for other hospitals to compare against their own radiation doses. Regular clinical audit should be employed to ensure that clinical practice is in line with the established LDRL.

Barnaoui et al.,(2014) [54], conducted a study to establish local reference levels (LRLs) for IC procedures frequently performed at the paediatric cardiac catheterization unit in one of paediatric hospital in France. This study covered the period between January 2010 and December 2011. They evaluated organ radiation dose and calculated conversion factors for the assessment of E. The x-ray machine used was biplane C-Arm Siemens Axiom Artis BC system. The clinical data of the

patients were collected for each producer and the dosimetric parameter (KAP, FT, and total number of cine frames [NF]) were retrieved retrospectively from automatic dose recording. The patients were < 16 years old and classified according to their weight into five groups (≤6.5, 6.5–14.5, 14.5–25.5, 25.5–43.5, and > 43.5 kg). The organ dose measurement was performed using Anthropomorphic epoxy phantom ranging from the newborn to the adolescent and TLD made of lithium fluoride (LiF) powder inserted into the predrilled holes corresponding organs of interest. Conversion factors from KAP to an E were calculated using the PCXMC 2.0 program. It is found that the KAP values increased relatively in relation to the weight increase. While FT and number of cine frames were not significantly correlated with weight. The mean effective dose for diagnostic procedure was 4.8 mSv and for the therapeutic procedure was 7.3 mSv. These values were comparable with other researcher values. Their study was the first in France in paediatric IC and concluded that in order to have better overview a national survey should be conducted.

Chapter 3: Methodology

The methodologies used in this study are based on the IAEA code of practice published at their Technical Report Series No. 457 (TRS 457) [14] and the IAEA series no. 24 [18]. It is stated that the dose measurement is made wherever possible both with phantoms and collected patient dosimetry data. Specifically, the report illustrates the code to measure the incident air kerma, K_i, in conventional x-ray and incident air kerma rate in IC. The dosimetry measurements rely on the use of polymethyl methacrylate (PMMA) slab phantom to represent the different thicknesses of paediatric patients. Furthermore, collection of relevant imaging data associated with clinical procedures is used to determine radiation dose quantities. The use of a phantom enables repeatable, standardized measurements to be made, with a rapid evaluation of results. The main purposes of these measurements are to contribute in setting local paediatric DRL and to allow for a comparison of patient dose measurements against DRLs published data worldwide. Moreover, these measurements may allow for evaluation of radiation risk assessment through Monte Carlo program PCXMC 2.0, aimed to estimate patient organ doses and the E in medical x-ray examinations.

3.1 Clinical Dose Measurement Methods in Conventional Radiography

In this part of the study, the measurements were made for two x-ray machines. The first one was the fixed digital x-ray machine (Philips, Digital Diagnostic) installed on July 2012 while the second was the mobile digital x-ray (SHIMADZU, MobileDaRt Evolution) installed on July 2014 at Dubai hospital (see both in Figure (6) and Figure (7)). The first machine is used for both adult and

paediatric examinations though the mobile one is dedicated for the neonate in the NICU.

Figure 6: Fixed Digital x-ray - Philips Digital Diagnostic

Figure 7: Mobile Digital x-ray- SHIMADZU MobileDaRt Evolution

For the fixed digital x-ray machine, five common radiological examinations were chosen for different paediatric age groups, where the age groups were classified as follow: newborn (0- 1 m), >1m – 1y, >1 -5y, >5 -10y and >10 -15y. For the first two age groups the selected common examinations were: Chest, Abdomen, combined Chest-Abdomen, Pelvis and Extremities while for the rest of the groups the following examinations were selected: Chest, Abdomen, Lat. Skull (post nasal space), Pelvis and Extremities.

The premature babies (neonates) commonly need to be treated for respiratory or digestive diseases in NICU. Thus, the most frequent requested radiological examinations in the NICU are chest, abdomen and combined chest-abdomen. For this study, combined chest-abdomen examination was selected.

The main dosimetric quantities used in conventional radiography were IAK, k_i, ESAK, k_e, and KAP, P_{KA}. Incident air kerma were measured and estimated by two procedures. The first one was performed by using PMMA phantom with different thicknesses to represent paediatric of different age groups. The second method was without phantom where the exposure factors extracted from the DICOM header. The ESAK calculated from the IAK and then executed with the application of the appropriate backscatter factor (BSF).

For each paediatric age group, it is noticed that a different field sizes were used in the clinical practices which reflects the actual differences of patient sizes. For this reason, an averaged field size for each age group was obtained from the DICOM data collection which was utilized for the phantom and free in air measurements.

Although, the data collection worksheets were distributed to the radiographers to collect the relevant clinical exposure parameters (specifically: date of examination, gender, age, weight, height, kVp, mAs, patient thickness, tube focus to table distance (d_{FTD}), tube focus to skin distance (d_{FSD}), type of examination and KAP reading) the collected data were insufficient to satisfy the requirement to establish local DRLs. Hence, the average values of kVp and mAs were obtained from the DICOM header.

3.1.1 Measurement of air kerma (with phantom) -Fixed x-ray machine

Since the machine is digital, the exposure parameters were selected automatically by the automatic exposure control (AEC). The measurements were carried out with different phantom thicknesses to represent the different age group of paediatric patients. The thickness layers chosen were based on the recommended

phantom thickness dimensions for paediatric dosimetry by IAEA document [18] as shown in Table (3).

Table 3: Recommended phantom thickness dimensions [18]

Phantom dimensions		Corresponding patient demographics		
Approximate tissue thickness[a] (cm)	Polymethyl methacrylate thickness (cm)	Approximate weight (kg)	Approximate height (cm)	Approximate age (USA)
5	5	[b]	[b]	Preterm
10	10	4.7	56	Newborn
15	15	31	138	10 years

[a] 60–70 kV with varying filtrations.
[b] Not possible to quantify.

List of equipments used:

a) Calibrated semiconductor dosimeter (Unfors Xi meter and RF detector) (See Appendix 1 and Appendix 2).

b) PMMA slabs phantom of dimension 25 cm x 25 cm and different thickness from 5 to15 cm and a Measuring tape.

Method:

1) For each phantom size and examination type, the phantom must be positioned according to the clinical protocol for that patient age group, using a vertical or table Bucky as appropriate.

2) Factors that require extra care to ensure clinical accuracy are multiple such as the use of a grid, choice of filtration, choice of focus to detector distance, and the use of AEC detectors.

3) Care must be taken to ensure that the phantom position should cover all detectors (ionization chambers) of the AEC to acquire the correct parameter.

4) The x-ray field size for the phantom measurements should be similar to the typical field size during clinical practice.
5) Measure and record the distance between the x-ray tube focus and the vertical Bucky or table Bucky, d_{FTD}.
6) Place the dosimeter in the probe holder. Care should be taken that the dosimeter placed at sufficient distance above the phantom surface and outside the AEC detectors to avoid any effect on the measurements.
7) The dosimeter should be placed as close to the central axis as possible to minimize the influence of the heel effect.
8) Measure and record the distance, d_m, between the reference point of the dosimeter and the table top.
9) To avoid large uncertainties arising from the measurement of low dose levels, expose the dosimeter for three times under AEC, and record the readings, M_1, M_2 and M_3 as well as HVL. Moreover, register the selected exposure parameters mainly: tube voltage (kVp), tube current (mAs) and displayed (indicated value) KAP reading on the monitor.

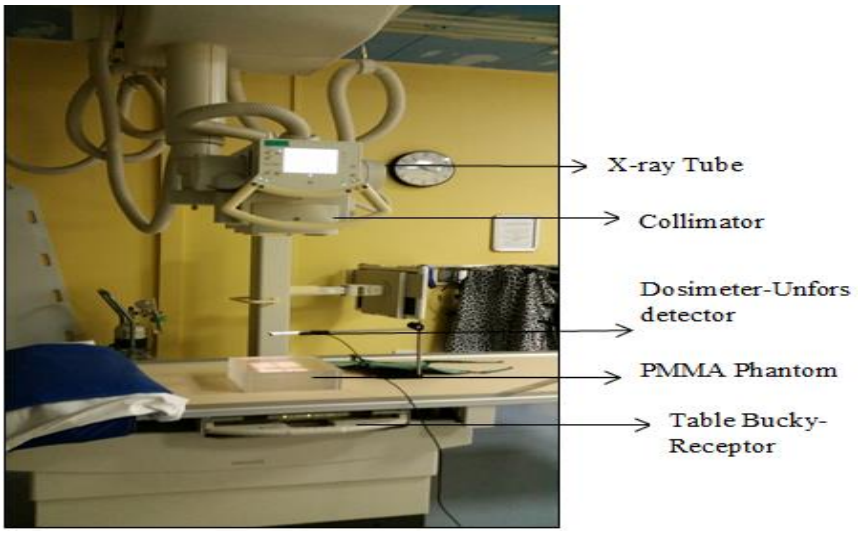

Figure 8: Phantom measurements setup - Fixed X-ray machine

3.1.2 Measurements of air kerma (without phantom) - Fixed x-ray machine

For each selected common examination, the clinical exposure parameters (kVp, mAs, filed size and KAP reading) were collected and averaged from the DICOM header for the different paediatric patient age groups. Then, exposure parameters were entered manually and the AEC detector was switched off. The same steps in section 3.1.1 were repeated but this time with phantom removed from the patient table. The results of this method is used to calculate the tube output Y (d) as shown in section 3.1.6.

Figure 9: Air kerma measurements setup- (Table Bucky)

Figure 10: Air kerma measurements setup-(Virtical Bucky)

3.1.3 Measurements of air kerma without phantom - mobile x-ray machine

According to the clinical protocol, the exposure parameters were entered manually. The air kerma values were measured free in air without using the phantom where ranges of kVp and mAs were used according to the clinical situation. Then, the same steps in section 3.1.1 were repeated. The results of this method were used for tube output Y (d) calculations as shown in section 3.1.6.

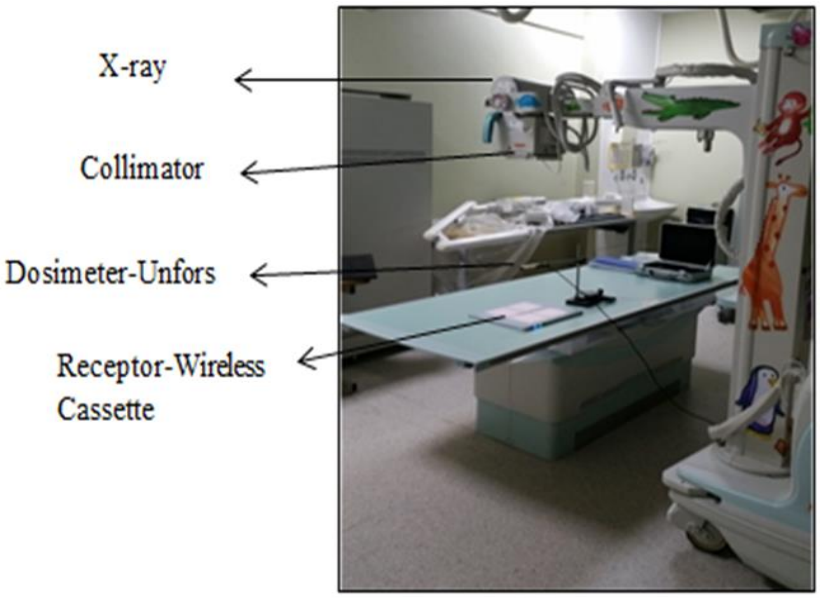

Figure 11: Air kerma measurements setup - Digital mobile x-ray

3.1.4 Calculations of incident air kerma

First the air kerma K (d) at the measurement point d_m was calculated according to the following equation:

$$\mathbf{K\,(d) = \overline{M}\,N_{K,Q_0}\;\;k_Q\,k_{TP}} \qquad (6)$$

Where $\overline{M}$ is the mean value of the dosimeter reading (M_1, M_2 and M_3);

N_{K,Q_0}: is the calibration factor of the dosimeter at beam quality Q_0;

k_Q: is the correction factor for dosimeter response at the clinical beam quality Q compared to Q_0;

k_{TP}: is the correction factor for temperature and pressure of the ionization chamber dosimeter. The values for this parameter were taken as unity for semiconductor detectors.

Then, the incident air kerma, K_i, values at the phantom position were determined using the inverse square law as shown in the following equation:

$$\mathbf{K_i \;=\; K\,(d)\,\left(\frac{d_{FTD}-d_m}{d_{FTD}-t_p}\right)^2} \qquad (7)$$

where t_p is the phantom thickness [18]. (See Appendix 3)

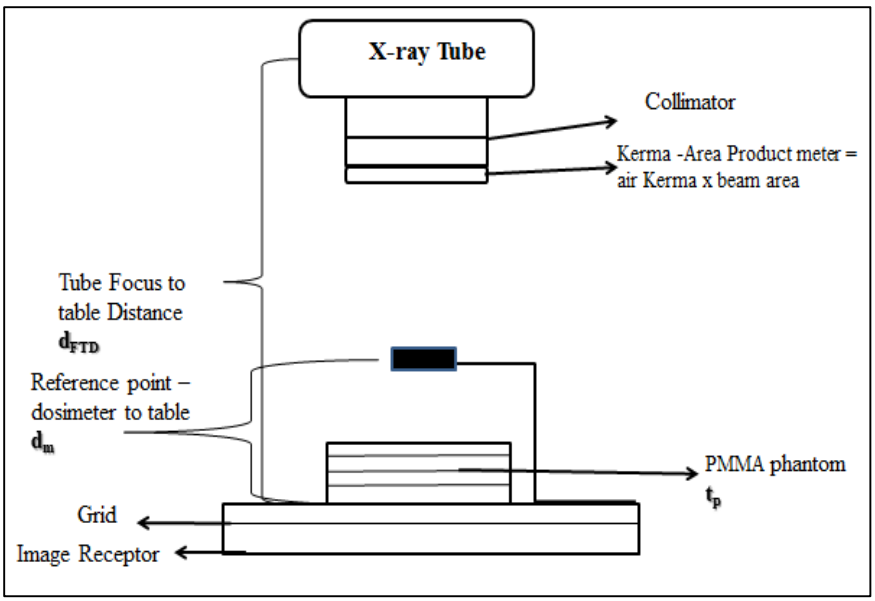

Figure 12: Schematic diagram show the required distances for air kerma measurment

3.1.5 Incident and surface air kerma for patients dosimetry

3.1.5.1 Calculation of the x-ray tube output Y (d)

The first step of this calculation was described in details in sections (3.1.2 - 3.1.4) where the air kerma was measured without phantom. The x-ray tube output, Y(d), was calculated using the following equation [18]:

$$\mathbf{Y(d)} = \frac{\mathbf{K(d)}}{\mathbf{P_{It}}} \qquad (8)$$

Where, P_{It} is the tube loading (mAs) during the exposure. The values of the x-ray tube output Y(d) were then plotted against the tube potential and the resulting curve was fitted using a power function.

Then, the incident air kerma, K_i, is estimated indirectly from the x-ray tube output Y(d) at the selected distance and exposure parameters using the inverse square law for each patient using the following formula [18]:

$$\mathbf{K_i = Y\,(d)\,P_{It}\left(\frac{d}{d_{FTD} - t_p}\right)^2} \qquad (9)$$

Where Y (d) is the x-ray tube output measured at a distance, d, from the tube focus; P_{It} is the tube loading (mAs) during the exposure of the patient;

d_{FTD} and t_P are the tube focus to patient support distance and the patient thickness, respectively.

The ESAK, K_e, is calculated based on K_i and appropriate backscatter factor (B) given in reference [14] by using the following equation:

$$\mathbf{K_e = K_i \times B} \qquad (10)$$

The selection of the backscatter factor (B) is based on the measured HVL and the field size used during the examination for each patient.

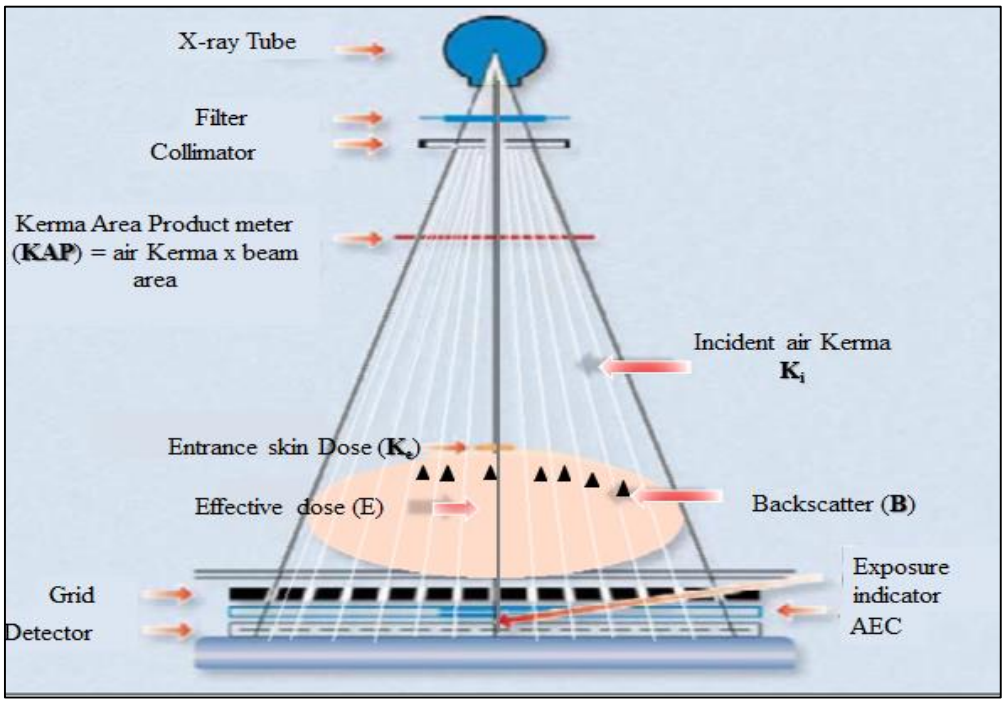

Figure 13: Typical examination beam geometry and related radiation dose quantities [20]

3.1.5.2 Calculation of entrance surface air kerma (ESAK)

The calculation of patient dosimetric value, ESAK, K_e, from incident air Kerma, K_i, is determined either by using patient exposure parameters and tube output Y(d) or derived from the displayed KAP value. To obtain the patient doses (ESAK) from the KAP value, the following steps are considered:

a) Calibration of KAP meter (see Appendix 4 and Appendix 5) and
b) Dividing the KAP value by the selected field size and then multiplied by an appropriate backscatter value.

3.2 Clinical Dose Measurement Methods in Interventional Cardiology

The IC procedures were performed using a Biplane system (Philips Allura Xper FD 10/10) equipped with flat panel detector as shown in (Figure 9). It is located in the cardiac center at Dubai hospital. The machine has three fluoroscopy mode (low, normal and high) and three fields of view (25, 20 and 15) cm. The inherent filtration in this system is 2.5 mm Al/75 and additional filtration of (1mm Al + 0.1 mm Cu) for defaulted protocol for Adult while (1mm Al + 0.4 mm Cu) for paediatric protocol. The pulse rate frequently used at pulsed fluoroscopy mode was 15 pulses/s and for cine mode was 30 pulses/s.

Focal spot to isocenter distance was 76.5 cm. The primary dosimetry quantities in the interventional cardiology are the entrance surface air Kerma rate, $\dot{\mathbf{K}}_\mathbf{e}$, and the air kerma-area product, KAP. The ESAK rate was measured with phantoms slabs, while for patient dosimetry evaluation the KAP was collected from calibrated KAP meter fitted within the x-ray tube.

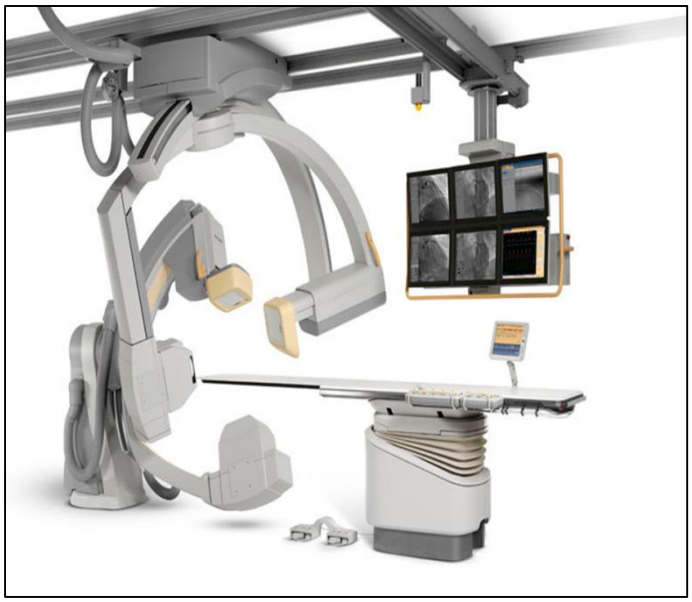

Figure 14: Biplane system - Philips Allura FD 10/10 [8]

3.2.1 Measurements with phantom

Ranges of PMMA phantom slab thicknesses were used 4.8, 7.4, 9.5, 12, 14.5 and 16.8 cm to carry out the entrance surface air kerma rate measurements. Since, the dosimeter used to measure the air kerma rate does not respond to backscattered radiation the entrance surface air kerma rate must be determined by applying an appropriate B to the measured incident air kerma rates [18]. The B values were given in Appendix VII of IAEA TRS No. 457 [14]. According to the clinical practices at Dubai hospital Cath lab, the adult default protocol was used for all paediatric patients. However, for newborn patients a paediatric protocol was used. The measurements were taken using normal fluoro mode and 25cm x-ray field size. This mode is used for the majority of acquisition runs during a coronary angiography procedure.

List of equipment:

a) Calibrated semiconductor dosimeter (Unfors Xi meter and RF detector) (See Appendix 1).
b) PMMA phantom slab thickness.
c) Measuring tape.
d) Rig to support the phantom above the detector

Method:

1) Position the phantom on the patient support resting on the rig. The space between the patient support and the phantom must be sufficient for positioning the detector between them.
2) The detector should be at the center and in contact with the phantom. The distance between the patient support and the detector was about 1 cm.
3) The distance between the exit surface of the phantom and the flat panel was 10 cm.
4) Focus to flat panel and focus to detector distances was measured and recorded.
5) The exposure parameters were selected automatically through the automatic exposure control (AEC). The default protocol was set for cardiac application where the left coronary procedure was selected as 15 frames per second (fps). For newborn patient, dedicated paediatric protocol was used.
6) The phantom was exposed under AEC. Dosimeter readings (dose rate),Ṁ, tube voltage, tube current and the flat panel setting were recorded. The measurements were repeated three times and dosimeter readings were recorded.

7) Same steps for all phantom thickness were repeated.

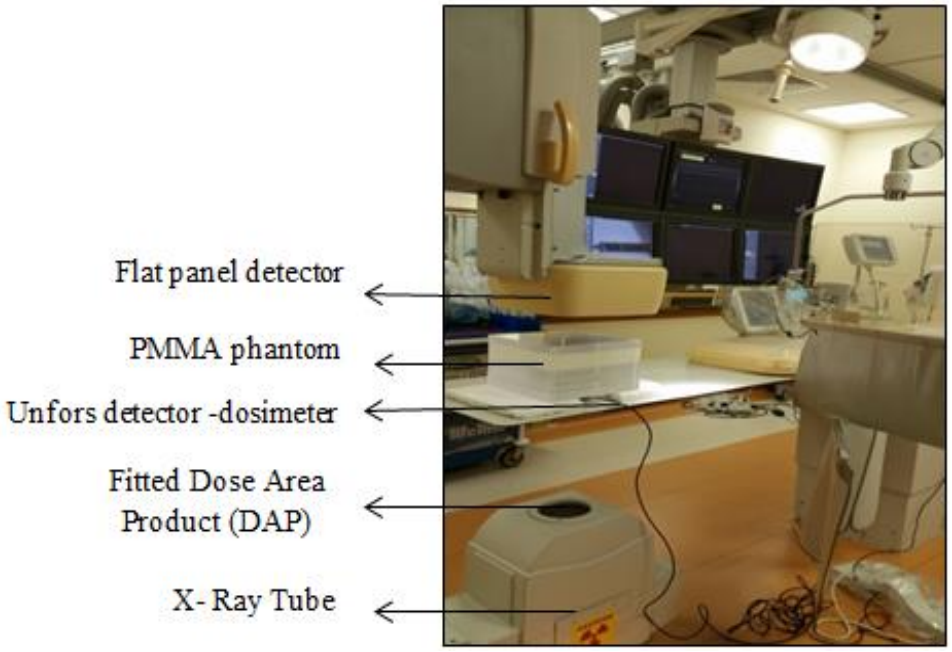

Figure 15: Cath lab - phantom measurments setup

3.2.2 Calculation of entrance surface air kerma rate

The mean dosimeter reading $\overline{\dot{M}}$ was calculated. Then the entrance surface air kerma rate, $\dot{K}_e$, calculated as follows

$$\dot{K}_e = \overline{\dot{M}}\, N_{K,Q_0}\, k_Q\, k_{TP}\, \left(\frac{B_w}{B_{PMMA}}\right) \qquad (11)$$

Where B_w and B_{PMMA} are the B for water and PMMA, respectively.

3.2.3 Verification of patient dose indicators

3.2.3.1 Kerma area product (KAP) and skin dose indicators (cumulative air kerma (CAK))

The main parameter to assess the patient dose value in the interventional cardiology is the displayed KAP reading (indicated KAP). Accordingly, the meter should be calibrated correctly and verified as described in the following steps [64]:

1) Measurements were taken free in air without the patient support.
2) It is recommended to position the dosimeter at the Interventional Reference Point (IRP) 61.5 cm from the focal spot or 15 cm below the isocenter toward the x-ray tube as illustrated in figures 11 and 12. However, in this study the Unfors detector was positioned at the level of isocentre where the bed was used to hold it. To apply these recommendations, corrections based on inverse square law should be used.
3) A proper square field size was selected to cover the sensitive part of the Unfors detector. The area of the field size at the level of detector is recommended to be about 10x10 cm^2. Since there was no tool provided to measure the field size, the beam was collimated to the size of the detector exactly which was 11 x 2.5 cm^2.
4) A Cu (1.5 mm) absorber was placed on the back of the detector to enhance the tube voltage.
5) Initial values for $(kAP_{cons})_{in}$ and $(CAK_{cons})_{in}$ displayed in console were registered. The x-ray beam was kept on for a period of time to measure the dose in a range of 30-40 mGy. Then, the final displayed values for $(KAP_{cons})_f$ and $(CAK_{cons})_f$ were recorded.
6) Measurements were repeated for at least 3 times for both fluoro and Cine mode for different fields of view.

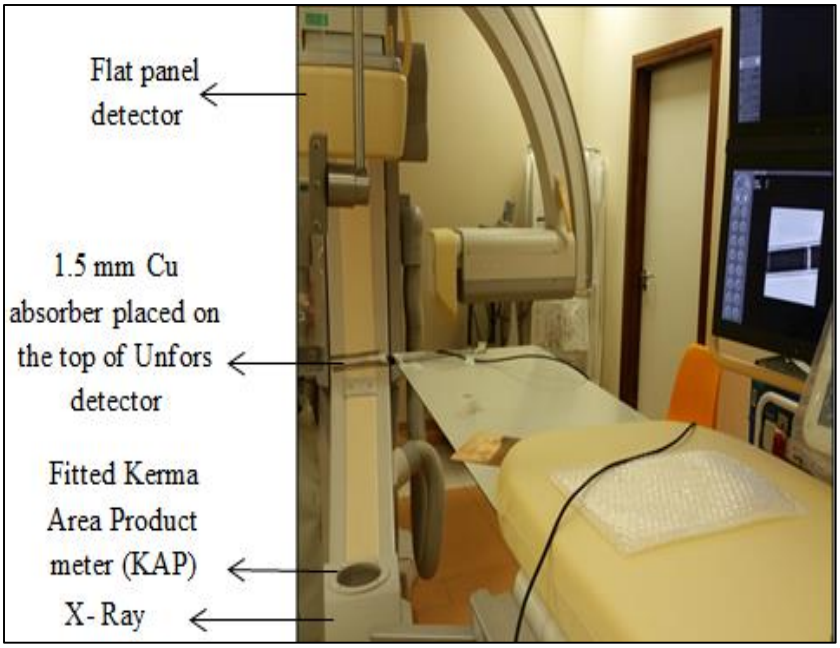

Figure 16: Verification of KAP & CAK setup

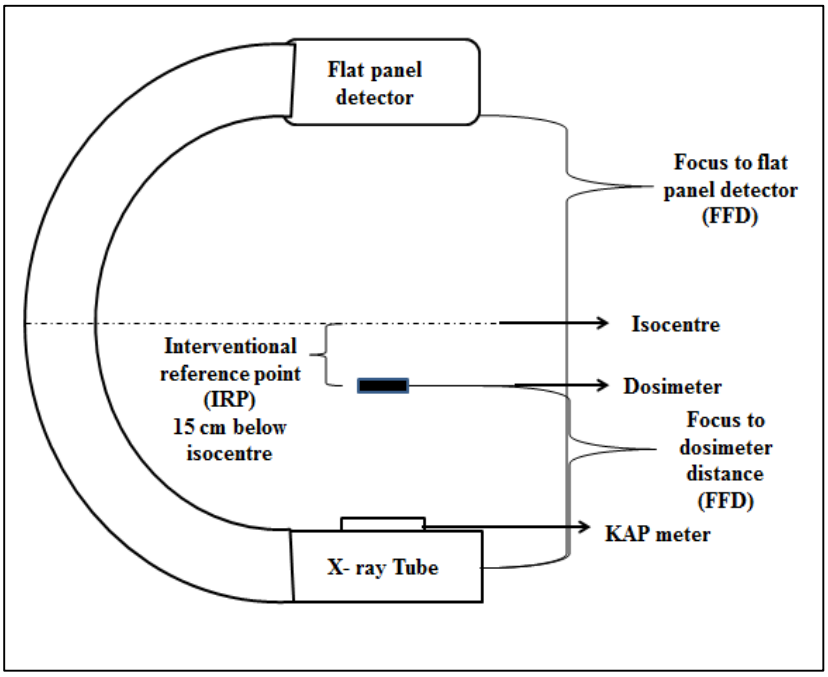

Figure 17: Schematic diagram for the KAP & CAK verification setup

3.2.3.2 Calculation of the calibration factor

For each measurement calculate

$$\mathbf{KAP_{cons}} = (\mathbf{KAP_{cons}})_{\mathbf{f}} - (\mathbf{KAP_{cons}})_{\mathbf{in}} \quad (12)$$

$$\mathbf{CAK_{cons}} = (\mathbf{CAK_{cons}})_{\mathbf{f}} - (\mathbf{CAK_{cons}})_{\mathbf{in}} \quad (13)$$

$$\mathbf{KAP_{meas}} = \mathbf{Air\ Kerma} \times \mathbf{Area} \quad (14)$$

For each measurement calculate the calibration factors for KAP and CAK:

$$\mathbf{CF^{KAP}} = \left(\frac{\mathbf{KAP}_{\mathbf{meas}}}{\mathbf{KAP}_{\mathbf{cons}}}\right) \quad (15)$$

$$\mathbf{CF^{CAK}} = \left(\frac{\mathbf{CAK}_{\mathbf{meas}}}{\mathbf{CAK}_{\mathbf{cons}}}\right) \quad (16)$$

3.3 Effective Dose and Risk Assessment

Effective dose (E) is the main parameter used to predict stochastic effects and assess the radiation risk. Therefore, it is extremely important to acquire E data in different paediatric age groups where it is clearly known that paediatric are more sensitive to radiation than adults [18]. In this study the Es were estimated for paediatric patient in both conventional radiology and interventional cardiology. The software PCXMC 2.0 was used to calculate the E and estimate the radiation risk. For this method of calculation, the following data should be fed into the PCXMC 2.0 program in order to have accurate calculations:

1- The patient demographic information: age, height and weight.
2- X-ray beam geometry: projection angle, focus to image distance and beam height and width.
3- Tube potential, filter material and total thickness.
4- The value of the KAP reading

3.3.1 Paediatric E in fixed and mobile x-ray

In this study, the patient age and exposure parameter were collected from the DICOM header in the period from 2012 to 2014. The objective was to collect twenty cases for each examination from each year. The exposure parameters collected were the peak tube voltage (kVp), exposure current time product (mAs), Field size (cm) and the KAP values. Paediatric patients were divided into five age groups: newborn (0- 1 m), >1m – 1y, >1 -5y, >5 -10y and >10 -15y.

Patient demographic information (weight and height) were not available in the DICOM header, therefore, the PCXMC 2.0 software settings for weight and height was used. The dose unit of KAP reading was $\mu Gy.m^2$ and it was converted into $mGy.cm^2$ then entered into PCXMC 2.0 program. The focuses to image distance, projection angles and half value layer for the five common examinations were derived from the phantom study descried in section 3.1.1.

The E estimated for the patient upper extremities examination was performed on the lower extremities of the phantom in the PCXMC 2.0 software. Then, paediatric patient stochastic radiation risks were estimated for both genders.

3.3.1 Paediatric E in interventional cardiology

For this part of study the patient demographic information and dosimetric parameter were collected manually because the interventional cardiology system was not integrated with the DICOM system. The patients were divided into five groups: newborn (0- 1 m), >1m – 1y, >1 -5y, >5 -10y and >10 -15y.

The entrance beam field size used for all age groups was 25 cm. Since the x-ray tube is under the couch; the projection angle selected in the PCXMC program

was PA with angle 90 degree. The focus to skin distance was kept as much as possible at 61 cm.

The collected readings for KAP, air kerma and fluoroscopic time were derived from the sum of both planes (frontal and lateral). The collected data were missing information related to the type of the clinical procedure. Hence, the collected dosimetric values were mixture of diagnostic and therapeutic procedures. It is noticed that the majority of the cases were described as therapeutic procedures.

The patient KAP readings were corrected for patient table absorption factor 0.75 and for KAP calibration factor 1.39. For CAK, the corrections for table absorption factor 0.75 and CAK calibration factor 1.07 were applied. The paediatric patient's stochastic radiation risks were estimated by the PCXMC 2.0 software for both genders.

Chapter 4: Results

4.1 Clinical Dose Measurements

4.1.1 Phantom measurements in digital x-ray fixed machine

Table (4) shows the results of phantom measurements carried out under full automatic exposure control (AEC) using clinical settings to determine the incident air kerma, K_i, and the ESAK for different paediatric age groups in the five common examinations. Also, it shows the difference between the displayed (indicated) air kerma and the measured incident air kerma.

Table 4: Fixed digital x-ray- Phantom measurements

Field size (cm) L X W		**Newborn (0-1m) clinical examinations – Phantom thickness = 4.8 cm - with Grid & AEC is not activated**	**kVp**	**mAs**	**Incident Air Kerma K_i (µGy)**	**Indicated Air Kerma (µGy)**	**% Dose diff.**	**ESAK K_e (µGy)**
18	15	Abdomen (AP) - Table Bucky - (AEC Off)	65	3.6	60.01	54.07	9.90%	84.62
18	15	Abdomen (AP) - Tabletop - (AEC Off)	65	2.9	47.90	43.70	8.77%	67.54
18	12	Abdomen (AP) - Table Buck - (AEC On)	65	2.6	40.18	43.36	-7.92%	56.65
12	14	chest (AP) - Table top -Supine	60	1.9	15.95	16.07	-0.75%	22.49
21	15	chest/Abdomen (chest protocol) -Table top	60	1.9	23.64	22.54	4.65%	33.33
21	15	chest/Abdomen (Abdomen protocol) – Table Top	65	2.9	48.32	45.40	6.05%	65.71
15	12	Pelvis (AP) - Table Bucky - (AEC Off)	65	4.9	82.37	71.11	13.67%	116.14
15	12	Pelvis (AP) - Table Bucky - (AEC ON)	65	2.7	41.21	32.04	22.26%	58.10
12	6	Extremities (upper) Hand (PA)- table top	50	2.4	51.44	49.54	3.69%	72.52
Field size (cm) L X W		**(>0- 1 y) clinical examinations - Phantom thickness = 9.5 cm - with Grid & AEC is not activated**	**kVp**	**mAs**	**Incident Air Kerma K_i (µGy)**	**Indicated Air Kerma (µGy)**	**% Dose diff.**	**ESAK K_e (µGy)**
24	19	Abdomen (AP) -Table Bucky (AEC Off)	65	3.6	66.61	52.85	20.65%	93.92
24	19	Abdomen (AP) - Table Top(AEC Off)	65	2.9	53.95	44.01	18.42%	76.06
24	19	Abdomen (AP)- Table Bucky (AEC ON)	65	6.1	111.15	78.95	28.97%	156.72
15	17	chest (AP) -Table top - supine	60	1.9	17.32	15.69	9.43%	24.42
26	17	chest/Abdomen (chest protocol) -Table top-supine	60	1.9	26.51	22.62	14.66%	37.38
26	17	chest/Abdomen (Abdomen protocol) -Table top-supine	65	2.9	54.50	43.36	20.43%	76.85
16	19	Pelvis (AP)- Table Bucky (AEC Off)	65	4.9	91.72	73.36	20.02%	129.32
16	19	Pelvis (AP)-Table Bucky (AEC ON)	65	6.4	116.22	81.80	29.62%	163.87
14	9	Extremities (upper) Hand (PA)- table top	50	2.4	51.69	49.21	4.80%	70.29
Field size (cm) L X W		**child (>1- 5)y clinical examinations - Phantom thickness = 9.5 cm - with Grid & the AEC is activated**	**kVp**	**mAs**	**Incident Air Kerma K_i (µGy)**	**Indicated dose (µGy)**	**% Dose diff.**	**ESAK K_e (µGy)**
31	23	Abdomen (AP) - Table Bucky	70	3.5	81.39	63.96	21.43%	128.60
21	22	Chest (PA) Vertical BUCKY	70	2.4	14.071	13.20	6.17%	22.23

21	22	Chest (AP) Supine- Table Bucky	70	1.9	28.23	26.55	5.95%	44.60
20	16	Lat. Skull (post Nasal space) - vertical Bucky	70	7.4	67.57	57.19	15.36%	106.76
20	23	Pelvis (AP)-Table Bucky	70	3.9	89.44	72.10	19.38%	141.31
14	10	Extremities (upper)–Hand(PA)-Table Top	50	3	67.73	60.71	10.35%	92.11
Field size (cm) L X W		**Normal Adult (>5-10)y clinical examinations - Phantom thickness =9.5 cm- with Grid & the AEC is activated**	**kVp**	**mAs**	**Incident Air Kerma K_i (µGy)**	**Indicated dose (µGy)**	**% Dose diff.**	**ESAK K_e (µGy)**
38	28	Abdomen (AP) - Table Bucky	85	1.2	109.77	86.22	21.46%	166.85
27	27	Chest (PA)- Vertical BUCKY	117	1.6	36.67	32.37	11.72%	61.24
21	17	Lat. Skull (post Nasal space) - Vertical Bucky	73	9.9	258.87	220.45	14.84%	409.02
27	30	Pelvis (AP)- Table Bucky	80	1.2	99.08	73.74	25.57%	150.60
21	13	Extremities (upper)- Hand(PA)- table top	52	1.9	46.03	43.35	5.84%	62.61
Field size (cm) L X W		**Normal Adult (>10- 15)y clinical examinations- Phantom thickness =9.5 cm - with Grid & the AEC is activated**	**kVp**	**mAs**	**Incident Air Kerma K_i (µGy)**	**Indicated dose (µGy)**	**% Dose diff.**	**ESAK K_e (µGy)**
42	33	Abdomen (AP) - Table Bucky	85	2.1	220.19	146.01	33.69%	334.70
33	33	Chest (PA)- vertical Bucky	117	3.1	76.18	64.65	15.14%	127.21
23	18	Lat. Skull (post Nasal space)- vertical Bucky	73	9.9	277.26	217.55	21.54%	438.07
30	35	Pelvis (AP)- Table Bucky	80	2.7	246.75	165.75	32.83%	375.06
23	15	Extremities (upper) Hand(PA)- table top	52	1.9	48.31	44.54	7.79%	65.70

Continuous-- Table 4: Fixed digital x-ray- Phantom measurements

4.1.2 Fixed digital x-ray - Incidinet air kerma measurements without phantom

Table (5) shows the exposure parameters and the calculated ESAK which were collected from the DICOM header. These parameters were averaged over the years 2012, 2013 and 2014. The objective was to collect 20 cases from each year for each five examinations for different age groups.

Table 5: DICOM system- patient exposure parameter and calculated ESAK

Newborn (0 - 1 m)										
Examination	**No. of patient**	**Statistic**	**Age (Days)**	**kVp**	**mAs**	**KAP ($\mu Gy.m^2$)**	**Field size (L) cm**	**Field size (w) cm**	**Incident air Kerma (K_i) µGy**	**ESAK (K_e) µGy**
chest (AP)	**60**	Mean	8.18	60.20	2.00	0.48	12.36	13.87	29.32	37.53
		3rd Quartile	14.00	60.00	2.00	0.58	13.06	14.80	35.75	45.77
		SD	9.30	1.09	0.00	0.18	2.83	2.64	10.14	12.99
Abdomen (AP)	**14**	Mean	7.86	65.36	3.57	1.40	19.48	15.73	48.58	62.18
		3rd Quartile	12.50	65.00	4.00	1.60	20.50	16.07	55.26	70.73
		SD	7.53	0.66	0.65	0.50	2.76	1.89	15.54	19.89
Chest/Abdomen(AP)	**18**	Mean	6.47	60.83	2.17	0.90	20.99	14.71	31.77	41.94
		3rd Quartile	12.00	60.00	2.00	1.10	22.71	15.37	38.41	50.70
		SD	6.55	1.39	0.28	0.30	2.05	1.54	11.80	15.57
Pelvis	**2**	Mean	28.00	67.50	5.00	1.70	49.50	12.16	52.61	69.44
		3rd Quartile	28.00	68.75	5.50	1.80	67.45	13.23	67.98	89.74
		SD	0.00	2.50	1.00	0.10	35.91	2.14	30.75	40.59

Extremities (Hand(AP))	**4**	Mean	9.50	50.00	2.00	0.80	13.61	6.94	89.72	112.16
		3rd Quartile	13.75	50.00	2.00	1.10	18.38	7.88	108.12	135.14
		SD	9.25	0.00	0.00	0.30	5.66	1.21	23.30	29.12
> 0 - 1 y										
Examination	**No. of patient**		**Age (months)**	**kVp**	**mAs**	**KAP (µGy.m2)**	**Field size (L) cm**	**Field size (w) cm**	**Incident air Kerma (K_i) µGy**	**ESAK (K_e) µGy**
chest (AP)	**59**	Mean	4.41	61.32	2.00	0.73	14.95	16.82	29.19	37.36
		3rd Quartile	6.50	60.00	2.00	0.86	16.76	18.09	32.84	42.03
		SD	3.17	2.51	0.00	0.36	2.89	2.22	11.76	15.05
Abdomen (AP)	**50**	Mean	5.25	67.00	4.82	4.05	23.54	18.65	88.71	117.10
		3rd Quartile	8.00	70.00	6.75	5.64	26.55	20.31	116.87	154.27
		SD	3.17	2.67	1.62	2.51	3.15	2.31	47.39	62.55
Chest/Abdomen(AP)	**21**	Mean	4.93	62.38	2.62	1.99	25.59	17.40	43.95	58.01
		3rd Quartile	8.00	66.00	3.00	1.92	27.78	18.86	49.42	65.24
		SD	3.38	3.73	1.02	1.50	3.86	2.37	30.35	40.06
Pelvis	**53**	Mean	4.83	66.32	4.64	3.30	16.35	19.08	122.94	162.29
		3rd Quartile	6.00	70.00	6.00	4.14	17.44	20.74	146.59	193.50
		SD	2.49	2.23	0.90	2.09	9.92	10.31	68.31	90.18
Extremities (Hand(AP))	**11**	Mean	6.91	50.00	2.82	0.89	13.42	8.93	87.06	108.83
		3rd Quartile	8.50	50.00	3.00	1.04	15.94	9.44	97.84	122.31
		SD	2.34	0.00	0.60	0.20	6.08	1.47	43.95	54.94
>1 - 5y										
Examination	**No. of patient**		**Age (Years)**	**kVp**	**mAs**	**KAP (µGy.m2)**	**Field size (L) cm**	**Field size (w) cm**	**Incident air Kerma (K_i) µGy**	**ESAK (K_e) µGy**
chest (AP)	**65**	Mean	2.86	68.83	2.02	1.24	20.50	21.66	29.80	40.52
		3rd Quartile	4.00	70.00	2.00	1.43	22.99	23.60	33.83	46.01
		SD	1.28	1.83	0.12	0.69	4.08	2.69	19.63	26.69
Abdomen (AP)	**64**	Mean	3.20	69.69	4.36	5.57	30.94	23.37	79.04	107.49

		3rd Quartile	4.00	70.00	6.00	6.79	34.00	24.91	95.07	129.30
		SD	1.24	1.75	1.88	2.76	4.67	3.75	41.38	56.28
Lat. Skull (Post Nasal space)	**63**	Mean	3.38	70.00	6.65	3.10	19.48	16.07	96.67	131.48
		3rd Quartile	4.00	70.00	7.00	3.50	22.02	17.76	120.68	164.13
		SD	1.16	0.00	0.81	2.26	3.81	3.17	63.96	86.99
Pelvis	**55**	Mean	3.04	69.87	5.58	5.54	20.27	23.46	121.37	165.06
		3rd Quartile	4.00	70.00	8.00	6.54	23.22	27.20	157.64	214.39
		SD	1.24	0.94	4.43	5.50	4.89	4.87	100.41	136.55
Extremities (Hand(AP))	**44**	Mean	2.92	50.13	3.23	1.38	14.44	10.18	97.72	125.08
		3rd Quartile	4.00	50.00	3.25	1.71	17.55	11.77	99.32	127.13
		SD	1.26	1.39	0.68	0.80	5.43	4.00	52.78	67.56
>5 - 10 y										
Examination	**No. of patient**		**Age (Years)**	**kVp**	**mAs**	**KAP ($\mu Gy.m^{2)}$**	**Field size (L) cm**	**Field size (w) cm**	**Incident air Kerma (K_i) µGy**	**ESAK (K_e) µGy**
chest (AP)	**57**	Mean	8.00	124.72	1.28	2.81	26.40	26.88	39.96	62.33
		3rd Quartile	9.00	125.00	1.00	3.10	28.02	27.88	44.54	69.48
		SD	1.12	0.55	0.42	1.26	2.41	2.35	17.17	26.79
Abdomen (AP)	**62**	Mean	8.00	84.60	2.35	16.78	38.38	28.21	147.06	207.35
		3rd Quartile	9.00	85.00	3.00	19.31	41.05	30.03	177.82	250.73
		SD	1.37	2.08	1.36	12.07	4.00	3.84	83.84	118.21
Lat. Skull (Post Nasal space)	**64**	Mean	8.06	72.64	9.88	13.12	21.40	16.96	368.70	508.81
		3rd Quartile	9.00	73.00	10.00	12.26	24.06	18.24	367.55	507.22
		SD	1.38	1.36	0.49	13.40	3.77	2.54	395.39	545.63
Pelvis	**44**	Mean	8.14	79.98	2.30	13.53	26.94	29.99	164.15	231.45
		3rd Quartile	9.00	80.00	3.00	20.41	29.22	32.77	202.89	286.08
		SD	1.19	1.00	2.11	9.73	4.62	4.10	125.99	177.65
Extremities (Hand(AP))	**55**	Mean	8.33	52.42	1.93	1.45	20.75	12.50	54.36	69.03
		3rd Quartile	9.00	52.00	2.00	1.81	23.73	14.70	62.47	79.34
		SD	1.29	1.13	0.33	0.69	4.33	4.26	12.26	15.57

>10 -15 y										
Examination	**No. of patient**		Age (Years)	kVp	mAs	KAP ($\mu Gy.m^2$)	Field size (L) cm	Field size (w) cm	Incident air Kerma (K_i) µGy	ESAK (K_e) µGy
chest (AP)	**62**	Mean	12.49	125.00	1.50	4.27	32.72	32.70	39.56	61.72
		3rd Quartile	13.00	125.00	2.00	4.96	35.50	34.96	46.85	73.09
		SD	4.56	0.00	0.84	2.62	5.13	4.64	20.66	32.23
Abdomen (AP)	**42**	Mean	12.91	85.00	4.36	39.97	41.84	32.87	281.07	396.31
		3rd Quartile	14.00	85.00	5.00	47.73	43.02	34.33	302.26	426.18
		SD	4.99	0.00	3.93	40.31	1.89	4.32	269.75	380.35
Lat. Skull (Post Nasal space)	**45**	Mean	12.71	73.00	10.04	15.78	23.20	18.37	367.20	506.74
		3rd Quartile	14.00	73.00	10.00	18.11	25.36	20.81	435.48	600.97
		SD	1.22	0.00	0.30	15.70	4.35	3.12	331.41	457.34
Pelvis	**37**	Mean	12.51	79.76	4.73	33.27	29.85	35.32	319.16	450.01
		3rd Quartile	14.00	80.00	5.00	39.09	30.76	36.94	386.41	544.84
		SD	1.22	0.83	3.55	20.17	3.03	3.85	205.46	289.69
Extremities (Hand(AP))	**42**	Mean	12.61	52.17	1.93	2.06	23.18	15.16	54.73	69.51
		3rd Quartile	13.00	52.00	2.00	2.33	25.46	16.70	61.63	78.27
		SD	2.18	0.85	0.26	1.35	4.48	5.23	13.51	17.16

Continuous- Table 5: DICOM system- patient exposure parameterand calculated ESAK

Table (6) shows the results of the measurements carried out to determine the incident air kerma K_i, and the ESAK without the presence of phantom. The exposure parameters from Table (5) were used to perform these measurements where the exposure parameters were entered manually. The results of the measured air Kerma were used later to calculate the tube output Y (d).

Table 6: Fixed digital x-ray incidinet air kerma measurments without phantom

Field size (cm) L X W		Newborn (0-1m) clinical examinations/ with Grid & the AEC is NOT activated	kVp	mAs	Measured Air Kerma (M) (µGy)	Incident Air Kerma, K_i (µGy)	Indicated Air Kerma (µGy)	% Dose diff.
18	15	Abdomen (AP) – Table Bucky	66	3.1	81.043	47.971	47.04	1.95%
12	14	chest (AP)- Table top	60	2	22.870	14.834	21.43	-44.46%
21	15	chest/Abdomen (chest protocol) - Table top	60	2	36.447	21.508	22.22	-3.32%
15	12	Pelvis (AP)- Table Bucky	66	5	133.900	79.258	76.67	3.27%
12	6	Extremities (upper) Hand(PA)- table top	50	2	69.437	40.663	43.06	-5.88%
Field size (cm) L X W		**Newborn (>0- 1 y) clinical examinations- with Grid & the AEC is NOT activated**	**kVp**	**mAs**	**Measured Air Kerma (M) (µGy)**	**Incident Air Kerma, K_i (µGy)**	**Indicated Air Kerma (µGy)**	**% Dose diff.**
24	19	Abdomen (AP) - Table Bucky	66	4	108.20	64.045	62.57	2.30%
15	17	chest (AP) -Table top	60	2	22.59	14.656	16.34	-11.49%
26	17	chest/Abdomen (Abdomen protocol) Table top	66	3.1	82.49	48.831	46.83	4.09%
26	17	chest/Abdomen (chest protocol) - Table top	60	2	136.27	22.001	22.32	-1.46%
16	19	Pelvis (AP)- Table Bucky	66	5	88.76	80.658	77.74	3.62%
14	9	Extremities (upper)Hand(PA)- Table top	50	2.5	37.28	51.977	53.97	-3.83%
Field size (cm) L X W		**child (>1- 5)y clinical examinations- with Grid & the AEC is NOT activated**	**kVp**	**mAs**	**Measured Air Kerma (M) (µGy)**	**Incident Air Kerma, K_i (µGy)**	**Indicated Air Kerma (µGy)**	**% Dose diff.**
31	23	Abdomen (AP) - Table Bucky	70	4	130.30	77.17	73.63	4.58%
21	22	Chest (PA)-Vertical Bucky	70	2.5	16.27	12.60	12.99	-3.08%
21	22	Chest (AP)- Table top- Supine	70	2	36.91	24.02	26.12	-8.72%
20	16	Lat. Skull (post Nasal space)- vertical Bucky	70	8	86.74	63.74	61.25	3.91%
20	16	Lat. Skull (post nasal space)- vertical Bucky	70	6.3	68.09	42.43	47.97	-13.06%
20	23	Pelvis (AP)- Table Bucky	70	5	163.50	96.83	92.68	4.28%
14	10	Extremities (upper) Hand(PA)- Table top	50	3.1	110.80	64.89	62.86	3.13%
Field size (cm) L X W		**Child (>5-10)clinical examination- with Grid & the AEC is NOT activated**	**kVp**	**mAs**	**Measured Air Kerma (M) (µGy)**	**Incident Air Kerma, K_i (µGy)**	**Indicated Air Kerma (µGy)**	**% Dose diff.**
38	28	Abdomen (AP)- Table Bucky	85	1.2	149.10	88.26	79.61	9.80%
27	27	Chest (PA)- Vertical Bucky	117	1.6	41.07	31.49	30.86	2.01%

27	27	Chest (PA)- Vertical Bucky	125	1.2	35.02	26.93	26.84	0.35%
21	17	Lat. Skull (post nasal space)- vertical Bucky	73	10	307.57	221.03	209.06	5.42%
27	30	Pelvis (AP)- Table Bucky	81	1.2	137.17	81.23	75.80	6.68%
27	30	Pelvis (AP)- Table Bucky	81	1.2	133.20	78.88	72.72	7.82%
27	30	Pelvis (AP)- Table Bucky	81	2	230.67	136.61	127.61	6.58%
21	13	Extremities (upper) Hand PA- table top	52	2	78.67	48.55	43.96	9.46%
Field size (cm) L X W		**Child (>10- 15)y clinical examinations - with Grid & the AEC is NOT activated**	**kVp**	**mAs**	**Measured Air Kerma (M) (µGy)**	**Incident Air Kerma, K_i (µGy)**	**Indicated Air Kerma (µGy)**	**% Dose diff.**
42	33	Abdomen (AP) - Table Bucky	85	2.5	322.60	190.95	167.53	12.26%
33	33	Chest (PA)- Vertical Bucky	117	3.1	82.21	62.66	60.54	3.37%
33	33	Chest (PA)- Vertical Bucky	125	1.6	41.53	31.74	35.72	-12.54%
23	18	Lat. Skull (post nasal space)- vertical Bucky	73	10	315.07	226.42	219.40	3.10%
30	35	Pelvis (AP)- Table Bucky	81	3.1	361.70	214.21	190.29	11.17%
30	35	Pelvis (AP)- Table Bucky	81	3.1	356.60	211.18	190.70	9.70%
23	15	Extremities (upper) Hand PA- table top	52	2	79.88	47.41	43.09	9.11%

Continuous-Table 6: Fixed digital x-ray incidinet air kerma measurments without phantom

4.1.3 Calculation of the tube output Y (d)

Table (7) displays the results of the tube output Y (d) that was calculated from the mean measurements of the air kerma k (d) and corrected by the use of dosimeter calibration factor $k_{Q.}$

Table 7: Fixed x-ray- Tube output calculation

Table Bucky Examination					
kVp	**P_{It} (mAs)**	**Mean Air Kerma (M) (µGy)**	**k_Q**	**K(d) =M * K_Q (µGy)**	**Y (d) (µGy/mAs)**
66	3.1	81.04	0.985	79.86	25.77
66	4	108.20	0.985	106.63	26.66
70	4	130.30	0.986	128.48	32.12
85	1.2	149.10	0.985	146.94	122.44
85	2.5	322.60	0.985	317.92	127.16
66	5	133.90	0.985	131.96	26.39
66	5	136.27	0.985	134.29	26.86
70	5	163.50	0.986	161.21	32.24
81	1.2	133.20	0.986	131.34	109.45
81	2	230.67	0.986	227.44	113.72
81	3.1	356.60	0.986	351.61	113.42
60	2	36.45	0.983	35.81	17.90
60	2	37.28	0.983	36.63	18.32
Chest (PA) -Vertical Bucky					
kVp	**P_{It} (mAs)**	**Mean Air Kerma (M) (µGy)**	**k_Q**	**K(d) =M * K_Q (µGy)**	**Y (d) (µGy/mAs)**
70	2.5	16.27	0.986	16.05	6.42
117	1.6	41.07	0.989	40.62	25.39
117	3.1	82.21	0.989	34.64	28.87
125	1.2	35.02	0.992	81.54	26.30
125	1.6	41.53	0.992	41.19	25.75
Lat. Skull (Post Nasal space) - Vertical Bucky					

kVp	P_{It} (mAs)	Mean Air Kerma (M) (µGy)	k_Q	K(d) = M * K_Q (µGy)	Y (d) (µGy/mAs)
70	6.3	68.08	0.986	67.13	10.65
70	8	86.74	0.986	85.52	10.6
73	10	307.57	0.987	303.54	30.3
73	10	315.07	0.987	310.94	31.093
Extremities (upper) Hand PA- Table top					
kVp	**P_{It} (mAs)**	**Mean Air Kerma (M) (µGy)**	**k_Q**	**K(d) =M * K_Q (µGy)**	**Y (d) (µGy/mAs)**
50	2	69.44	0.975	67.70	33.85
50	2.5	88.76	0.975	86.54	34.62
50	3.1	110.80	0.975	108.03	34.85
52	2	78.67	0.977	76.82	38.41
52	2	79.88	0.977	78.00	39.00
Chest (AP) - Table top					
kVp	**P_{It} (mAs)**	**Mean Air Kerma (M) (µGy)**	**k_Q**	**K(d) =M * K_Q (µGy)**	**Y (d) (µGy/mAs)**
60	2	22.87	0.983	22.47	11.23
60	2	22.60	0.983	22.20	11.10
70	2	36.91	0.986	36.39	18.19

Countinious-Table 7: Fixed x-ray- Tube output calculation

Graphs from 18 to 22 have been plotted between the tube potential kVp and the values of the x-ray tube output Y(d) to find out the fitted equations (y) that will be used to figure out the K_i & K_e for each paediatric patient.

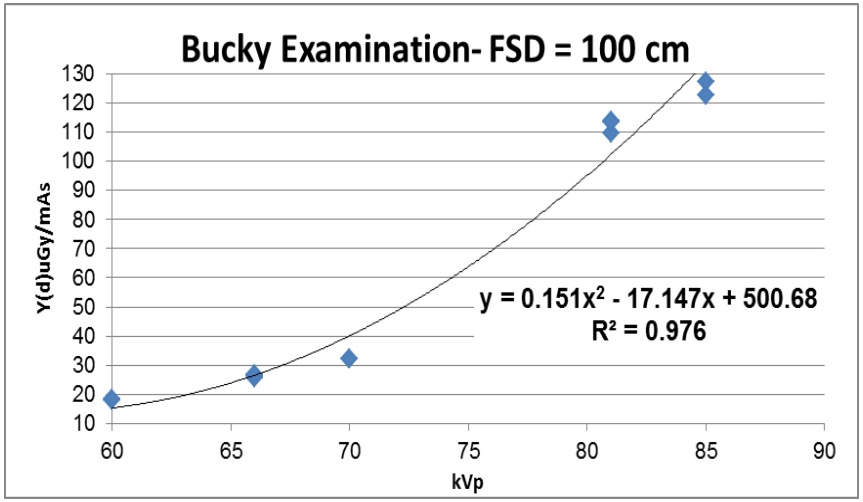

Figure 18: The releation between the tube out put and kVp - Bucky examination

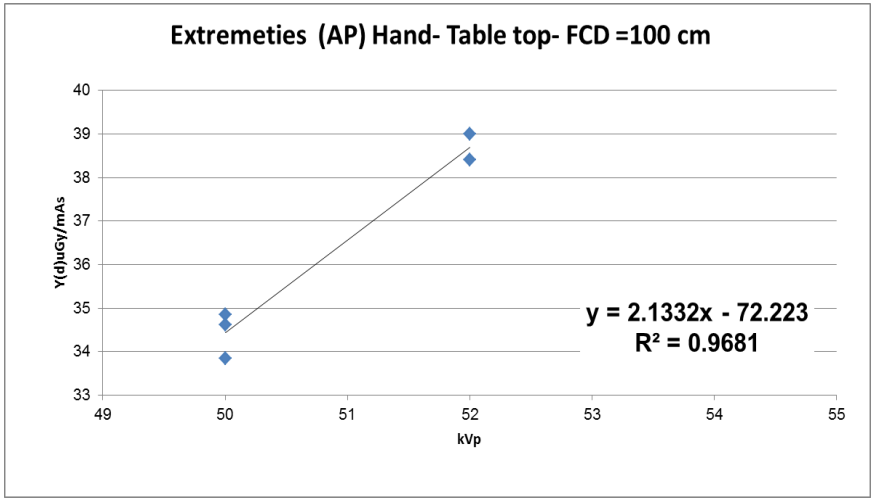

Figure 19: The relation between the tube out put and the kVp - Upper extremeties

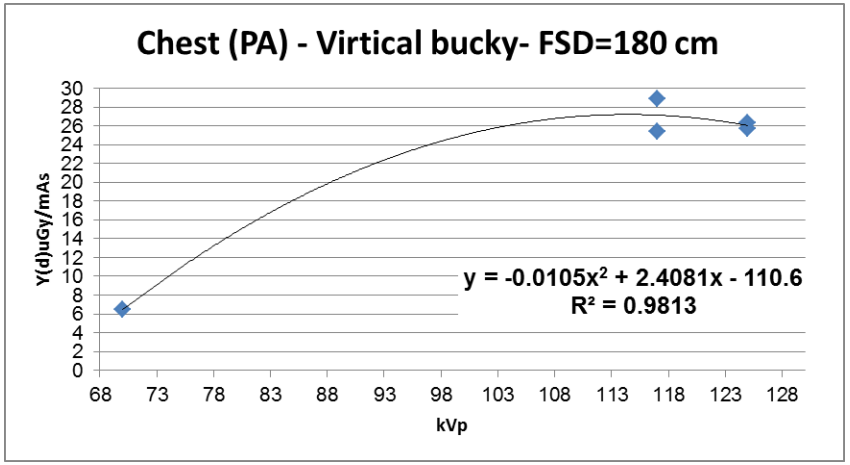

Figure 20: Relation between the tube out put and the kVp – Chest Virtical Bucky

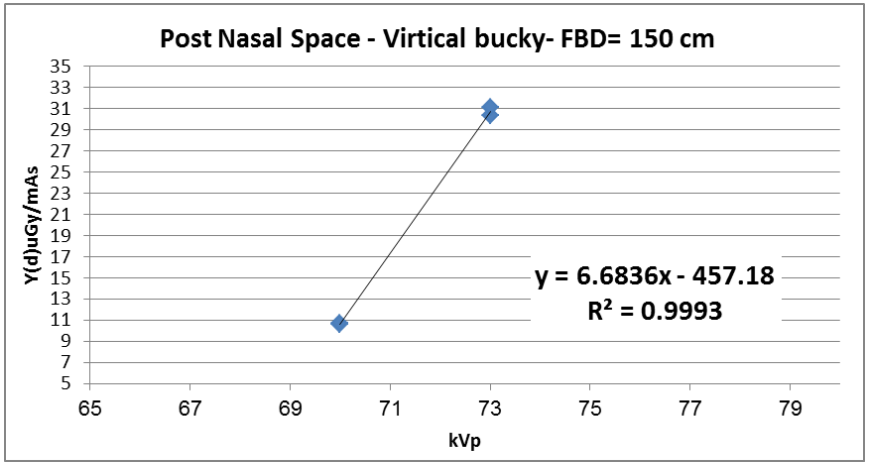

Figure 21: Relation between the tube out put and the kVp – Lat. Skull (Post Nasal Space) -Virtical Bucky

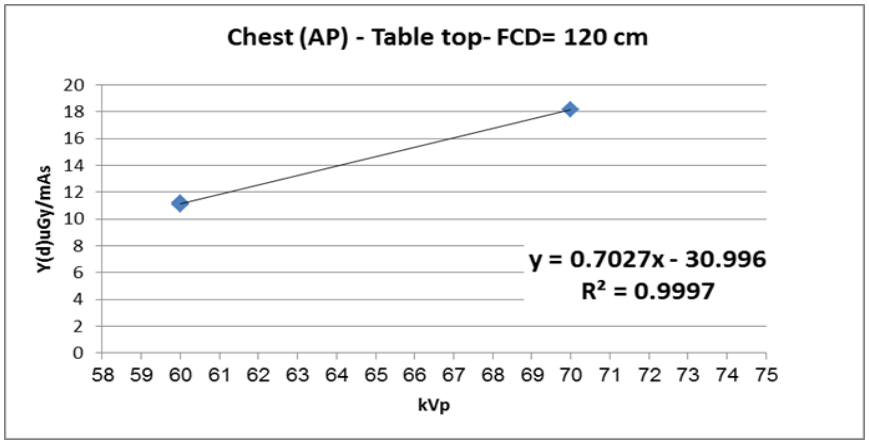

Figure 22: Relation between the tube out put and the kVp - Chest table top

4.2 Clinical dose measurements without phantom in digital x-ray mobile machine

Table (8) illustrates the measurements of the Air kerma, Ki, K_e, and the difference between the indicated and the measured doses, K_i. Furthermore, the dose measurements were performed for two different filed sizes.

Table 8: Mobile digital x-ray incidinet air kerma measurment without phantom

Field size (cm) L X W	Neonatal (0-1m) examination (NICU)	kVp	mAs	Measured Air Kerma (M) (µGy)	Incident Air Kerma, K_i (µGy)	Indicated Air Kerma (µGy)	% Dose diff.	ESAK K_e (µGy)
25.5 x 26	Chest /Abdomen	49	1.8	50.46	31.58	27.15	14.02%	42.94
25.5 x 26	Chest /Abdomen	50	1.8	53.15	33.47	28.66	14.38%	45.52
25.5 x 26	Chest /Abdomen	52	1.6	50.99	32.10	28.66	10.72%	43.66
25.5 x 26	Chest /Abdomen	52	2	63.88	40.21	35.19	12.49%	54.69
25.5 x 26	Chest /Abdomen	55	2	74.21	46.67	42.23	9.50%	63.47
25.5 x 26	Chest /Abdomen	57	2	81.83	51.40	46.76	9.03%	72.98
25.5 x 26	Chest /Abdomen	59	2	89.45	56.17	51.28	8.70%	79.76
25.5 x 26	Chest /Abdomen	60	1	47.18	29.61	27.65	6.61%	42.05
Field size (cm) L X W	**Neonatal (0-1m) examination (NICU)**	**kVp**	**mAs**	**Measured Air Kerma (M) (µGy)**	**Incident Air Kerma, K_i (µGy)**	**Indicated Air Kerma (µGy)**	**% Dose diff.**	**ESAK K_e (µGy)**
17 x 13	Chest /Abdomen	49	1.8	47.04	29.43	22.62	23.13%	40.03
17 x 13	Chest /Abdomen	50	1.8	51.08	32.17	27.15	15.60%	43.75
17 x 13	Chest /Abdomen	52	1.6	49.13	30.93	24.13	21.97%	42.06
17 x 13	Chest /Abdomen	52	2	61.25	38.56	31.67	17.85%	52.44
17 x 13	Chest /Abdomen	55	2	70.99	44.65	36.20	18.92%	60.72
17 x 13	Chest /Abdomen	57	2	78.37	49.22	40.72	17.27%	69.90
17 x 13	Chest /Abdomen	59	2	86.19	54.12	45.25	16.39%	76.85
17 x 13	Chest /Abdomen	60	1	45.65	28.65	22.62	21.03%	40.68

Table (9) shows the exposure parameter that was extracted from the DICOM header for the neonatal patients in the NICU and the calculation of the mean ESAK for 41 patients.

Table 9: DICOM system- Neonatal exposure parameter and calculated ESAK

Neonatal (NICU)										
Examination	**No. of patient**		**Age (Days)**	**kVp**	**mAs**	**KAP ($mGy.cm^2$)**	**Field size (L) cm**	**Field size (w) cm**	**Incident air Kerma (K_i) µGy**	**ESAK (K_e) µGy**
chest/ Abdomen	41	Mean	2.59	53.05	1.98	8.93	14.77	11.86	45.26	56.58
		3^{rd} Quartile	3.00	55.00	1.92	10.00	16.80	13.01	50.27	62.83
		SD	4.33	2.40	0.31	6.69	4.45	1.99	16.45	20.56

4.2.1 Calculation of the tube output Y (d)

Table (10) shows the result of the tube output for the two different field sizes where the upper half of the table related to the large field size (25.5 x 26) cm and the lower half for the small field size which is used clinically by the radiographer (17 x 13) cm.

Table 10: Mobile x-ray Tube output calculation

kVp	P_{It} (mAs)	M (µGy)	k_Q	K(d) =M * K_Q (µGy)	Y (d) µGy/mAs
49	1.8	50.463	0.990	49.959	28.035
50	1.8	53.147	0.997	52.961	29.526
52	1.6	50.993	0.996	50.789	31.871
52	2	63.883	0.996	63.628	31.942
55	2	74.210	0.995	73.839	37.105
57	2	81.827	0.994	81.319	40.913
59	2	89.450	0.994	88.869	44.725
60	1	47.180	0.993	46.850	47.180
kVp	**P_{It} (mAs)**	**M (µGy)**	**k_Q**	**K(d) =M * K_Q (µGy)**	**Y (d) µGy/mAs**
49	1.8	47.037	0.99	46.566	26.131
50	1.8	51.077	0.997	50.898	28.376
52	1.6	49.133	0.996	48.937	30.708
52	2	61.250	0.996	61.005	30.625
55	2	70.997	0.995	70.642	35.498
57	2	78.370	0.994	77.884	39.185
59	2	86.190	0.994	85.630	43.095
60	1	45.650	0.993	45.330	45.650

Graphs 18 and 19 describe Table (10) and the fitting equations (y) where the equations show that there is a slight difference between the field sizes.

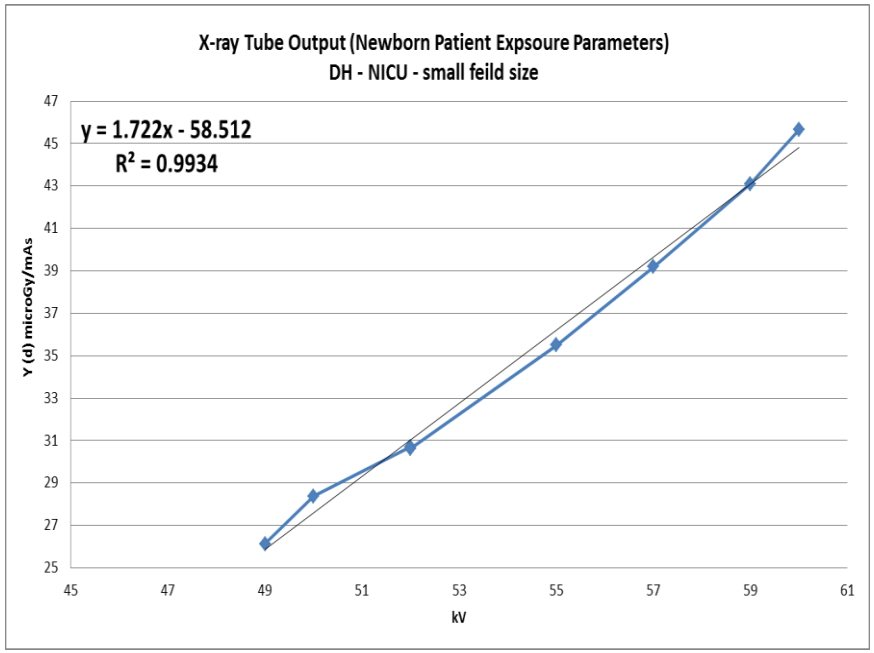

Figure 23: Relation between the tube out put and the kVp - Mobile X-ray –Samll field size

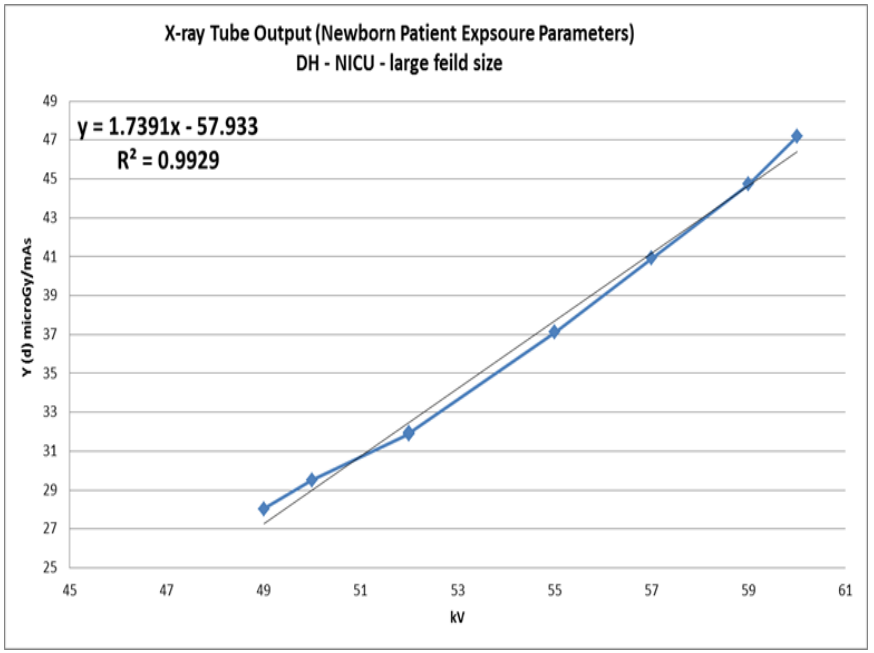

Figure 24: Relation between the tube out putand the kVp - Mobile X-ray – Large field size

4.3 Clinical Dose Measurement in the Interventional Cardiology

4.3.1 General kerma measurements assessment with phantoms

Table (11) shows the difference between the measured incident air kerma rate (mGy/min) and the air kerma (mGy) from the displayed (indicated) readings. For Frontal tube, the Focus to chamber distance (FCD) = 62 cm while for the lateral tube the FCD = 70 cm. The measurements were corrected for both tubes at the level of the IRP using the invers square law.

Table 11: Cath lab- Dose rate diferences between measured and indicated vlaues for frontal and lateral tubes.

Frontal Tube						
Phantom thickness: 9.5 cm						
Mode & field size	**Measured Ki (mGy/min)**	**Indicated dose rate mGy/min**	**% difference mGy/min**	**Measured Air Kerma (mGy)**	**Indicated Air Kerma (mGy)**	**% difference mGy**
Normal (25 cm)	4.81	5.40	13.59%	1.24	1.41	12.21%
Normal (20 cm)	9.54	10.800	11.87%	2.38	2.51	13.27%
Normal (15 cm)	14.28	16.200	15.30%	3.60	4.15	13.43%
Phantom thickness: 12 cm						
Normal (25 cm)	8.68	10.200	15.55%	2.21	2.56	17.52%
Normal (20 cm)	14.25	16.200	14.95%	3.59	4.13	13.69%
Normal (15 cm)	21.66	25.800	16.79%	5.48	6.40	19.13%
Lateral Tube						

Phantom thickness: 9.5 cm						
Mode & field size	**Measured Ki (mGy/min)**	**Indicated dose rate mGy/min**	**% difference mGy/min**	**Measured Air Kerma (mGy)**	**Indicated Air Kerma (mGy)**	**% difference mGy**
Normal (25 cm)	3.51	4.2	19.81%	0.89	1.08	21.81%
Normal (20 cm)	4.25	5	17.70%	1.27	1.29	2.44%
Normal (15 cm)	7.73	6.6	-14.63%	1.61	1.65	2.37%
Phantom thickness: 12 cm						
Normal (25 cm)	7.83	6.6	-15.70%	1.66	1.65	-0.54%
Normal (20 cm)	10.01	8.6	-14.06%	2.16	2.17	0.65%
Normal (15 cm)	12.80	11	-14.08%	2.71	2.77	2.21%

Continuous- Table 11: Cath lab- Dose rate diferences between measured and indicated vlaues for frontal and lateral tubes.

Table (12) shows the measurements of default procedures under the clinical examination protocol that performed on different phantom thickness starting form 4.8 cm that represent the newborn patient tell the 16.5 cm which represent the adolescence. These measurements were only for the frontal tube.

Table 12: Cath lab- Phantom measurements under clinical procedures

Fluoro mode								
Age Band	**Phantom size (cm)**	**Procedure**	**Fluoro pre Filter selected**	**K_i (mGy/min)**	**ESAK, K_e (mGy/min)**	**kVp**	**mA**	**ms**
Neonatal (0-1m)	4.8	Cardiac- paediatric- cardio 15 fr low contrast	0.4Cu + 1 mm Al	1.73	1.56	64	78	3
(> 1 - 10 y)	7.4	Default	0.1Cu + 1 mm Al	3.32	2.99	61	129	3
(> 1 - 10 y)	9.5	Default	0.1Cu + 1 mm Al	4.98	4.50	62	188	3
(> 10-15 y)	12	Default	0.1Cu + 1 mm Al	7.90	7.14	64	271	4
(> 10-15 y)	14.5	Default	0.1Cu + 1 mm Al	11.77	10.64	65	358	4
(> 10- 15y)	16.8	Default	0.1Cu + 1 mm Al	17.88	16.19	68	475	5
Cine mode								
Age Band	**Phantom size (cm)**	**Procedure**	**Exposure pre Filter selected**	**K_i (mGy/min)**	**ESAK, K_e (mGy/min)**	**kVp**	**mA**	**ms**	**µGy /fr**
Neonatal (0-1m)	4.8	Cardiac- paediatric- cardio 15 fr/s low contrast	0.1Cu + 1 mm Al	5.01	4.53	64	78	3	5.50
(> 1 - 10 y)	7.4	Default	0	15.99	14.43	61	129	3	17.75
(> 1 - 10 y)	9.5	Default	0	26.89	24.28	62	188	3	29.53
(> 10-15 y)	12	Default	0	44.11	39.87	64	271	4	48.43
(> 10-15 y)	14.5	Default	0	68.70	62.14	65	358	4	75.49
(> 10- 15y)	16.8	Default	0	108.60	98.32	68	475	5	119.23

Graphs 25 and 26 show the linear relationship between the phantom thickness and the air kerma rate where it is increased with phantom size for both mode fluoro and cine.

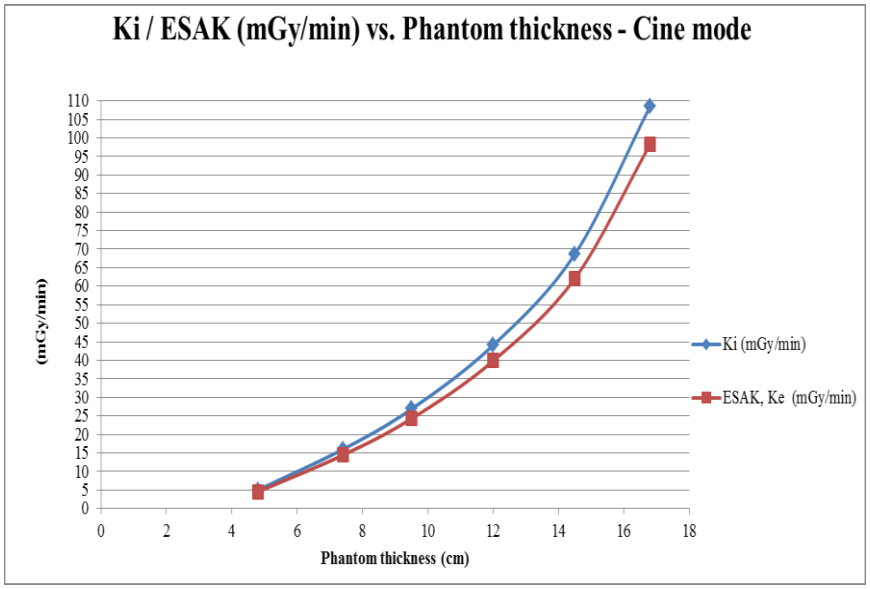

Figure 26: Proportional relation between the phantom thickness and the incident air keram rate - Cine mode

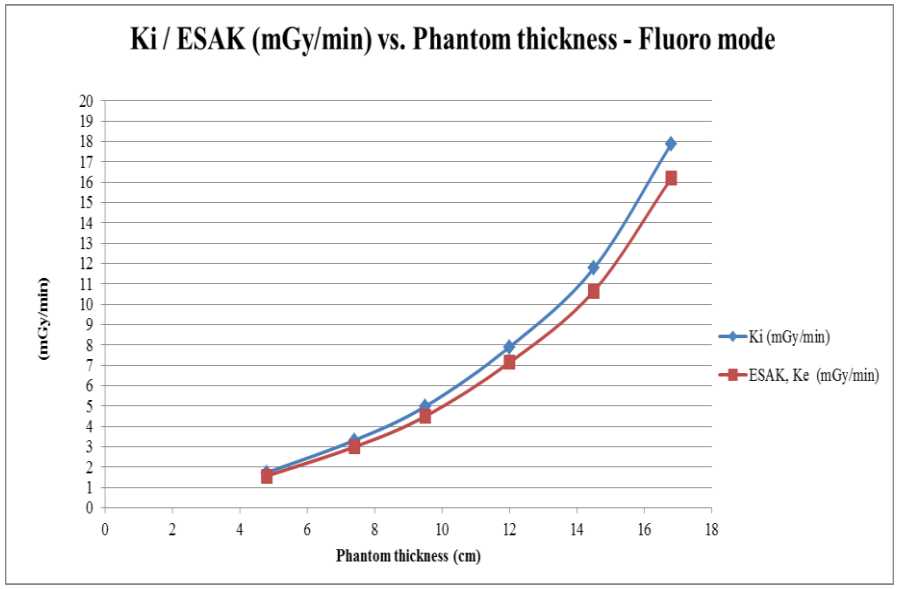

Figure 25: Propotional relation between the the phantom thickness and the incident air keram rate - Fluoro mode

Table (13) shows the measurements when paediatric protocols were selected on different phantom thickness. These measurements were performed only for the frontal tube.

Table 13: Cath lab- Phantom measurment using paediatric protcol

Fluoro mode								
Age Band	**Phantom size (cm)**	**Procedure**	**Fluoro pre Filter selected**	**K_i (mGy/min)**	**ESAK, K_e (mGy/min)**	**kVp**	**mA**	**ms**
Newborn (0-1m)	4.8	paediatric- cardio 15 fr low contrast- (< 5 kg)	0.4 Cu + 1 mm Al	1.76	1.59	68	108	4
> 1 - 10 y	7.4	paediatric- cardio 15 fr low contrast- (5-15) kg	0.4 Cu + 1 mm Al	2.83	2.56	67	100	4
> 1 - 10 y	9.5	paediatric- cardio 15 fr low contrast- (15-40) kg	0.4 Cu + 1 mm Al	4.34	3.92	63	241	4
> 10 - 15 y	12	paediatric- cardio 15 fr low contrast- (15-40) kg	0.4 Cu + 1 mm Al	6.26	5.66	64	310	4
> 10 - 15 y	14.5	paediatric- cardio 15 fr low contrast- (40- 55) kg	0.4 Cu + 1 mm Al	9.82	8.89	67	422	4
> 10 - 15y	16.8	paediatric- cardio 15 fr low contrast- (55- 70) kg	0.4 Cu + 1 mm Al	14.05	12.73	69	548	5
Cine mode								
Age Band	**Phantom size (cm)**	**Procedure**	**Exposure pre Filter selected**	**K_i (mGy/min)**	**ESAK, K_e (mGy/min)**	**kVp**	**mA**	**ms**	**µGy /fr**
Newborn (0-1m)	4.8	paediatric- cardio 15 fr low contrast- (< 5 kg)	0.1Cu + 1 mm Al	3.13	2.84	68	108	4	3.44
> 1 - 10 y	7.4	paediatric- cardio 15 fr low contrast- (5-15) kg	0.1Cu + 1 mm Al	8.15	7.38	67	101	4	8.96

> 1 - 10 y	9.5	paediatric- cardio 15 fr low contrast- (15-40) kg	0.1Cu + 1 mm Al	16.31	14.73	63	241	4	17.91
> 10 - 15 y	12	paediatric- cardio 15 fr low contrast- (15-40) kg	0.1Cu + 1 mm Al	24.54	22.18	64	310	4	26.95
> 10 - 15 y	14.5	paediatric- cardio 15 fr low contrast- (40- 55) kg	0.1Cu + 1 mm Al	41.65	37.71	67	422	4	45.75
> 10 - 15y	16.8	paediatric- cardio 15 fr low contrast- (55- 70) kg	0.1Cu + 1 mm Al	66.90	60.60	69	548	5	73.47

Continuous- Table13: Cath lab- Phantom measurment using paediatric protcol

Figure (27 and 28) shows the comparison between the two protocols (the default and the selected paediatric protocol) for both modes fluoro and cine, respectively.

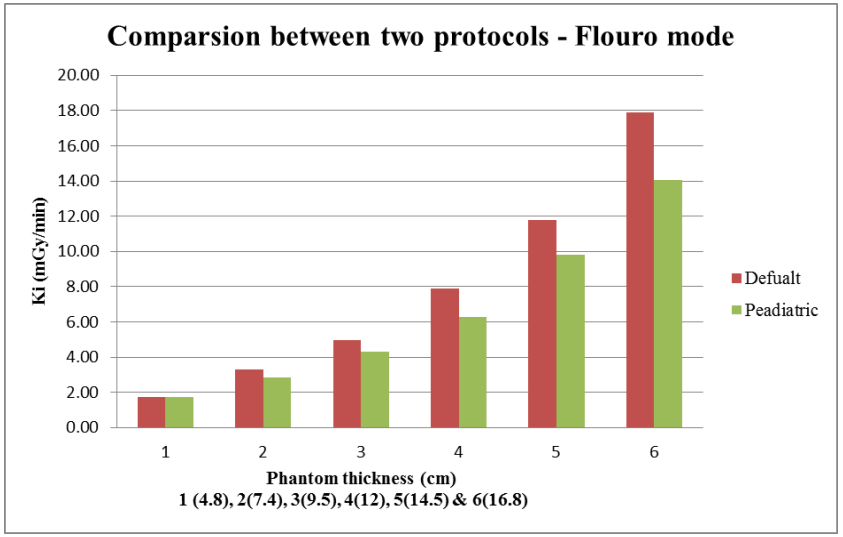

Figure 28: Cath lab- Comparsion between the two protocol- Fluoro mode

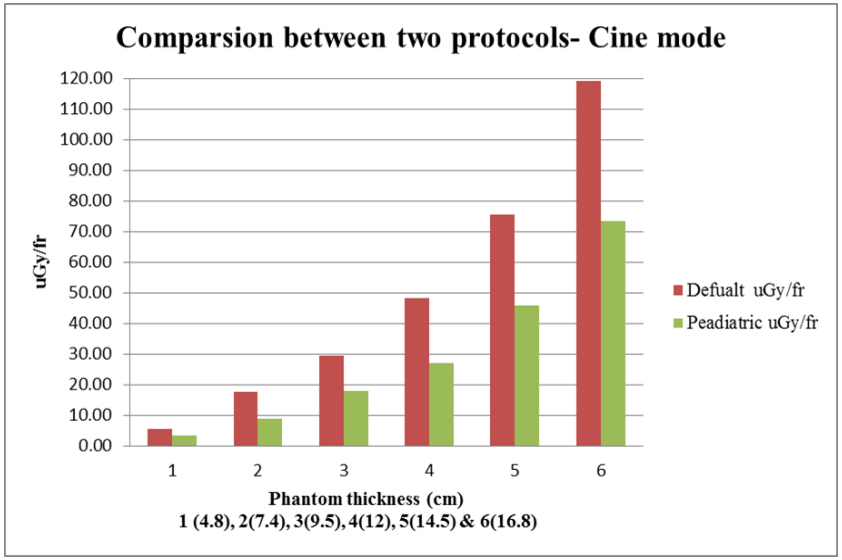

Figure 27: Cath lab - Comparison between two protocols - Cine mode

4.3.2 Verification of patient dose indicator

Table (14) shows the difference in the reading between the indicated KAP reading in the console and the measured KAP using the diagnostic dosimeter for both mode Fluoro and Cine.

Table 14: KAP verification for fluoro and cine mode

Fluoro mode								
Mode & field size (cm x cm)	**kVp**	**mA**	**K_i (mGy)**	**Area (cm2)**	**Calculated KAP (mGy.cm2)**	**Indicated KAP (mGy.cm2)**	**diff %**	**CF**
Low (25)	92	777	29.75	27.5	818.17	603.67	-26.22%	1.36
Normal (25)	92	777	30.50	27.5	838.74	603.33	-28.07%	1.39
High (25)	91	784	30.51	27.5	839.04	613.00	-26.94%	1.37
Normal (20)	94	763	30.49	27.5	838.41	609.67	-27.28%	1.38
Normal (15)	97	738	30.39	27.5	835.77	498.67	-40.33%	1.68
Cine mode								
Mode & field size (cm x cm)	**kVp**	**mA**	**K_i (mGy)**	**Area (cm2)**	**Calculated KAP (mGy.cm2)**	**Indicated KAP (mGy.cm2)**	**diff %**	**CF**
Low (25)	92	777	44.04	27.5	1211.01	844.00	-30.31%	1.43
Normal (25)	92	777	51.43	27.5	1414.33	1006.00	-28.87%	1.41
High (25)	91	784	44.75	27.5	1230.69	894.00	-27.36%	1.38
Normal (20)	94	763	44.21	27.5	1215.81	875.00	-28.03%	1.39
Normal (15)	97	738	52.03	27.5	1430.85	836.00	-41.57%	1.71

Table (15) shows the difference in the reading between the indicated CAK reading in the console and the measured CAK using the diagnostic dosimeter for both mode Fluoro and Cine.

Table 15: Cumulative air kerma (CAK) verification for fluoro and cine mode

Fluoro mode								
Mode & field size (cm x cm)	**kVp**	**mA**	**Ki (mGy)**	**FDD**	**Calculated Ki @ IRP**	**Indicated CAK (mGy)**	**diff %**	**CF**
Low (25)	92	777	29.75	76.5	46.03	42.80	-7.02%	1.08
Normal (25)	92	777	30.50	76.5	47.19	44.04	-6.67%	1.07
High (25)	91	784	30.51	76.5	47.21	44.23	-6.31%	1.07
Normal (20)	94	763	30.49	76.5	47.17	44.28	-6.13%	1.07
Normal (15)	97	738	30.39	76.5	47.02	43.96	-6.51%	1.07
Cine mode								
Mode & field size (cm x cm)	**kVp**	**mA**	**Ki (mGy)**	**FDD**	**Calculated Ki @ IRP**	**Indicated CAK (mGy)**	**diff %**	**CF**
Low (25)	92	777	44.04	76.5	68.14	65.44	-3.96%	1.04
Normal (25)	92	777	51.43	76.5	79.58	77.72	-2.34%	1.02
High (25)	91	784	44.75	76.5	69.24	69.18	-0.10%	1.00
Normal (20)	94	763	44.21	76.5	68.41	67.74	-0.97%	1.01
Normal (15)	97	738	52.03	76.5	80.51	79.50	-1.25%	1.01

Table (16) illustrates the patient demographic information's and the dosimetric values that collected manually by the technicians at the interventional cardiology.

Table 16: Cath lab- Patient demographic and dosimetric information

Age group	No. of patient	Statistic	Weight (kg)	Height (cm)	Age	Total KAP (mGy. cm2)	Total Air Kerma (mGy)	No. of series	No. of Images	f/s	FT (min)
Newborn (days)	3	Mean	3.63	49.33	5.8	2258.4	26.76	5.00	542.00	15	7.03
		3rd Quartile	3.85	50	8.2	2703.2	31.51	6.00	587.50	15	7.83
		SD	0.51	1.15	7.5	815.33	8.59	2.83	128.69	0	1.41
>0-1y (months)	30	Mean	7.14	67.31	7.0	10682.7	10.68	149	8.45	1138	17.5
		3rd Quartile	7.5	69	8.9	10294.4	10.29	160.5	10.00	1338	15
		SD	3.50	14.53	2.9	9255.87	9.26	124.1	3.89	605	5.69
>1-5y	30	Mean	12.16	92.46	2.9	20454.4	217.19	9.83	1164.6	16.0	14.4
		3rd Quartile	15.75	108	4.50	19476.8	223.28	13.75	1557.8	15	20.2
		SD	4.16	18.04	1.55	31969.2	282.71	6.04	801.35	4.80	11.9
>5- 10y	20	Mean	18.34	103.9	6.58	19089.8	175.57	7.05	876.35	15.8	10.6
		3rd Quartile	20.22	119.5	7.25	25494.9	207.76	7.25	1058.5	15	13.0
		SD	5.58	32.97	1.11	14239.9	139.64	5.55	660.73	3.35	6.81
>10-15y	5	Mean	52.33	151.2	12.3	53622.8	538.52	7.40	888.40	15	30.3
		3rd Quartile	59.15	153.2	12.6	85646.6	1010.9	14.00	1428	15	35.3
		SD	21.65	5.87	1.4	63515.8	492.10	6.19	920.28	-	34.6

4.4 Effective Dose and Risk Assessment

4.4.1 Paediatric E in fixed and mobile x-ray

Table (17) displays the E for the paediatric patient in different five examinations and the stochastic radiation risk for both genders in the fixed x-ray unit.

Table 17: Fixed x-ray-Effective dose for paediatric patient and the stochastic radiation risk for both genders

Age Group	**Newborn (0 - 1 m)**		**>0 - 1 y**		**>1 - 5y**		**>5 - 10 y**		**>10 - 15 y**	
Examination	**KAP ($\mu Gy.m^2$)**	**Effective dose (E) (µSv)**	**KAP ($\mu Gy.m^2$)**	**Effective dose (E) (µSv)**	**KAP (µGy.m2)**	**Effective dose (E) (µSv)**	**KAP ($\mu Gy.m^2$)**	**Effective dose (E) (µSv)**	**KAP ($\mu Gy.m^2$)**	**Effective dose (E) (µSv)**
chest (AP)	0.48	15.81	0.73	12.89	1.24	12.63	2.81	22.11	4.27	22.73
Abdomen (AP)	1.40	35.07	4.05	37.02	5.57	36.78	16.78	80.73	39.97	103.3
Chest/Abdomen (AP)	0.90	28.50	1.99	28.28	3.10	4.16	13.12	10.75	15.78	9.722
Pelvis	1.70	9.02	3.30	30.75	5.54	29.56	13.53	41.78	33.27	68.6
Extremities (Hand(AP))	0.80	0.844	0.89	0.375	1.37	0.25	1.45	0.09	2.06	0.054

Chest	Male -Stochastic radiation risk		Female Stochastic radiation risk	
Age Group	**Risk of Exposure -Induced cancer death (REID) %**	**Loss of life expectancy (LLE)**	**Risk of Exposure -Induced cancer death (REID) %**	**Loss of life expectancy (LLE)**
Newborn	1.59E-04	0.5 hr	3.99E-04	0.8 hr
> 0 - 1 y	1.03E-04	0.3 hr	3.34E-04	0.5 hr
>1 - 5y	9.71E-05	0.2 hr	2.64E-04	0.4 hr
>5 - 10 y	1.62E-04	0.4 hr	3.70E-04	0.6 hr
>10 -15 y	1.33E-04	0.3 hr	2.99E-04	0.5 hr
Abdomen	**Male -Stochastic radiation risk**		**Male -Stochastic radiation risk**	
Age Group	**Risk of Exposure -Induced cancer death(REID) %**	**Loss of life expectancy (LLE)**	**Risk of Exposure -Induced cancer death(REID) %**	**Loss of life expectancy (LLE)**
Newborn	3.82E-04	1.1 hr	6.66E-04	1.6 hr
> 0 - 1 y	4.71E-04	1.2 hr	5.13E-04	1.5 hr
>1 - 5y	3.91E-04	0.8 hr	4.35E-04	1 hr
>5 - 10 y	6.73E-04	1.4 hr	9.20E-04	1.9 hr
>10 -15 y	8.37E-04	1.7 hr	9.08E-04	2.0 hr
Chest-Abdomen	**Male -Stochastic radiation risk**		**Female Stochastic radiation risk**	
Age Group	**Risk of Exposure -Induced cancer death(REID) %**	**Loss of life expectancy (LLE)**	**Risk of Exposure -Induced cancer death(REID) %**	**Loss of life expectancy (LLE)**
Newborn	2.96E-04	0.9 hr	6.02E-04	1.4 hr
> 0 - 1 y	2.86E-04	0.7 hr	6.18E-04	1.2 hr
Lat. Skull (post nasal space)	**Male -Stochastic radiation risk**		**Male -Stochastic radiation risk**	
Age Group	**Risk of Exposure -Induced cancer death(REID) %**	**Loss of life expectancy (LLE)**	**Risk of Exposure -Induced cancer death(REID) %**	**Loss of life expectancy (LLE)**
>1 - 5y	3.37E-05	0.1 hr	3.81E-05	0.2 hr
>5 - 10 y	6.57E-05	0.2 hr	7.53E-05	0.3 hr
>10 -15 y	4.69E-05	0.1 hr	5.45E-05	0.2 hr
Pelvis	**Male -Stochastic radiation risk**		**Female Stochastic radiation risk**	
Age Group	**Risk of Exposure -Induced cancer death(REID) %**	**Loss of life expectancy (LLE)**	**Risk of Exposure -Induced cancer death(REID) %**	**Loss of life expectancy (LLE)**
Newborn	1.03E-04	0.4 hr	6.90E-05	0.3 hr

> 0 - 1 y	3.11E-04	1.1 hr	2.12E-04	0.7 hr
>1 - 5y	2.23E-04	0.6 hr	1.47E-04	0.4 hr
>5 - 10 y	2.52E-04	0.6 hr	1.65E-04	0.4 hr
>10 -15 y	3.43E-04	0.7 hr	2.29E-04	0.5 hr
Extremities	**Male -Stochastic radiation risk**		**Female Stochastic radiation risk**	
Age Group	**Risk of Exposure -Induced cancer death(REID) %**	**Loss of life expectancy (LLE)**	**Risk of Exposure -Induced cancer death(REID) %**	**Loss of life expectancy (LLE)**
Newborn	9.08E-06	0.1 hr	8.28E-06	0.1 hr
> 0 - 1 y	3.62E-06	0 hr	3.51E-06	0 hr
>1 - 5y	1.96E-06	0 hr	1.91E-06	0 hr
>5 - 10 y	5.35E-07	0 hr	5.72E-07	0 hr
>10 -15 y	2.66E-07	0 hr	3.26E-07	0 hr

Continuous- Table17: Fixed x-ray-Effective dose for paediatric patient and the stochastic radiation risk for both genders

Table (18) displays the E for the neonatal patient in the intensive care unit and the stochastic radiation risk fort both genders using the mobile x-ray.

Table 18: Mobile x-ray - Effective dose and stochastic radiation risk

Neonatal			**Male -Stochastic radiation risk**		**Female Stochastic radiation risk**	
Examination	**KAP ($mGy.cm^2$)**	**Effective dose E (µSv)**	**Risk of Exposure -Induced cancer death(REID) %**	**Loss of life expectancy (LLE)**	**Risk of Exposure -Induced cancer death(REID) %**	**Loss of life expectancy (LLE)**
chest/ Abdomen	8.93	23.03	2.45E-04	0.7 hr	5.71E-04	1.2 hr

4.4.1 Paediatric E in interventional cardiology

Table (19) displays the E for the paediatric patient in the interventional cardiology and the stochastic radiation risk for both genders.

Table 19: Cath lab-Effective dose and stochastic radiation risk

Interventional Cardiology			Male -Stochastic radiation risk		Female Stochastic radiation risk	
Age group	**Total KAP (Gy.cm2)**	**Effective dose E (mSv)**	**Risk of Exposure -Induced cancer death(REID) %**	**Loss of life expectancy (LLE)**	**Risk of Exposure -Induced cancer death(REID) %**	**Loss of life expectancy (LLE)**
Newborn	2.26	2.44	3.01E-02	3.4 days	5.10E-02	6.5 days
> 0 - 1 y	10.68	6.35	9.23E-02	11.6 days	1.42E-01	18.3 days
>1 - 5y	20.45	12.24	1.39E-01	14.4 days	2.49E-01	23.5 days
>5 - 10 y	19.09	9.78	9.74E-02	9.2 days	1.66E-01	15.7 days
>10 -15 y	53.62	14.04	1.22E-01	11.2 days	2.08E-01	20.2 days

4.5 LDRL Comparison with other worldwide published surveys

Table (20) shows the LDRL comparison between the results obtained from this study and the other worldwide surveyor's results for the paediatric patient undergoing radiological procedures in the digital fixed x-ray.

Table 20: Fixed x-ray- LDRL Comparison between current study and other surveyor's results

Examination	Age group	ESAK (K_e) (µGy)							
		Current study	DHA- Children and women's hospital (2015) [63]	Austria (2010) [10]	Sudan - Omdurman hospital (2008) [40]	UNSCARE (2008) [2]	Italy (2005) [57]	Ireland (2004) [55]	UK (2000) [56]
Chest	Newborn	37.53	54.69	55	52	60	80	-	50
	>0-1y	37.36	68.87	69	80	80	-	57	50
	>1-5 y	41.00	45.84	82	192	110	100	53	70
	>5 - 10 y	62.33	64.3	108	157	70	-	66	120
	>10 - 15 y	61.78	136.44	112	222	110	-	88	-
Abdomen	Newborn	62.18	56.4	100	145	110	-	-	-
	>0-1y	117.10	65.3	172	209	340	-	330	400
	>1-5 y	107.49	94.88	511	465	590	1000	752	500
	>5 - 10 y	207.35	284.95	966	-	860	-	-	800

	>10 - 15 y	396.31	-	-	-	2010	-	-	1200
Examination	**Age group**	**ESAK (Ke) (µGy)**							
		Current study	**DHA- Children and women's hospital (2015) [63]**	**Austria (2010) [10]**	**Sudan - Omdurman hospital (2008) [40]**	**UNSCARE (2008) [2]**	**Italy (2005) [57]**	**Ireland (2004) [55]**	**UK (2000) [56]**
Pelvis	Newborn	69.44	-	-	204	170	200	-	-
	>0-1y	162.29	-	-	234	350	-	265	500
	>1-5 y	165.06	-	-	354	510	900	475	600
	>5 - 10 y	231.45	-	-	504	650	-	807	700
	>10 - 15 y	450.01	-	-	-	1300	-	892	2000
Lat. Skull (Post Nasal Space)	Newborn	-	-	294	-	-	-	-	-
	>0-1y	-	-	700	-	340	-	-	500
	>1-5 y	131.92	-	506	-	580	1000		800
	>5 - 10 y	508.81	-	557	-	-	-	-	800
	>10 - 15 y	506.74	-	676	-	-	-	-	800

Continuous- Table 20: LDRL Comparison between current study and other surveyor's results

Table (21) displays the KAP values that obtained in this study compared to the KAP values in other published surveys for the fixed x-ray machine.

Table 21: Fixed x-ray- KAP comparison with other surveyor's

Examination	Age group	KAP (P_{KA}) (mGy . cm^2)		
		Current study	Ireland (2013)[43]	Austria (2010)[10]
Chest	Newborn	4.80	-	17
	> 0 - 1y	7.28	8.6	23
	> 1 - 5 y	12.37	15.3	26
	> 5 - 10 y	28.06	21.1	37
	> 10 - 15 y	42.69	41	73
Abdomen	Newborn	14.00	-	60
	> 0 - 1y	40.46	10	90
	> 1 - 5 y	55.68	116	200
	> 5 - 10 y	167.76	325.5	500
	> 10 - 15 y	399.66	503.8	700
Pelvis	Newborn	17.00	-	-
	> 0 - 1y	32.98	22	-
	> 1 - 5 y	55.42	49.9	-
	> 5 - 10 y	135.29	140.5	-
	> 10 - 15 y	332.68	174.1	-
Lat. Skull (Post Nasal Space)	Newborn	-	-	100
	> 0 - 1y	-	-	200
	> 1 - 5 y	30.96	-	250
	> 5 - 10 y	131.23	-	300
	> 10 - 15 y	157.85	-	350

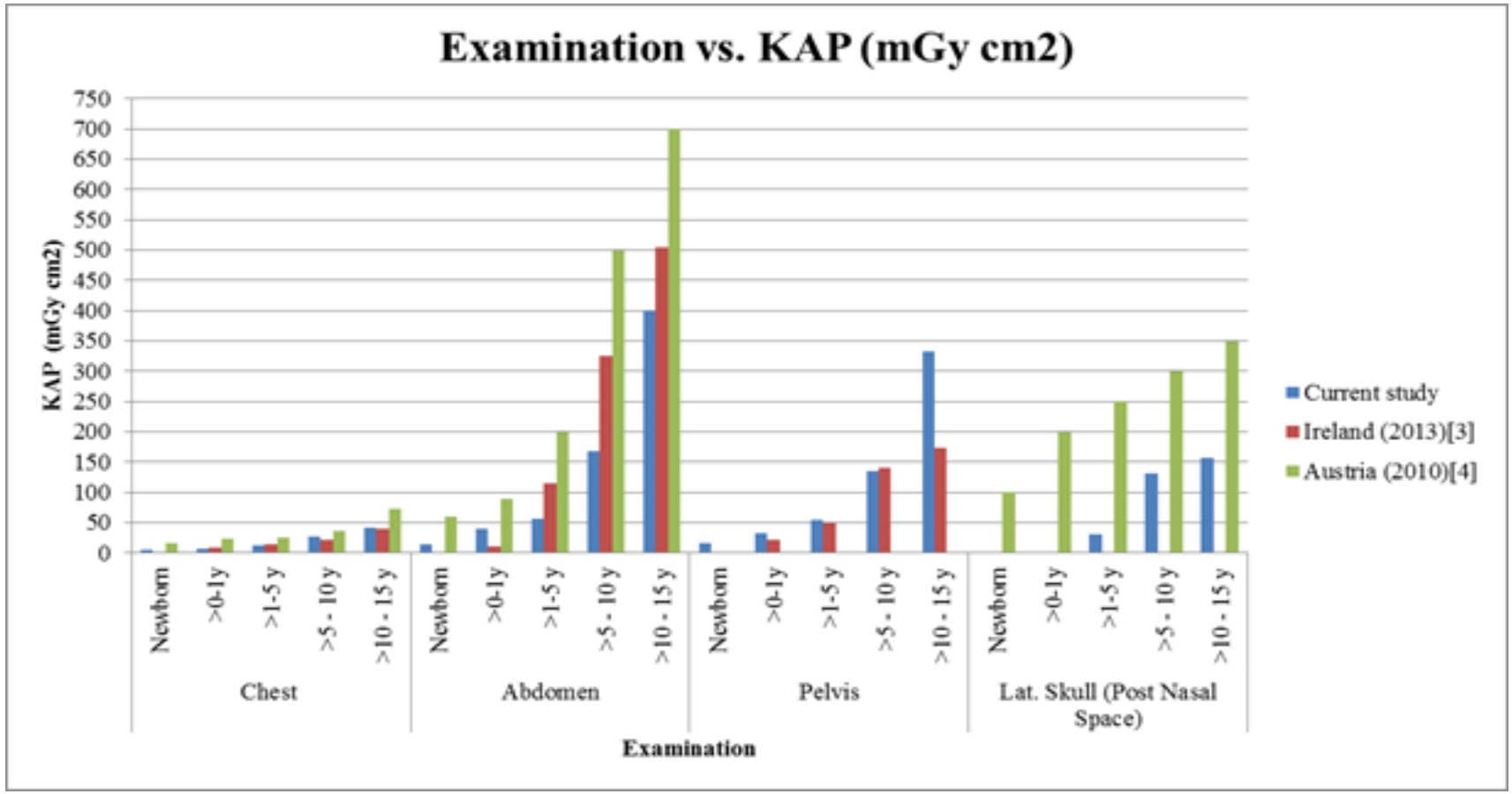

Figure 29: Comparison between current study KAP values and other published surveys

Table (22) shows the LDRL comparison between present study findings for the combined chest-abdomen examination in the NICU at Dubai hospital and other surveyors form different countries. The comparison includes the number of patients, ESAK, KAP and E.

Table 22: Mobile x-ray- LDRL ESAK and KAP comparison with other surveyor's

Neonatal – Combined Chest-Abdomen				
Surveyors	**No. of patient**	**ESAK (µGy)**	**KAP (P_{KA}) (mGy . cm2)**	**E (µSv)**
Current study	41	56.58	8.93	23.03
KSA (2014) [48]	135	80	-	20
Greece (2007) [60]	378	38.2	7.2	-
Belgium (2013) [47]	285	43	11	-

Table (23) displays the LDRL comparing the KAP findings in this study for IC to the other published surveys data from selected countries. Also, it includes the data that was collected between 2010 and 2012 for the same IC system in Dubai hospital. Table (24) compares the E findings in this study to selected countries.

Table 23: Interventional Cardiology- LDRL KAP values comparison with other published surveys

Examination	Age group	KAP (P_{KA}) (Gy . cm^2)							
		Current study	DHA- DH (2012) [63]	UK (2010) [58]	UK (2013)[52] Diagnostic procedure	Belgium (2008)[59]		Sweden(2009)[61]	
						Diagnostic 75th percentile	Therapeutic 75th percentile	Diagnostic	Therapeutic
Interventional cardiology	Newborn	2.25 ± 0.815	-	-	-	4.1	6.5	3.7 ±2.6	3.2 ±4.1
	>0-1y	10.68 ± 9.25	11.43	4.12	1.9 ±1.52	5.4	9.2	6.0 ±5.8	2.6 ±5.1
	>1-5 y	20.45 ±31.96	10.35	9.23	4.21 ±5.76	8.7	17.35	7.6 ±9.5	7.8 ±11.8
	>5 - 10 y	19.08 ± 4.23	20.01	18.11	5.82 ± 4.78	12.3	27	15.9 ±12.9	10.0 ±9.7
	>10 -15y	53.62 ± 63.51	13.41	28.14	12.89 ± 12.22	16.6	74.4	37.9 ±52.3	34.2 ±38.9

Table 24: Interventional Cardiology- Effective Dose comparison with others published surveys

Examination	Age group	E (mSv)				
		Current study	UK (2010) [58]	Belgium (2008) [59]		Sweden (2009) [61]
				Diagnostic 75th percentile	Therapeutic 75th percentile	
Interventional cardiology	Newborn	2.438	-	11.3	22.6	13
	>0-1y	6.352	8.45	9.7	18.6	8.6
	>1-5 y	12.24	7.52	8.55	17.4	6.4
	>5 - 10 y	9.776	7.52	7	17.8	8.6
	>10 -15y	14.04	3.63	7	34.1	12.7

Chapter 5: Discussion

This study was conducted at Dubai hospital to evaluate the radiation exposure for paediatric patients. It was designed to reflect authentic clinical imaging situations for paediatric patients in the general x-ray and interventional cardiology practices. The major aim of this study is to participate in establishing the LDRL for paediatric patients at Dubai hospital. It is expected that the radiology quality control programs and the radiation exposure levels {IAK (K_i), ESAK (K_e), EASK rate ($\dot{K}_e$) and KAP values} for the paediatric patients are within the recommended standards and are comparable with other published studies. Furthermore, this study evaluates the radiation risk (effective dose).

The outcomes of the present work in Chapter 4 (Results) based on phantom study and clinical data derived from the DICOM header for both fixed x-ray and mobile x-ray machines while for interventional cardiology procedures the patient exposure data were collected manually by the Cath lab technicians. In general, mean ESAK results in Table (4) and (20) for the paediatric patients who have undergone diagnostic procedures using fixed x-ray were lower than the findings of other researchers. Moreover, for the mean KAP values, readings were comparable and lower than other published values [43, 10]. Evidently, the mean ESAK values in Table (22) obtained from mobile x-ray procedures for neonatal in the NICU was found to be comparable and slightly higher than other literature findings that were reviewed in this study [47, 48, 60].

The patient radiation exposure data in the interventional cardiology were collected by the technicians. Mixtures of data were found between diagnostic and

interventional procedures, but the majority was for the therapeutic procedures. In comparing KAP results in this study with those mentioned in the selected literature, the results of this study were higher [52, 58, 59, 61].

5.1 Digital Fixed X-ray

The number of diagnostic examinations for paediatric patients is increasing over the years in Dubai hospital as shown in Table (25). Hence, an evaluation for the radiation exposure received by this group of patients is very important. It has been known that paediatric patients are at higher risk form radiation exposure than the adults. Although the amount of dose in diagnostic radiology is not significant for tissue reaction effects, but the long life expectancy for the paediatric patients makes the occurrence of stochastic effects of a high possibility [14].

Table 25: Fixed x-ray - Statistic on the number of paediatric patient in Dubai hospital

Year	Total no. of patient	Female	Male	(0 -1) Y	(>1- 5) Y	(>5 - 10) Y	(>10 - 15) Y
2012	5612	2448	3164	133	3747	1001	732
2013	6545	2749	3796	2113	2204	1174	1054
Aug-14	4613	1985	2628	1391	1592	963	667

The digital Philips machine in room 1 shown in Figure (6) at Dubai hospital was used to perform the majority of the paediatric x-ray examinations. The exposure parameter (kVp & mAs) were fully selected by the AEC. The phantom study in Table (4) shown that for the patient of age groups (newborn (0-1m), > 0-1y and > 1-3 y) the AEC is off for the abdomen and pelvis examinations. For other examinations: Chest, combined chest–abdomen and extremities they were performed on the table where the digital cassette was under the patient directly. Moreover, all the x-ray bucky examinations were performed in the presence of the grid for all age groups.

Phantom study was repeated for the **abdomen** examination for the patient of age group (newborn and > 0-1y) when the acquisition is table top (no grid) and the cassette is directly under the patient. In this set up, it was found that there is a reduction in the dose by 25% for newborn and 19% for >0-1y. Moreover, the study was repeated while the AEC was switched on for both age groups but taken into considerations that the AEC ionization chamber is activated and covered by the phantom. The results shown that there is a dramatic reduction for the newborn by 49 % while for the age group >0-1y the dose increased dramatically by 40%.

For the **pelvis** examinations, the phantom study was repeated while the AEC is switched on for both previous groups. The reduction was for the newborn by 50% while dose increased for the group >0 -1y by 21%.

This variation in the dose for both age groups for the abdomen and pelvis examinations shown that the AEC is not sensitive for the patients below 3 years old and an exposure chart based on the patient weight is recommended for patients of age less than 3 years old. The same recommendations are written in the ICRP 121 [1]; it is much safer to use exposure chart based on weight for the trunk examinations and patient age for extremities examinations.

For the combined **chest-abdomen** examinations, there was a clear difference in the patient dose when using chest protocol and abdomen protocol wherein the dose was lower by using the chest protocol. Hence, it is highly recommended the use of the chest protocol for this combined examination. Furthermore, it is recognized from Table (4) and the below graph (Figure 30) that the ESAK increases as patient age group increase except for the extremities examinations. The highest extremities value were found for the age group >1-5y; because the mAs was higher than the

other age groups. Moreover, to reduce child dose in the chest examinations, specially the age group (>1-5y), vertical bucky is recommended with cooperative patients otherwise the grid should not be used for lying position.

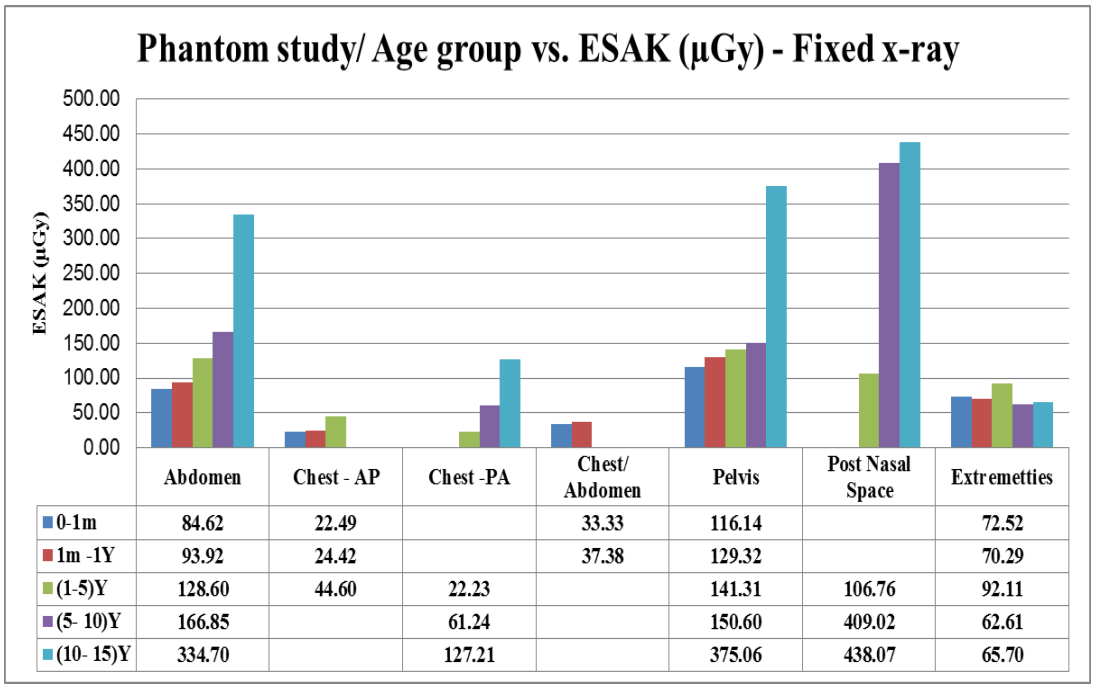

	Abdomen	Chest - AP	Chest -PA	Chest/ Abdomen	Pelvis	Post Nasal Space	Extremetties
0-1m	84.62	22.49		33.33	116.14		72.52
1m -1Y	93.92	24.42		37.38	129.32		70.29
(1-5)Y	128.60	44.60	22.23		141.31	106.76	92.11
(5- 10)Y	166.85		61.24		150.60	409.02	62.61
(10- 15)Y	334.70		127.21		375.06	438.07	65.70

Figure 30: Phantom study- ESAK vs. Patient age groups

The patient data which was collected from the DICOM header were displayed in Table (5) revealed the authentic situation of the patient radiation doses. It is considered as one of the most efficient methods used recently for estimating the patient ESAK indirectly form the digital system. A number of surveyors and organizations recommended the use of this method as it is more straightforward and systematic [18, 43, 41]. The data collected shows that the numbers of the cases for newborn patients were 2 and 4 for the pelvis and extremities examinations, respectively. The results of this group were limited because the sample is very small. The mean ESAK values published by different surveyors were summarized in the graph (Figure 31) for the five common examinations covered in this study. The dose levels for **chest** examinations of the first two age groups (newborn and > 0-1y) were

almost identical. This is because AEC was switched off for these two age groups. This dose level similarity also observed for the last two age groups (> 5-10 y and >10 – 15 y). That is due to the automatic selection of same exposure parameters.

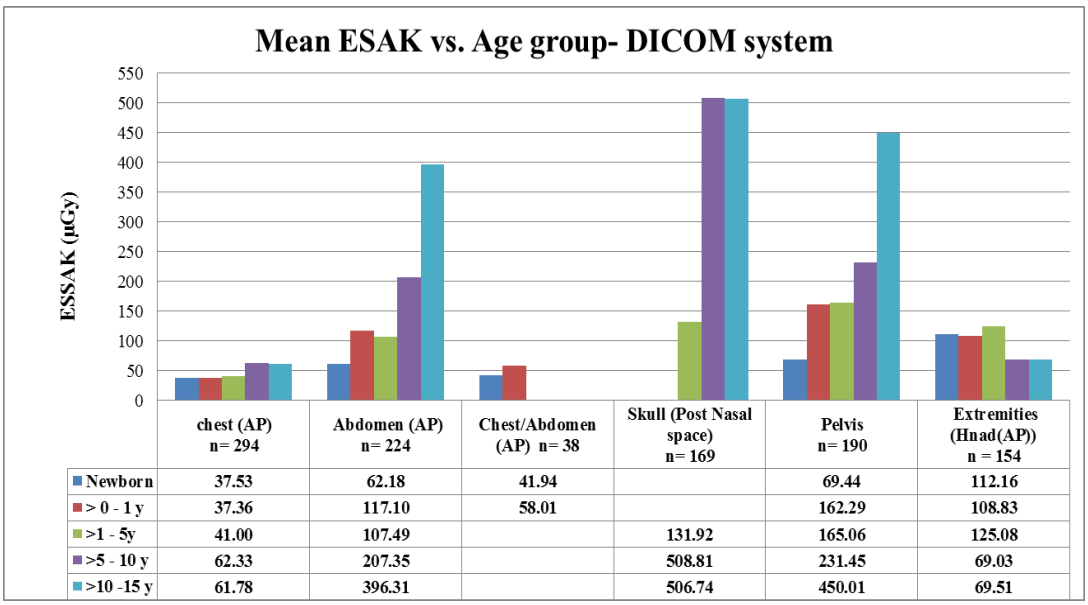

	chest (AP) n= 294	Abdomen (AP) n= 224	Chest/Abdomen (AP) n= 38	Skull (Post Nasal space) n= 169	Pelvis n= 190	Extremities (Hnad(AP)) n = 154
Newborn	37.53	62.18	41.94		69.44	112.16
> 0 - 1 y	37.36	117.10	58.01		162.29	108.83
>1 - 5y	41.00	107.49		131.92	165.06	125.08
>5 - 10 y	62.33	207.35		508.81	231.45	69.03
>10 -15 y	61.78	396.31		506.74	450.01	69.51

Figure 31: Mean ESAK vs. Age groups - DICOM system

The **abdomen** examinations have shown an increasing trend with the increase of the patient age except for the group (> 0-1y). The ESAK value for the group (> 0-1y) was 117.1 µGy which is higher than the group (>1-5y) where the value was 107.49 µGy. There was no clear reason except that there is a variation between the patient sizes within the same age group. Similar findings were observed by Matthews K. et al., (2013) [43], where he stated that the reason for the variation in the KAP values was not related to the radiographer technique; it was due to the variation in the patient size within the same age category. Moreover, the ICRP and IAEA mentioned this issue in their publications [14, 18, 1]. Similar dose levels were observed for the skull examinations of the last two age groups; the ESAK values for the (>5-10 y) was 508.81 µGy while for the (>10-15y) was 506.74 µGy. However,

the dose difference between these two groups was not significant. It is expected that the reason behind this situation is that the exposure parameters were similar.

The **pelvis** examinations demonstrated smooth linear relationship with the increasing of the patient age. For the extremities, the mean ESAK values were fluctuating between the patient age groups; the main reason was the limited number of the patients in the first two age groups and the collimation selected by the radiographer. In general, the trend is that the patient radiation dose is increasing with the increasing of the age group which has been also stated in Linet et al., (2009) survey [38].

Another method to calculate the patient ESAK was intended to be used indirectly through the fitting function (y) in (Figures from 18 to 22), which derived from measurements of the x-ray tube output Y (d) in Table (7). The patient's data collection samples were very limited. Due to the time limitation it was not possible to complete the patient dose calculations using the tube output method as had been described it in Chapter 3 (Methodology). In future, if the hospital collects significant number of patients data samples for the different x-ray examinations and the machine is maintained stable through systematic quality control, they can utilize the fitting functions (y) that were produced form this work to estimate the patients ESAK. Furthermore, this method is considered as a backup in case of the KAP damage or corruption in the DICOM system.

Table (20) together with graph (Figures 32) illustrated the LDRL comparison between the ESAK obtained from this study and other published data. It is clearly shown that our ESAK values were the lowest among the other published data. Also, it is noticed that there is no data by the other surveyors on the radiation dose for the

combined chest-abdomen and extremities examinations. Furthermore, Table (21) and Figure 29 show that the KAP values in this study for the five common examinations were lower than the values of Austria [10] and Ireland [43]. Apart for the pelvis examinations, our KAP values were higher than the values mentioned in the Ireland reference.

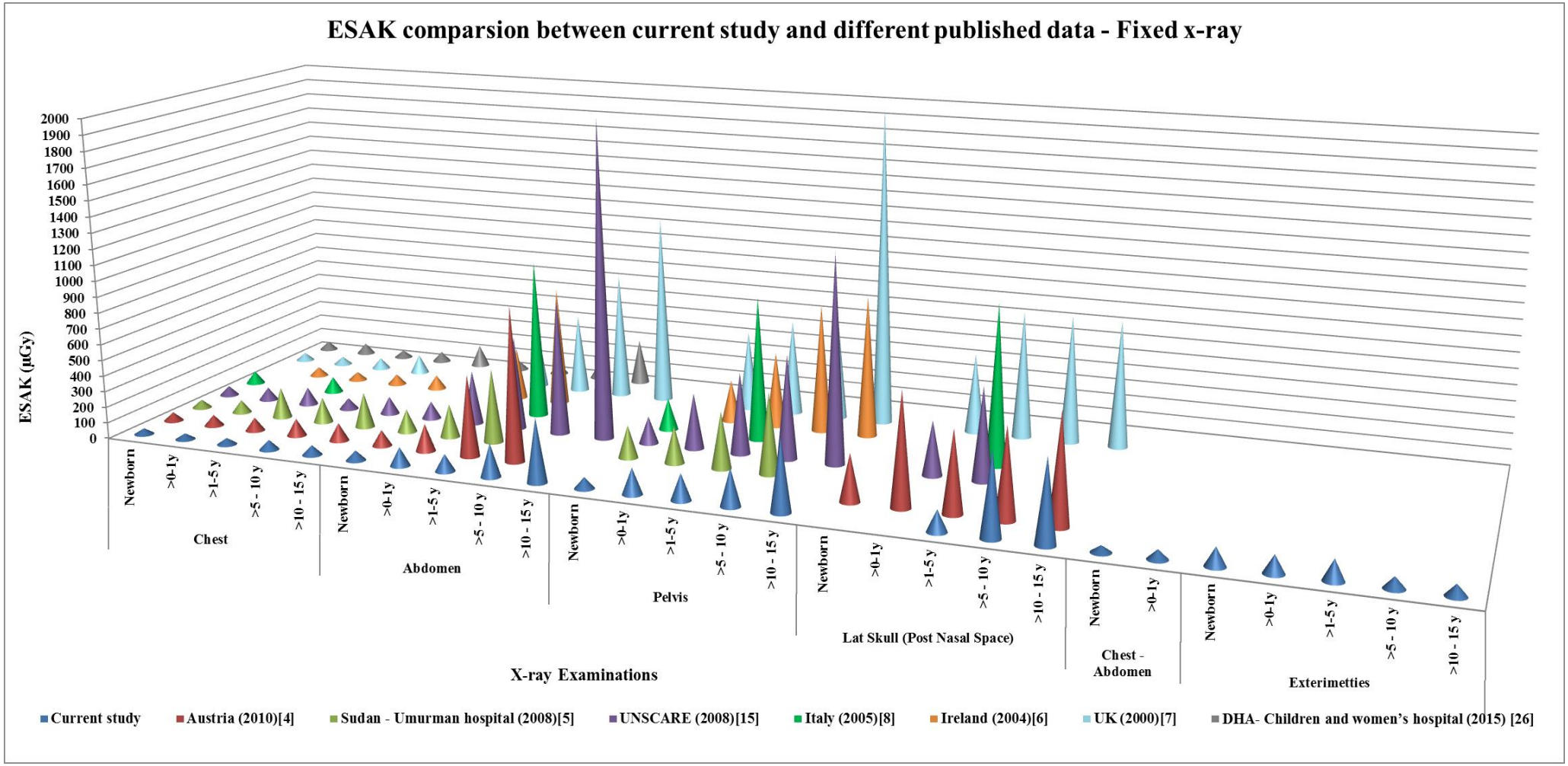

Figure 32: Fixed x-ray- LDRL ESAK Comparison between current study and other published surveys

5.2 Digital Mobile X-ray (Neonatal Intensive Care Unit)

The use of mobile x-ray machine in diagnostic radiology is a helpful tool for the immobilized patients who are admitted in the hospital. According to the statistics on the number of the mobile x-ray machine examinations at Dubai hospital, as displayed in the Table (26), it is noticed that the highest percentage of the examinations performed was for the paediatric patients of age group (0-1) y. Hence, 41 patients were selected from the DICOM system at Dubai hospital NICU to investigate the radiation dose level delivered to them during their hospitalization as shown in Table (9).

Table 26: Statistic on the number of the mobile x-ray examination

YEAR	Total no. of patient	Female	Male	(0 -1) Y	(>1- 5) Y	(>5 - 10) Y	(>10 - 15) Y
2012	1789	825	964	1389	320	45	36
2013	1939	789	1150	1362	389	72	106
Aug-14	1258	505	753	1031	149	43	35

In addition, the free in air measurements performed on the mobile x-ray with different tube potentials, as presented in Table (8), shows that the maximum difference between the measured and indicated air kerma was 14.38 % while the minimum was 6.6% for the field size of 25.5 cm x 26 cm. For the filed size 17 cm x 13 cm, the maximum was 23.1% and minimum was15.6 %. The tube output was calculated and fitting function was generated from these measurements as had been done with the fixed x-ray machine.

The mean ESAK that derived from the DICOM header in Table (9) and the values measured in Table (8), using the same exposure parameters (kVp and mAs), were similar; they were 56.58 µGy and 52.44 µGy, respectively. We predict that in

this age group of patients most of the radiographers using the same exposure parameters. Moreover, the mean value for the exposure parameters that used for the neonates in this study were 53 kVp and 1.98 mAs, were less than those recommended by the Commission of the European Communities (CEC) (CEC, 1996) [13], where the voltage of kVp ranged from 60 to 65. The ESAK value of this study was lower than the value recommended by the CEC (80 µGy); this is due to the fact that this recommendation was for screen film system whereas our system is digital.

From Table (22) and Figure (33), it is noticed that the mean ESAK values for the combined chest –abdomen examination for this work was higher than the data published for Greece and Belgium [60, 47] and lower than those for Kingdom of Saudi Arabia (KSA) [48]. The KAP readings in this study were lower than the readings from Belgium [47] and comparable to those from Greece [60]. The main reasons for this variation in the ESAK doses among the surveyors are mainly due to the use of different exposure factors, type of the x-ray machines used (digital, computed tomography or screen film), tube filtration and collimation.

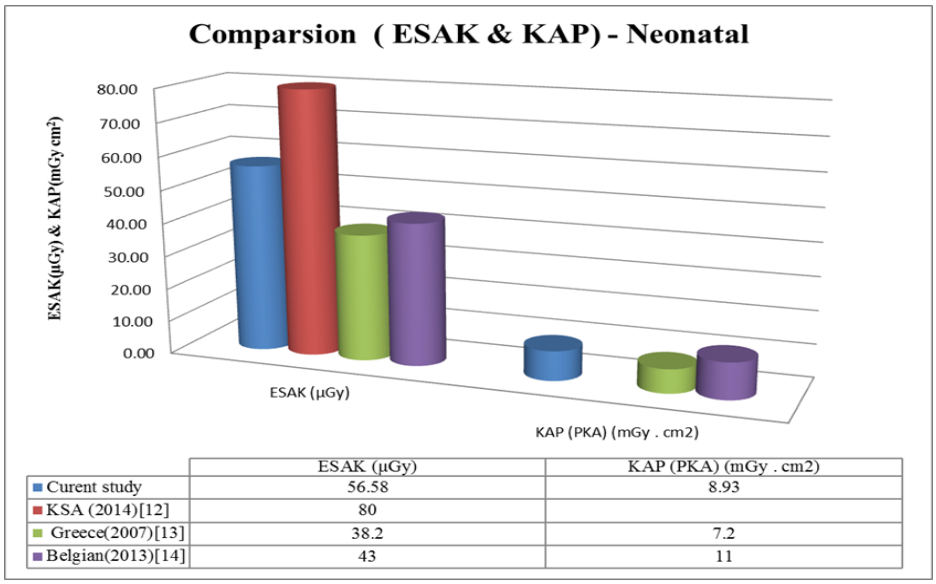

	ESAK (µGy)	KAP (PKA) (mGy . cm2)
Curent study	56.58	8.93
KSA (2014)[12]	80	
Greece(2007)[13]	38.2	7.2
Belgian(2013)[14]	43	11

Figure 33: Neonatal (NICU) - Comparison the LDRL with other published surveys

5.3 Interventional Cardiology

Interventional cardiology is considered as the x-ray modality that delivers the highest radiation dose to the patients compared to the fixed and mobile x-ray units. As a first step, the performance of this imaging system was assessed. Table (11) shows that the general evaluation of the biplane interventional fluoroscopy using different field size for both tubes (frontal and lateral). Two different phantom sizes were used 9.5 cm and 12 cm. For frontal tube, the percentage of the differences between measured and indicated air kerma at the IRP were 12.21% and 17.52%, respectively, of field size 25 cm. For the Lateral tube, the differences were 21.81% and 0.54%, for measured and indicated air kerma respectively. Moreover, it is recognized that when the field size decreases the radiation dose increases for both measured and indicated values.

Table (12) shows the ESAK values for the different six phantom thicknesses used under preset clinical conditions. Both Fluoro mode and image acquisition (cine mode) showed a linear relationship between the phantom thicknesses and the ESAK values. This relationship has strong correlation, it was R^2= 0.93 as shown in (Figure 20 and Figure 21) in Chapter 4.The same trend observed for the exposure parameters (kVp and mAs).

The phantom study was repeated using the paediatric protocol as demonstrated in Table (13), reduction on air kerma rate was observed in fluoro mode as follow: 1.85%, 17.05%, 14.75%, 26.13%, 19.82% and 27.26% for phantom sizes 4.8, 7.4, 9.5, 12, 14.5 and 16.8 cm, respectively. Moreover, a significant reduction in dose per frame was found in the cine mode. It is acknowledged that the cine mode deliver the higher dose to the patient compared to the fluoro mode. The dose

reductions in our measurements were as follow: 59.64%, 98.08%, 64.85%, 79.68%, 65.02% and 62.69% for phantom sizes 4.8, 7.4, 9.5, 12, 14.5 and 16.8 cm, respectively.

It is believed that the main reason for these reduction percentages in the doses are the pre filter that selected by the machine. For the default protocol, the filter presetting for the fluoro mode was 0.1 Cu + 1 mm Al while for the cine mode there was no filter. Considering paediatric protocol the presetting filter was 0.4 mm Cu + 1mm Al for fluoro mode and 0.1 mm Cu + 1 mm Al for cine mode. Therefore, the use of additional filtration for the paediatric patient is crucial to reduce the dose as mentioned by Bacher.k et al., (2005) [62], and also recommended by the ICRP 121 (2013) [1]. The difference in the amount of the radiation dose level reduction for both modes was displayed in Figure (27) for fluoro mode and in Figure (28) for cine mode. The x-axis represents the six phantom thicknesses and the y-axis represents the incident air kerma rate for the fluoro mode and the dose per frame for the cine mode.

Since the system is integrated with KAP meter, a verification of the meter accuracy was performed before starting the patient dosimetric data collection. Table (14) shows that the maximum difference for the fluoro procedures between the measured KAP and indicated KAP was found 40.3% in the normal mode and 15 cm field size option. The minimum difference was found 26.22% in the low mode and 25 cm field size. The difference for the clinical mode (normal mode and 25 cm field size option; which is the most used option at the Dubai hospital Cath lab) was 28.07% which is lower than the level mentioned in the IAEA scientific presentation

(it was mentioned as 30% to 40%). The calibration factor was found 1.39 for the normal mode with 25 cm field size.

For the cine procedures, the maximum difference was found 41.5% in the normal mode with 15 cm field size and the minimum was found 27.36% in the high mode with 25 cm field size. The calibration factor was found 1.41 for the option of normal mode with 25 cm field size.

Table (15) shows that the maximum difference for the CAK in fluoro procedure was found 7.02% in the low mode with 25 cm field size option whereas the minimum difference was found 6.13% in normal mode with 15 cm field size. The difference for the common clinical used mode and field size used was 6.67% and the calibration factor was found 1.07. In the cine mode procedures, the maximum difference was found 3.96% and the minimum was found 0.1 %. The calibration factor was found 1.02 and the difference was found 2.34% for the option of common clinical mode.

The total number of paediatric patients collected with sufficient information was 88 patients. Table (16) revealed analytically the paediatric demographic information and the dosimetric values where the mean weight were 3.36, 7.14, 12.16, 18.34 and 52.33 kg and mean ages were 5.8 day, 7 month, 2.9 year, 6.58 year and 12.3 year for the five age groups, respectively. The highest number of cases of paediatric patients were for the two age groups (>0-1y and >1-5y) while the lowest number of cases was for the newborn. For the dosimetric values, the data collections were total KAP, Air kerma value and Fluoro Time (FT).

The mean KAP values were 2.258 ± 0.82, 10.682 ± 9.26, 20.454 ± 31.96, 19.09 ± 14.23 and 53.622 ± 63.52 Gy.cm^2 for the newborn, >0-1y, >1-5y, >5-10y and >10-15y, respectively. It is noticed that the KAP value of age group (>1-5 y) is slightly higher than the second one (>5-10), this is possibly due to the limited number of the collected cases in the second group and the heterogeneous of the patient in the same age group. The mean value for the skin dose (Air kerma) were 26.76 ± 8.59, 10.68 ± 9.26, 217.19 ± 282.71, 175.57 ± 139.64 and 538.2 ± 492.1 mGy for the newborn, >0-1y, >1-5y, >5-10y and >10-15y, respectively. The mean FT were 7.03 ± 1.4, 17.5 ± 5.69, 14.4 ± 11.9, 10.6 ± 6.8 and 30.3 ± 34.6 minutes (min) for the five age groups, respectively. This large variation in the range of the paediatric dosimetric values (KAP, Air Kerma and FT) in the interventional cardiology also observed and stated by several researchers such as McFadden et al.,(2013) [52], Tsapaki V. et al., (2007) [50] , Bacher K. et al., (2005) [62] and Barnaoui et al.,(2014) [54].

Investigations of the KAP correlation with the technical data collected are shown on the following graphs. Figure (34) shows a strong correlation (R^2= 0.90) between the KAP values and Air Kerma. Figure (35) and Figure (36) show poor correlation (R^2= 0.14) and (R^2 = 0.26) between the KAP and both FT and patient weight, respectively. The variation can be explained by the complexity of the cardiac procedures, the variation in the anatomy from one patient to anther and the practice of the technicians or the cardiologists [54, 51].

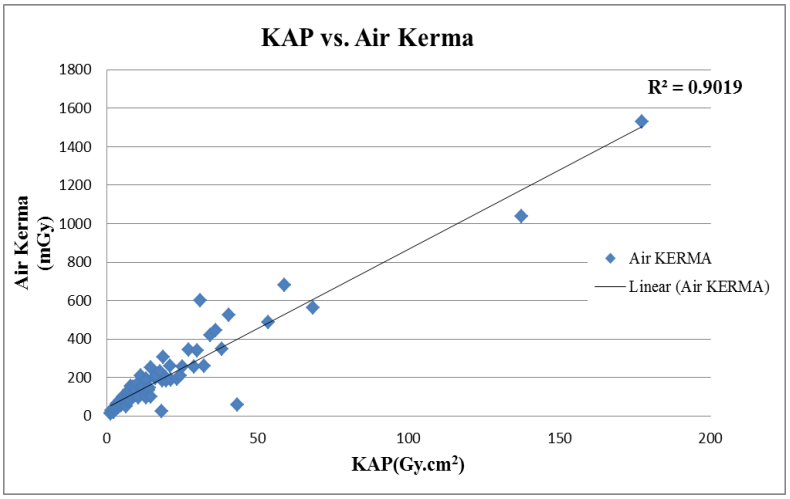

Figure 34: Correlation of KAP vs. Air Kerma

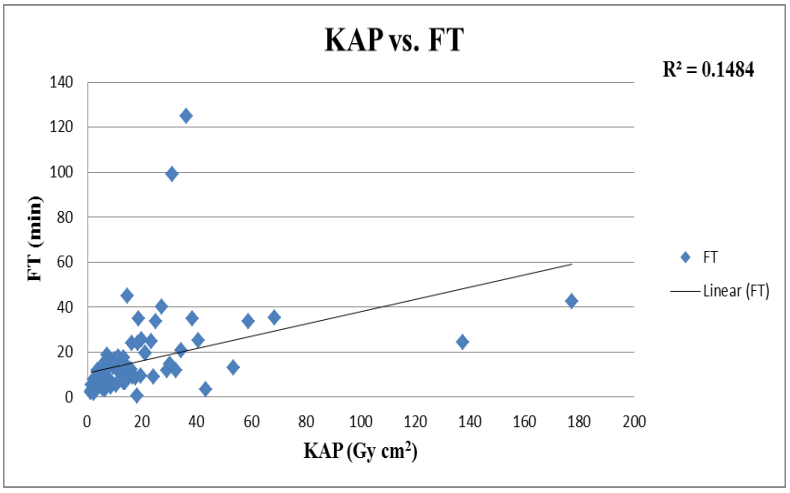

Figure 35: Correlation of KAP vs. FT

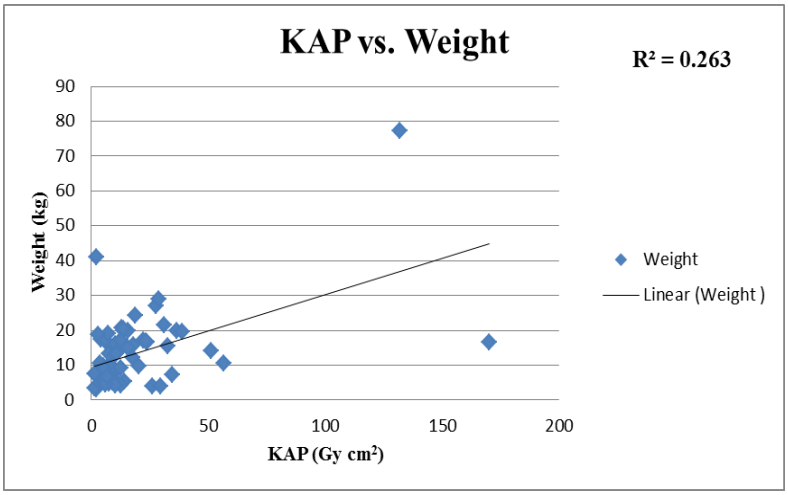

Figure 36: Correlation of KAP vs. Weight

Table (23) displays the comparisons of LDRL KAP values for this work and other published data using the same classification of paediatric age groups. The KAP values in this study were higher compared to the data from UK (2010) [58]. Moreover, these values were higher than data from Sweden (2009) [61] except for the newborn age group. While the data from Belgium (2008) [59] were higher than our values except for the age groups (>0-1y and >1-5y). Moreover, in comparing the findings in this research to a previous study done on same machine in 2012 [51], the present findings were found higher for age groups (>1-5 and > 10-15). This difference was mainly due to slight difference in age groups classification (it was as follow: 0-<1y, 1-<5y, 5-<10y and 10-≤15y). Figure (37) summarized the comparison shown in Table (23), where the therapeutic procedures were included only in this graph.

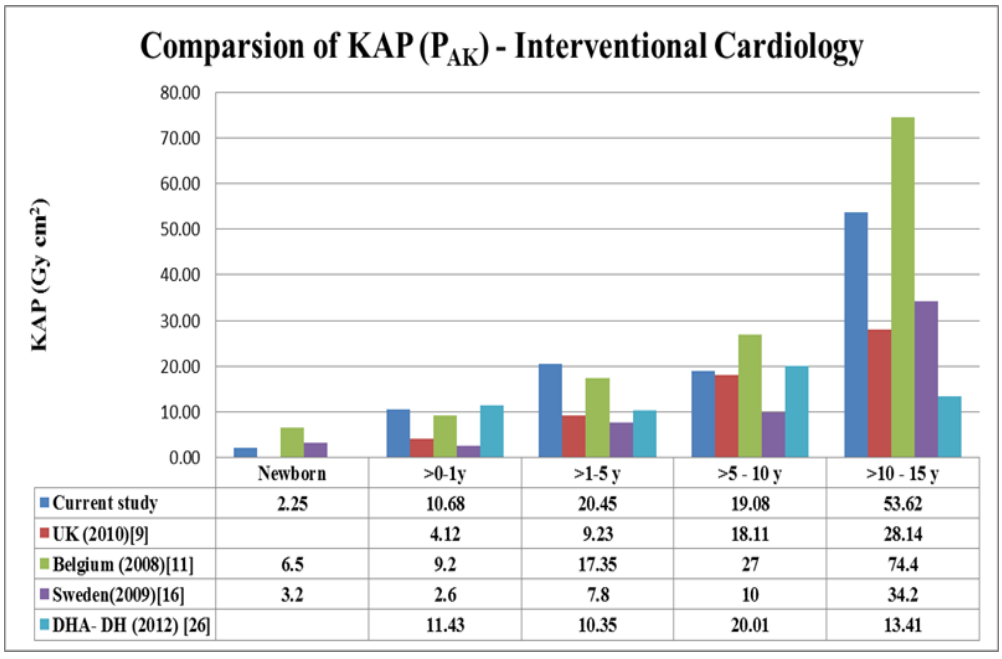

Figure 37: Comparison of KAP values with other published surveys - Interventional cardiology

5.4 Effective dose and Risk Assessment

For the paediatric patient, effective doses were calculated and the risk assessments were estimated in different examinations via the PCXMC 2.0 Monte Carlo software for fixed x-ray, mobile x-ray and IC. The KAP values were fed into software to estimate the Es. Table (17) illustrates the value of E for each age group at the fixed x-ray and it is noticed that in the chest examinations the Es for newborn was higher (15 µSv) than the following two groups. However, the KAP value for the newborn was the lowest and the maximum E was for age group >10-15y. For the abdomen examinations the E for the first three age groups were comparable to each other while their KAP values showed significant difference. The Es for the combined chest-abdomen examinations of the newborn and >0-1y age groups were almost similar although that their KAP values were different.

The Es of the previous examinations (chest, abdomen and combined chest-abdomen) show how much the paediatric groups are sensitive to radiation, where the sensitivity increases as the age decrease.

Figure (38) shows that the Es for the skull and extremities examinations are smaller compared to the other examinations, which is expected since these two parts of patient's body do not contain sensitive organs. Apart from the pelvis examination, it is found that the stochastic radiation risk for the female patient was higher than the male. This is may attribute to the tissue weight factors where for the breast is higher than gonads as stated on the ICRP publication (2007) [20].

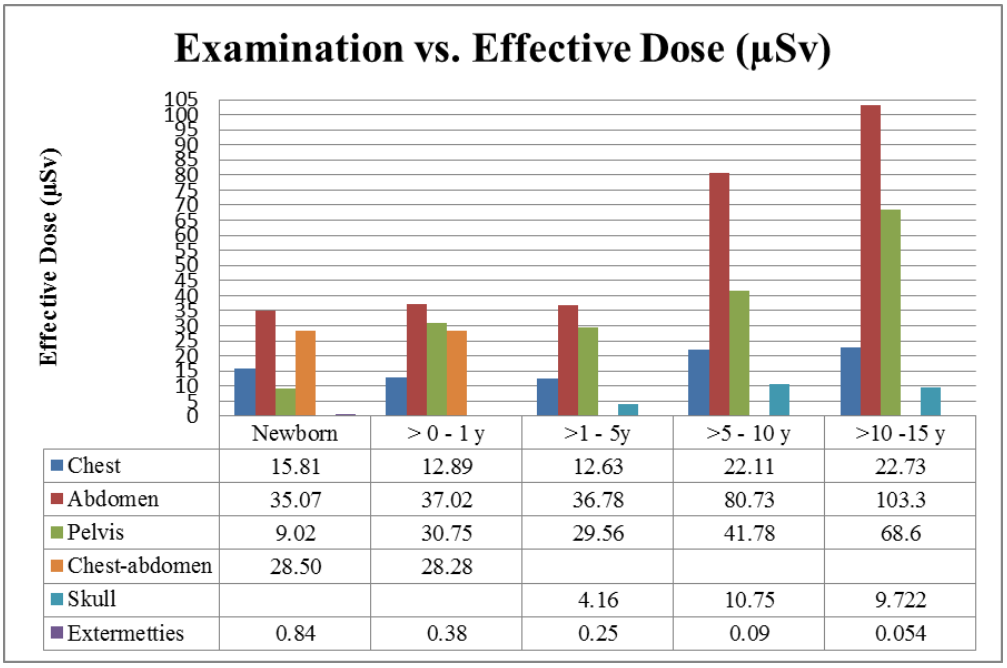

	Newborn	> 0 - 1 y	>1 - 5y	>5 - 10 y	>10 -15 y
Chest	15.81	12.89	12.63	22.11	22.73
Abdomen	35.07	37.02	36.78	80.73	103.3
Pelvis	9.02	30.75	29.56	41.78	68.6
Chest-abdomen	28.50	28.28			
Skull			4.16	10.75	9.722
Extermetties	0.84	0.38	0.25	0.09	0.054

Figure 38: Examination vs. Effective dose - Fixed x-ray

For the neonatal patients in the NICU, the values of the Es in Table (18) shows that the E for the combined chest-abdomen was (23.03 µSv) which is comparable to that for the newborn patient (28.5 µSv) in the fixed x-ray. This is may be due to the radiation dose delivered from the mobile x-ray which was comparable to that from the fixed x-ray. Moreover, the exposure parameters used with neonatal patient were (kVp=53 and mAs=1.98) lower than those used for the newborn in fixed x-ray (kVp =60.8 and mAs=2.17) as extracted from the DICOM header. It has to be kept in mind that the risk of ionizing radiations is strongly dependent on the child's age and the time of exposure as revealed by IAEA and ICRP [18, 1].

Table (19) illustrates the E for the paediatric patients in the IC; it is clearly shown that the Es and the radiation risk from this type of ionizing procedure are higher than what is demonstrated earlier. The IC effective dose is given in mSv while in general x-ray was given in µSv and the loss of life expectancy given in days while

in general x-ray was given in hours. In terms of gender sensitivity in IC, the similarity was observed as in general x-ray. That is the female is more sensitive than male by a factor of around 1.7.

When the findings of E values in IC in this research compared to other published data findings, as displayed in Table (24), it was found that the present research findings remained higher than the UK [58] and Sweden [61] but lower than that of Belgium [59]. It has to kept in mind that the principle of E (i.e. the effective dose is a good indicator for the risk of radiation induces cancer) should not be applied to the paediatric patients, since the tissue weight factors that suggested by the ICRP and used in the PCXMC 2.0 software were averaged over several populations involving both genders and all ages [18].

This study has limitations such as for the general x-ray the DICOM header does not have information of the patient demographic data (weight and height) and exposure factors (the distance from tube focus to table and from the tube focus to patient surface). This information was needed to calculate the patient ESAK through the fitting function generated from the tube output measurements and to estimate the E dose using the PCXMC 2.0 software. Moreover, the IC was not integrated with the DICOM system which raises the human errors when collecting the patient dosimetric values manually. The numbers of the paediatric patient in the IC were approximately 50 patients per year which is lower than other surveyor’s data.

Chapter 6: Summary of Results and Conclusions

(1) This study was conducted to evaluate paediatric patient radiation dose levels in digital conventional radiology (both fixed x-ray and mobile x-ray) and interventional cardiology at Dubai Hospital. The results of this study are expected to contribute in establishing the local and national DRLs in UAE. The number of the x-ray examinations for the paediatric patients were increasing over the years. Hence, paediatric radiation safety is one of the critical issues in the diagnostic radiology. It has been known that they are at higher risk form ionizing radiation than adults if they receive same amount of dose. At Dubai hospital it is expected that paediatric patient radiation dose levels in digital conventional radiology and interventional cardiology are within the recommended standards and comparable with the others published data.

(2) The indirect measurements of the ESAK in digital fixed x-ray examinations were not exceeding the recommended values reported by international organizations and they were lower than other published data. DICOM system was a very useful tool to extract the patient demographic and dosimetric information. Moreover, the tube output measurements also are considered a very good alternative method for indirect measurement of the ESAK in case of KAP damage or DICOM system corrupted.

(3) It was clearly shown form the results in the fixed and mobile x-ray that the chest and combined chest-abdomen examinations have the lowest radiation dose among the other x-ray examinations. Nevertheless, it has to be borne in mind that the frequent request of this type of examinations result in relatively high cumulative radiation doses. These examinations are safe if used with care and if

the professionals (paediatrations, radiologists and radiographers) have a good training on patient radiation protection and biological effects of x-rays.

(4) Neonates at NICU may need long hospitalization according to their clinical conditions that require several x-ray examinations to follow their clinical improvements. The referral physicians and paediatricians should outweigh the benefit to the risk for their patients and if possible ask for an alternative non-ionizing modality in consultation with the radiologists. The radiographers should optimize patient dose by reducing the number of radiation exposure, selecting the correct exposure factors and collimate the radiation beam to the area of interest as much as possible.

(5) In interventional cardiology, apart from the newborn, technicians were using the defaulted protocol for all patients with normal mode and field size of 25 cm. The machine has the options for the paediatric protocol and the phantom study shows the significant reduction in the dose when paediatric protocol is selected. Moreover, the big reduction was clear in the cine mode. Hence, the technicians are strongly encouraged to select the paediatric protocol when handling paediatric patients. The patient collected data shown that our KAP readings were higher than some of other published data and comparable to one of them. A wide variety found between the patient KAP values, even with same age group, may be due to the complexity of some of IC procedures and different patient sizes.

(6) Patient effective doses were easy to be estimated by using the Monte Carlo software PCXMC 2.0. The results show that the highest values were found in newborns compared with other paediatric age groups, even though newborns having the lowest KAP values. This shows how the paediatric group is so sensitive to radiation and this sensitivity is increased with the smaller age.

Moreover, female patients have higher stochastic radiation risk than male in all chest, abdomen and combined chest- abdomen examinations, whereas for the pelvis examination male were higher.

(7) Obviously, this study focused on patient dose and optimizing this dose with inevitable slight changes related to the protocols. Further studies are needed to include the image quality assessment to find the optimum image quality with lower radiation dose.

(8) This study suggests that there is a need to develop further radiation protection and education programs for paediatric patients, along with patient dosimetric monitoring, recording and reviewing within the UAE.

(9) In order to manage the establishment of DRLs (local and national), it is important to collect more patient dosimetry data and cover more x-ray systems.

Bibliography

1. Khong PL, Ringertz H, Donoghue V, Frush D, Rehani M, Appelgate K, et al. ICRP publication 121: radiological protection in paediatric diagnostic and interventional radiology. Annals of the ICRP. 2013; 42(2):1–63.
2. United Nnations, Sources and Effects of Ionizing Radiation, UNSCEAR 2008 Report to the General Assembly, with Scientific Annexes, Scientific Committee on the Effects of Atomic Radiation (UNSCEAR), UN, New York (2010).
3. Tsapaki V, Ahmed NA, AlSuwaidi JS, Beganovic A, Benider A, BenOmrane L, et al. Radiation Exposure to Patients During Interventional Procedures in 20 Countries: Initial IAEA Project Results. American Journal of Roentgenology. 2009 Aug; 193(2):559–69.
4. Rehani M, International Atomic Energy Agency. Safety Reports Series No. 71, Radiation protection in paediatric radiology. Vienna; 2012
5. International Atomic Energy Agency. Radiation protection and safety of radiation sources: international basic safety standards, general safety requirements. Vienna: International Atomic Energy Agency; 2011.
6. Linet MS, pyo Kim K, Rajaraman P. Children's exposure to diagnostic medical radiation and cancer risk: epidemiologic and dosimetric considerations. Pediatric radiology. 2009;39(1):4–26
7. Suliman II, Elawed SO. Radiation dose measurements for optimisation of chest X-ray examinations of children in general radiography hospitals. Radiation protection dosimetry. 2013; nct 073.
8. Allura Xper FD10/10 - Philips [Internet]. [Cited 2015 Apr 12]. Available from:http://www.healthcare.philips.com/main/products/interventional_xray/product/interventional_cardiology/imaging_systems/intcardio_fd1010.wpd
9. Hart D, Wall BF, Shrimpton PC, Dance DR. The establishment of reference doses in paediatric radiology as a function of patient size. Radiation protection dosimetry. 2000; 90(1-2):235–8.

10. Billinger J, Nowotny R, Homolka P. Diagnostic reference levels in pediatric radiology in Austria. European Radiology. 2010 Jul; 20(7):1572–9.
11. Şorop I, Dădulescu E. Assessment of entrance surface doses for newborn babies within an intensive care unit. Romanian Reports in Physics. 2011; 63(2):401–10.
12. Schultz FW, Geleijns J, Spoelstra FM, Zoetelief J. Monte Carlo calculations for assessment of radiation dose to patients with congenital heart defects and to staff during cardiac catheterizations. The British journal of radiology. 2003; 76(909): 638-647
13. Kohn M M, Moores BM, Schibilla H, Schneider K, Stender HS, Stieve FE, et al. European guidelines on quality criteria for diagnostic radiographic images in paediatrics. Luxembourg: Office for Official Publications of the European Communities; 1996.
14. Pernička F, McLean ID, International Atomic Energy Agency. Dosimetry in diagnostic radiology: an international code of practice TRS No. 457. Vienna: International Atomic Energy Agency; 2007.
15. VALENTIN J. ICRP Publication 103: The 2007 Recommendations of the International Commission on Radiological Protection. Annals of the ICRP.2007; 37(2.4):2.
16. European Society of Radiology (ESR). White paper on radiation protection by the European Society of Radiology. Insights into Imaging. 2011 Aug; 2 (4):357–62.
17. Kiljunen T. Patient doses in CT, dental cone beam CT and projection radiography in Finland, with emphasis on paediatric patients. 2008 [cited 2015 Apr 12]; Available from: https://helda.helsinki.fi/handle/10138/23235
18. Delis H, Mclean I D, Van W. Dosimetry in diagnostic radiology for paediatric patients. IAEA human Health Series No.24. Vienna; 2013.
19. International Commission on Radiological Protection. ICRP Publication 60: 1990 Recommendations of the International Commission on Radiological Protection. Annals of the ICRP.1990; 21 (1-3).

20. Neitzel U. Management of pediatric radiation dose using Philips digital radiography. Pediatric Radiology. 2004 Oct; 34(S3):S227–33.

21. McCollough CH, Christner JA, Kofler JM. How Effective Is Effective Dose as a Predictor of Radiation Risk? American Journal of Roentgenology. 2010 Apr;194(4):890–6.

22. Ullman G. Quantifying image quality in diagnostic radiology using simulation of the imaging system and model observers. [Thesis]. Institutionen för medicin och hälsa; 2008. Linköping University Medical Dissertations, 1050.

23. Tapiovaara M, Siiskonen T. PCXMC 2.0: a PC-based Monte Carlo program for calculating patient doses in medical X-ray examinations. Helsinki: Finnish Centre for Radiation and Nuclear Safety; 2008.

24. Liaparinos PF. Monte Carlo simulations in medical imaging. 2010 Apr [cited 2015 Apr 1]; 5(2). Available from: http://e-jst.teiath.gr/issue_15/Liaparinos_15.pdf

25. Carroll QB. Radiography in the Digital Age: Physics - Exposure - Radiation Biology. 1 edition. Springfield, Ill: Charles C Thomas Pub Ltd; 2011. 882 p.

26. Bushberg JT, Seibert JA, Jr EML, Boone JM. The Essential Physics of Medical Imaging. 2.00 edition. Philadelphia: Lippincott Williams & Wilkins; 2001. 933 p.

27. Information for Public [Internet]. [Cited 2015 Apr 1]. Available from: https://rpop.iaea.org/RPOP/RPoP/Content/InformationFor/Patients/information-public/

28. Balter S, Miller DL. Patient Skin Reactions From Interventional Fluoroscopy Procedures. American Journal of Roentgenology. 2014 Apr; 202(4):W335–42.

29. Vano E, Padovani R, Neofotistou V, Tsapaki V, Kottou S, Ten JI, et al.

Improving patient dose management using DICOM header information. The European SENTINEL experience. Proceedings of the International Special Topic Conference on Information Technology in Biomedicine Available at http://medlab cs uoi gr/itab2006/proceedings/Medical% 20Imaging/149 pdf, Accessed [Internet]. 2010 [cited 2015 Apr 13]. Available from: http://www.researchgate.net/profile/Keith_Faulkner/publication/237461991_Improving_patient_dose_management_using_DICOM_header_information._The_European_SENTINEL_experience/links/00b7d5266498f43d44000000.pdf

30. International Atomic Energy Agency, European Commission. Radiation protection and safety of radiation sources: international basic safety standards : general safety requirements. 2014.
31. Radiology, News, Education, Service [Internet]. [Cited 2015 Apr 13]. Available from: http://www.auntminnieeurope.com/index.aspx?sec=ser&sub=def&pag=dis&ItemID=610921
32. Geijer H. Radiation dose and image quality in diagnostic radiology: optimization of the dose - image quality relationship with clinical experience from scoliosis radiography, coronary intervention and a flat-panel digital detector. [Thesis]. Linköping: Linköpings universitet; 2001. Linköping University Medical Dissertations, 706.
33. Faulkner K. Dose audit and optimization for radiological and interventional procedures. [Ph.D. thesis]. Journal of Medical Physics .Association of Medical Physicists of India. 2008; 33(1):35.
34. International Commission on Radiological Protection. ICRP Publication 105: Radiological Protection in Medicine. Annals of the ICRP.2007; 37:6.
35. International Commission on Radiological Protection. ICRP Publication 113: Education and Training in Radiological Protection for Diagnostic and Interventional Procedures. Annals of the ICRP.2009; 39:5.
36. Hart D, Hillier M. C, Wall BF. Doses to patients from medical X-ray examinations in the UK 2000 review. National Radiological Protection Board (United Kingdom). 2002.

37. Hart D, Hillier M. C. Doses to patients from radiographic and fluoroscopic X-ray imaging procedures in the UK-2005 review. Health Protection Agency. Radiation Protection Division. 2007.
38. Linet MS, pyo Kim K, Rajaraman P. Children's exposure to diagnostic medical radiation and cancer risk: epidemiologic and dosimetric considerations. Pediatric radiology. 2009; 39(1):4–26.
39. Yakoumakis EN, Tsalafoutas IA, Aliberti M, Pantos GI, Yakoumakis NE, Karaiskos P, et al. Radiation doses in common X-ray examinations carried out in two dedicated paediatric hospitals. Radiation Protection Dosimetry. 2007 May 25;124(4):348–52.
40. Suliman II, Elshiekh EHA. Radiation doses from some common paediatric X-ray examinations in Sudan. Radiation Protection Dosimetry. 2008 Aug 4;132(1):64–72.
41. Smans K, Vano E, Sanchez R, Schultz FW, Zoetelief J, Kiljunen T, et al. Results of a European survey on patient doses in paediatric radiology. Radiation Protection Dosimetry. 2008 Feb 18;129 (1-3):204–10.
42. Ribeiro LA, Yoshimura EM. Entrance surface dose measurements in pediatric radiological examinations. Radiation Measurements. 2008 Feb;43(2-6):972–6.
43. Matthews K, Patrick C. Brennan, McEntee MF. An evaluation of paediatric projection radiography in Ireland. Radiography. 2014; 20: 189-194.
44. Akhdar HF. Assessment of Entrance Skin Dose and Effective Dose of Some Routine X-ray Examinations Using Calculation Technique. [PhD thesis]. King Saud University; 2007. Available from: http://repository.ksu.edu.sa/jspui/handle/123456789/8706
45. Brindhaban A. Radiation dose to premature infants in neonatal intensive care units in Kuwait. Radiation Protection Dosimetry. 2004 Jul 20; 111(3):275–81.
46. Frayre AS, Torres P, Gaona E, Rivera T, Franco J, Molina N. Radiation dose reduction in a neonatal intensive care unit in computed radiography. Applied Radiation and Isotopes. 2012 Dec; 71:57–60.

47. Dabin J, Struelens L, Vanhavere F. Radiation dose to premature new-borns in the Belgian neonatal intensive care units. Radiation Protection Dosimetry. 2014 Jan 1; 158(1):28–35.
48. Alzimami K, Sulieman A, Yousif A, Babikir E, Salih I. Evaluation of radiation dose to neonates in a special care baby unit. Radiation Physics and Chemistry. 2014 Nov; 104:150–3.
49. Donadieu J, Zeghnoun A, Roudier C, Maccia C, Pirard P, André C, et al. Cumulative Effective Doses Delivered by Radiographs to Preterm Infants in a Neonatal Intensive Care Unit. Pediatrics. 2006 Mar 1; 117(3):882–8.
50. Tsapaki V, Kottou S, Korniotis S, Nikolaki N, Rammos S, Apostolopoulou SC. Radiation doses in paediatric interventional cardiology procedures. Radiat Prot Dosimetry. 2008 Dec 1; 132(4):390–4.
51. Dragusin O, Gewillig M, Desmet W, Smans K, Struelens L, Bosmans H. Radiation dose survey in a paediatric cardiac catheterisation laboratory equipped with flat-panel detectors. Radiat Prot Dosimetry. 2008 Mar 1; 129(1-3):91–5.
52. McFadden S, Hughes C, D'Helft CI, McGee A, Rainford L, Brennan PC, et al. The establishment of local diagnostic reference levels for paediatric interventional cardiology. Radiography. 2013 Nov; 19(4):295–301.
53. Karambatsakidou A, Sahlgren B, Hansson B, Lidegran M, Fransson A. Effective dose conversion factors in paediatric interventional cardiology. BJR. 2009 Sep 1; 82(981):748–55.
54. Barnaoui S, Rehel JL, Baysson H, Boudjemline Y, Girodon B, Bernier MO, et al. Local Reference Levels and Organ Doses from Pediatric Cardiac Interventional Procedures. Pediatr Cardiol. 2014 Mar 21; 35(6):1037–45.
55. Medical Council- Diagnostic-Referance-Levels-03-12-2004.pdf [Internet]. [cited 2015 Apr 13]. Available from: https://www.medicalcouncil.ie/About-Us/Legislation/Medical-Ionising-Radiation/Diagnostic-Referance-Levels-03-12-2004.pdf
56. Hart D, Wall BF, Shrimpton PC, Dance DR. The establishment of reference doses in paediatric radiology as a function of patient size. Radiation protection dosimetry. 2000;90(1-2):235–8.

57. Compagnone G, Pagan L, Bergamini C. Effective dose calculations in conventional diagnostic X-ray examinations for adult and paediatric patients in a large Italian hospital. Radiat Prot Dosimetry. 2005 May 17;114(1-3):164–7.

58. Moores BM, Charnock P, Ward M. Web-based tools for quality assurance and radiation protection in diagnostic radiology. Radiat Prot Dosimetry. 2010 Apr 1;139(1-3):422–9

59. Dragusin O, Gewillig M, Desmet W, Smans K, Struelens L, Bosmans H. Radiation dose survey in a paediatric cardiac catheterisation laboratory equipped with flat-panel detectors. Radiat Prot Dosimetry. 2008 Mar 1;129(1-3):91–5.

60. Dougeni ED, Delis HB, Karatza AA, Kalogeropoulou CP, Skiadopoulos SG, Mantagos SP, et al. Dose and image quality optimization in neonatal radiography. BJR. 2007 Oct 1;80(958):807–15.

61. Karambatsakidou A, Sahlgren B, Hansson B, Lidegran M, Fransson A. Effective dose conversion factors in paediatric interventional cardiology. BJR. 2009 Sep 1;82(981):748–55.

62. Bacher K, Bogaert E, Lapere R, Wolf DD, Thierens H. Patient-Specific Dose and Radiation Risk Estimation in Pediatric Cardiac Catheterization. Circulation. 2005 Jan 4; 111(1):83–9.

63. AlSuwaidi JS, AlMazrouei NK, Pottybindu S, Siraj M, Mathew D, Blooshi AAA, et al. Patient dose monitoring in Dubai in radiography and interventional procedures. Ann ICRP. 2015 Mar 12;0146645315575875

64. Handouts from the IAEA Training Course on patient dose assessment and dose management in diagnostic radiology.

APPENDIX 1: Semiconductor Calibration Coefficient 1

Unfors Xi (Semiconductor based detector) calibrated on: 22-Sep-14			**Alain Hospital**	**S/N : 159970**
All below data were obtained from the calibration certificate of this device				
Calibration Curve (R/F Low)				
kVp	**mA**	**Ref Dose**	**Xi Dose**	**Cal. Coeff.(Ref Dose/Xi Dose)**
50	32	410.7	418.8	1.02
70	16	273.1	275.6	1.01
100	8	269.9	270.3	1.00
150	5	327.1	355.1	1.09
Calibration Curve (R/F High)				
kVp	**mA**	**Ref Dose**	**Xi Dose**	**Cal. Coeff.(Ref Dose/Xi Dose)**
50	51	6249	6404	0.98
70	26	3313	3358	0.99
100	10	2466	2503	0.99
150	5	4248	4251	1.00

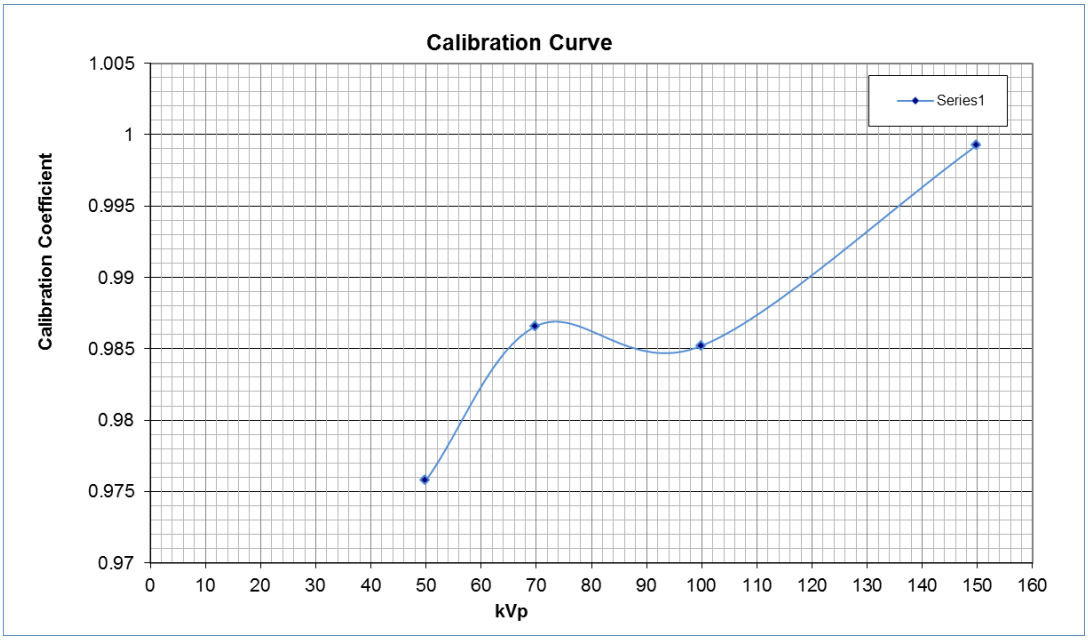

APPENDIX 2: Semiconductor Calibration Coefficient 2

Unfors Xi (Semiconductor based detector) calibrated on: 04-Jul-14			**Zayed Military Hospital**	**S/N : 149732**
All below data were obtained from the calibration certificate of this device				
Calibration Curve (R/F Low)				
kVp	**mA**	**Ref Dose**	**Xi Dose**	**Cal. Coeff.(Ref Dose/Xi Dose)**
50	32	218.2	219.3	1.01
70	16	227.8	230.5	1.01
100	8	219.9	222.4	1.01
150	5	354.5	352.3	0.99
Calibration Curve (R/F High)				
kVp	**mA**	**Ref Dose**	**Xi Dose**	**Cal. Coeff.(Ref Dose/Xi Dose)**
50	51	4362	4377	1.00
70	26	4595	4639	0.99
100	10	3539	3556	1.00
150	5	4407	4342	1.01

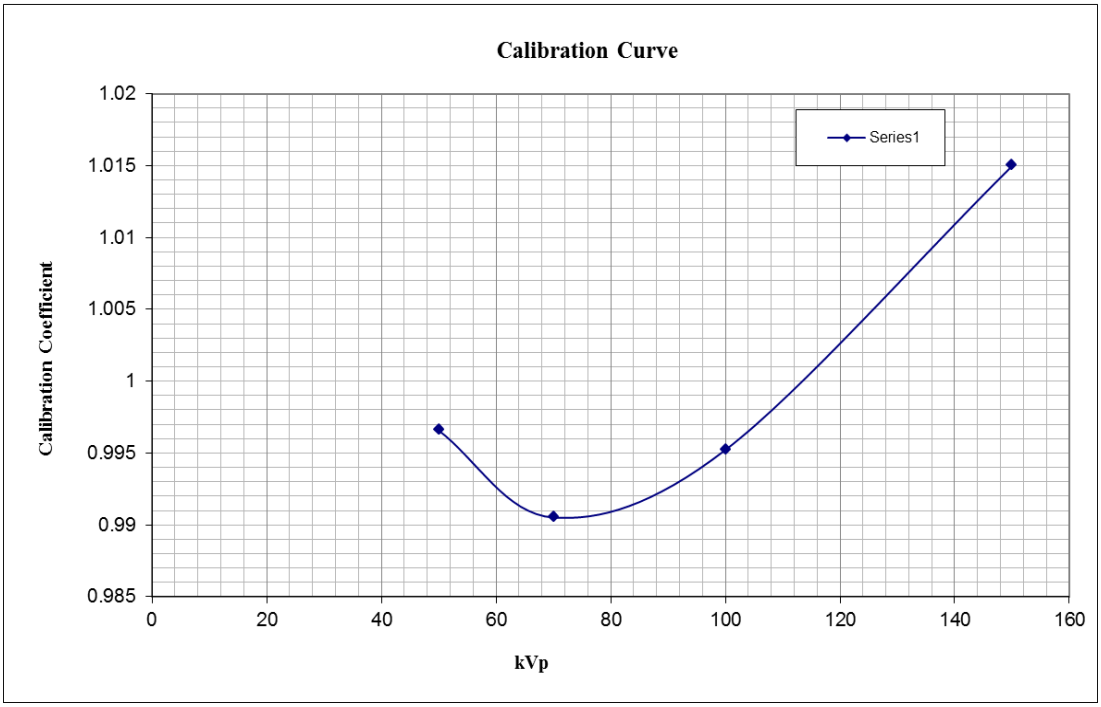

APPENDIX 3: Example on Phantom Dosimetry Calculation

Newborn (0-1m) clinical examinations - Phantom= 4.8 cm - with Grid & the AEC is NOT activated	**kVp**	**mAs**	**M**	**kQ**	**k(d) µGy**	**d_{FTD} mm**	**d_m mm**	**d_p mm**	**d_{FTD} - d_m mm**	**d_{FTD} - dp mm**	**(d_{FTD} - d_m) / (d_{FTD} - dp) mm**	**[(d_{FTD} - d_m) / (d_{FTD} - dp)]2 mm**	**Incident Air Kerma, Ki µGy**	**Indicated Air Kerma, Ki, (µGy)**	**% Variation**	**ESAK Ke = Ki * B**
Abdomen (AP) - BUCKY - FSD=100cm Dosimeter Phantom Distance = 18.7 cm , LFS	65	3.6	94.35	0.99	92.94	1000	235	48	765	952	0.80	0.65	60.02	54.07	9.90%	84.62
chest (AP) Table top- FSD=120 Dosimeter Phantom Distance = 16.2 cm , LFS	60	1.9	21.98	0.98	21.60	1200	210	48	990	1152	0.86	0.74	15.95	16.07	-0.75%	22.49
chest/Abdomen (chest protocol) - TABLE TOP- FSD=100 cm ,Dosimeter Phantom Distance = 16.2 cm , LFS	60	1.9	34.94	0.98	34.33	1000	210	48	790	952	0.83	0.69	23.64	22.54	4.65%	33.33
Pelvis (AP)-BUCKY - FSD=100 cm - Dosimeter Phantom Distance = 18.7 cm - LFS	65	4.9	129.5	0.99	127.56	1000	235	48	765	952	0.80	0.65	82.37	71.11	13.67%	116.14
Extremities (upper) Hand PA- table top- FSD = 100 cm , Dosimeter cassette Distance = 20.7 cm - SFS	50	2.4	83.89	0.98	81.79	1000	207	0	793	1000	0.79	0.63	51.44	49.54	3.69%	69.95
chest/Abdomen (Abdomen protocol) - TABLE TOP- FSD=100 cm ,Dosimeter Phantom Distance = 16.2 cm, LFS	65	2.9	71.23	0.99	70.17	1000	210	48	790	952	0.83	0.69	48.32	45.40	6.05%	68.13
Abdomen (AP) - tabletop - FSD=100cm , -Dosimeter Phantom Distance = 16.2 cm -Dosimeter cassette Distance= 20.7cm , LFS	65	2.9	70.09	0.99	69.04	1000	207	48	793	952	0.83	0.69	47.90	43.70	8.77%	67.54

APPENDIX 4: KAP Calibration for Fixed X-ray Unit

X-ray machine	PHILIPS - Digital Diagnostic	
X-ray tube Serial No:	246415	
Dosimeter	Alain hospital Unfors Xi meter	
Serial No	base unit: 164021	R/F detector: 159970
Exposure parameter		
Field size at Dosimeter level (cm) = 22.4 x 15	Machine field size (cm) = 19 x 26	
Focus to dosimeter distance = 80.5 cm		
Focus to table distance = 100 cm		

kVp	**mAs**	**Measured Air Kerma (µGy)**	**Indicated KAP (uGym^2)**	**Calculated KAP ($uGy.m^2$)**	**KAP %Difference**	**Incident Air Kerma, Ki (µGy)**	**Indicated Air Kerma (µGy)**	**Dose %Difference**	**KAP CF**
50	40	843.51	40.80	43.74	6.71%	843.51	885.34	-4.96%	1.07
60	25	821.05	39.90	42.50	6.13%	821.05	807.69	1.62%	1.07
70	8	142.31	7.19	7.38	2.56%	142.31	145.55	-2.28%	1.03
81	25	1517.46	75.59	78.68	3.93%	1517.46	1530.16	-0.84%	1.04
85	32	2141.51	106.71	111.04	3.90%	2141.51	2160.12	-0.87%	1.04
90	25	1864.80	93.01	96.69	3.81%	1864.80	1882.79	-0.97%	1.04
117	2.5	301.14	15.09	15.61	3.36%	301.14	305.47	-1.44%	1.03
125	2.5	331.68	16.93	17.20	1.53%	331.68	342.65	-3.31%	1.02

APPENDIX 5: KAP Calibration for Mobile X-ray Unit

X-ray machine	SHEMADZU – Digital mobile unit	
X-ray tube Serial No:	CM74B5943021	
Dosimeter	Zayed Military hospital Unfors Xi meter	
Serial No	base unit: 145378	R/F detector: 149732
Exposure parameter		
Field size at Dosimeter level (cm) = 10 cm x 12.6	Machine field size (cm) = 17 cm x 13	
Focus to dosimeter distance = 79.5 cm		
Focus to table distance = 100 cm		

kVp	**mAs**	**Measured Air Kerma (µGy)**	**Indicated KAP (mGy.cm^2)**	**Calculated KAP (mGy.cm^2)**	**KAP %Difference**	**Incident Air Kerma, Ki (µGy)**	**Indicated Air Kerma (µGy)**	**Dose %Difference**	**KAP CF**
49	1.8	47.04	5	5.92	18.53	29.43	22.62	23.13%	1.18
50	1.8	51.08	6.00	6.44	7.26	32.17	27.15	15.60%	1.07
52	1.6	49.13	5.33	6.19	16.08	30.93	24.13	21.97%	1.16
52	2	61.25	7.00	7.72	10.25	38.56	31.67	17.85%	1.10
55	2	71.00	8.00	8.95	11.82	44.65	36.20	18.92%	1.11
57	2	78.37	9.00	9.87	9.72	49.23	40.72	17.27%	1.09
59	2	86.19	10.00	10.86	8.60	54.12	45.25	16.39%	1.08
60	1	45.65	5.00	5.75	15.04	28.65	22.62	21.03%	1.15

APPENDIX 6: Patient Data Collection Form for both Fixed and Mobile Unit

Date of examination	ID	Age (Days)	Gender (F/M)	Weight (Kg)	Height (cm)	kVp	mAs	Patient thickness (cm)	FSD (Focus to skin distance) cm	FBD (Focus to bucky distance) cm	Field size (mm x mm)	Filtration (mm Al)	DAP (uGy.m^2)	Type of Examination	Clinical condition

APPENDIX 7: Patient Data Collection Form for Interventional Cardiology

Date of Procedure	Date of Birth/ Age	Gender	Weight KG	Height cm	Plane A			Plane B			Cine mode			DAP mGycm2
					FT min	Fluoro DAP	AK mGy	FT min	Fluoro DAP	AK mGy	No. of Series	No. of images	Frame rate(f/s)	